

**POLITECNICO DI TORINO**

**Corso di Laurea Magistrale**

**In Ingegneria Aerospaziale**

Tesi di Laurea Magistrale

**In-space and for-space Additive Manufacturing**

**Topology Optimization for future secondary structures**



**Relatore:**

Prof. Paolo Maggiore

Prof. Piero Messidoro

**Tutor Aziendale:**

Arch. Giorgio Musso

**Candidato**

Luigi Villari



## **Summary**

List of figures.....	5
List of Tables .....	7
Abstract.....	8
General Overview .....	9
1. In-space manufacturing .....	11
1.1 Use of space .....	11
1.2 In-space manufacturing. What is it? .....	11
1.2.1 Challenges for in-space manufacturing.....	12
1.2.2 Benefits of in-space manufacturing and assembly .....	13
1.3 State of the art in-space manufacturing & assembly.....	15
1.3.1 ISM for space .....	15
1.3.2 The case of In-space repair.....	17
1.4 A long-term vision .....	18
2. Additive Manufacturing .....	21
2.1 Classification AM Process.....	22
2.2 AM: state of the art.....	24
3. Optimization: introduction .....	26
3.1 The problem of optimization .....	26
3.2 Structural Optimization .....	27
3.2.1 Topology Optimization .....	28
4. Case Study.....	32
4.1 Altair solidThinking Inspire.....	32
4.2 Geometry and materials .....	33
4.3 Load and constraints conditions: Mass Acceleration Curve .....	34
4.4 Set-up linear static analysis.....	37
4.4.1 Model 0 - the original component.....	38
4.5 Project specifications .....	43
5. Optimization phase .....	44
5.1 Non-Design Space .....	44
5.2 Design Space.....	45
5.3 Results DS-Original and DS-Full .....	49
5.3.1 DS-Original .....	49

5.3.2 DS-Full.....	51
5.4 DS-Hybrid – Model 1 .....	53
5.4.1 Result DS-Hybrid.....	54
5.4.2 Analysis of Hybrid-Model .....	57
5.4.3 Result Hybrid-Model Lightened – Model 2 .....	58
5.5 DS-Lattice – Model 3 .....	60
5.5.1 Results of Lattice-Model.....	62
5.6 Final-Model .....	65
5.6.1 Result of ground-based scenario – Model 4.....	68
5.6.2 Result for space-based scenario – Model 5/6 .....	69
5.7 Model Comparison.....	72
6. Conclusion and future developments.....	73
References .....	74

## List of figures

Figure 1: Use cases categorized by depth of technology and business focus [3];	12
Figure 2: Change in launch cost over time [6];	13
Figure 3: Additive Manufacturing Facility (AMF) [10];	15
Figure 4: (A) Archinaut manufactures nodes and (B) struts, (C) Archinaut's robotic manipulators, (D) Archinaut autonomous assembles structural element [10];	16
Figure 5: P3DP Overall Architecture [11];	17
Figure 6: ISS Integrated Truss Structure detailing all ORU in situ [12];	18
Figure 7: Wonhrad Station, Nordung (1928) [13];	19
Figure 8: Functional layout of Orbitecture [13];	20
Figure 9: AM publications per year [16];	21
Figure 10: Electron Beam Free Fabrication Process [18];	24
Figure 11: WAAM Equipment [19];	25
Figure 12: The three types of Structural Optimization [22];	28
Figure 13: Domain for Optimization [22];	29
Figure 14: View 1 (left) and view 2 (right) of the model;	33
Figure 15: Physical Mass Acceleration Curve for STS/IUS [23];	35
Figure 16: Physical Mass Acceleration Curve for Titan 4/IUS [23];	36
Figure 17: Fasteners (left), support (right);	37
Figure 18: Original model contacts;	38
Figure 19: Point A of the model;	39
Figure 20: Number of elements VS Mean size;	39
Figure 21: Execution Time VS Mean Size;	40
Figure 22: Displacement (point A) VS Mean Size;	41
Figure 23: Factor of Safety Original-Model;	42
Figure 24: Displacement Original-Model;	42
Figure 25: von Mises stress Original-Model;	43
Figure 26: NDS;	44
Figure 27: DS-Original, view 1;	45
Figure 28: DS-Original, view2;	46
Figure 29: DS-Original, view3;	46
Figure 30: DS-Full, view1;	47
Figure 31: DS-Full, view2;	48
Figure 32: View of the three through-holes of DS-Full;	48
Figure 33: Shape Explorer	49
Figure 34: Optimized DS-Original max stiffness, view1;	50
Figure 35: Optimized DS-Original max stiffness, view 2;	50
Figure 36: Optimized DS-Original max stiffness, view 3;	51
Figure 37: Optimized DS-Full, minimize mass, view1;	52
Figure 38: Optimized DS-Full, minimize mass, view2;	52
Figure 39: Optimized DS-Full, minimize mass, view3;	53
Figure 40: DS-Hybrid, view1;	54
Figure 41: DS-Hybrid, view2;	54
Figure 42: Optimized DS-Hybrid, max stiffness, view1;	55

Figure 43: Optimized DS-Hybrid, max stiffness, view2;.....	55
Figure 44: Hybrid-Model, view1; .....	56
Figure 45: Hybrid-Model, view2; .....	56
Figure 46: Hybrid-Model, view3; .....	57
Figure 47: Hybrid-Model lightened, view1; .....	58
Figure 48: Hybrid-Model lightened, view2; .....	59
Figure 49: Hybrid-Model lightened, view3; .....	59
Figure 50: Factor of Safety of Hybrid-Model Lightened; .....	60
Figure 51: Displacement of Hybrid-Model Lightened; .....	60
Figure 52: DS-Lattice, view1; .....	61
Figure 53: DS-Lattice, view2; .....	61
Figure 54: Lattice-Model, view1; .....	62
Figure 55: Lattice-Model, view2; .....	63
Figure 56: Factor of Safety of Lattice-Model; .....	64
Figure 57: Displacement of Lattice-Model; .....	64
Figure 58: MAC Data Interpolation;.....	65
Figure 59: Space debris classification [25];.....	66
Figure 60: Final-Model, view1; .....	67
Figure 61: Final-Model, view2; .....	67
Figure 62: Factor of safety of Final-model, ground-based; .....	68
Figure 63: Displacement of Final-model, ground-based; .....	69
Figure 64: Factor of Safety of Final model, space-based production, standard 0.2[g]; ....	69
Figure 65: Displacement of Final model, space-based, standard 0.2 [g];.....	70
Figure 66: Factor of safety of the final model, space-based, debris impact; .....	71
Figure 67: Displacement of the final model, space-based, debris impact; .....	71

## **List of Tables**

Table 1: Classification of AM processes [17]; .....	22
Table 2: Mechanical properties of Aluminium; .....	34
Table 3: Mechanical properties of Kevlar; .....	34
Table 4: Original model weights; .....	34
Table 5: Load Case Original Model; .....	36
Table 6: Original model: result envelope for different mesh size; .....	40
Table 7: Results Original-Model, MS=2[mm];.....	41
Table 8: Acting forces of Hybrid-Model;.....	57
Table 9: Hybrid Model, results linear static analysis; .....	58
Table 10: Acting forces on Hybrid-Model Lightened;.....	59
Table 11: Hybrid Model Lightened, results linear static analysis; .....	59
Table 12: Lattice optimization constraints; .....	62
Table 13: Lattice-Model, linear static analysis results;.....	63
Table 14: Data for interpolation; .....	65
Table 15: Acting forces on Final-Model; .....	65
Table 16: Mechanical Properties of ULTEM 9085; .....	67
Table 17: Results for Final Model, ground-based production; .....	68
Table 18: Results for Final Model, space-based production, standard 0.2 [g];.....	69
Table 19: Results for Final Model, space-based production, impact with debris; .....	70
Table 20: Review of the model; .....	72

## ***Abstract***

The recent developments in the manufacturing process and the entry of new private companies in the space segment are feeding the in-space manufacturing theme. The development of a technology that combines manufacturing and assembly capabilities, practicable in a space environment, is a necessary step to improve safety and to reduce the cost of future space explorations and many other activities. Additive Manufacturing, between the several technologies tried in space, is the one that for different reasons, guarantee the highest percentage of success. Many activities can be performed in-space: manufacturing and assembly of large-structures, systems' components, servicing, repair, and many others. Among these, the case of repairing on demand any failed components could dramatically reduce the risks and cost in comparison to the sequence of tasks today needed to achieve the same goal (ground-based manufacturing/assembly and transfer to orbit). The project of thesis here presented, carried out in collaboration with Thales Alenia Space, focuses on topology optimization of an impact shield for protection from collisions with micrometeoroids and orbital debris, which is a thin wall structure, in two different scenarios: (i) additive manufacturing ground-based production and transfer to orbit, (ii) in-space additive manufacturing production. After analyzing the structural performance of the original model, two topological optimizations were carried out whose results are analyzed and presented. A third optimization, of the lattice type, was carried out to propose another optimized configuration that respects the project requirements and the physics of the problem. The aim is to exploit all the potential of Additive Manufacturing via the most recent topology optimization tools. The thesis includes a review of the trends and state of the art of in-space manufacturing technologies with focus on additive manufacturing, presenting the benefits and current challenges to be overcome. In conclusion, possible future developments and studies are proposed.

## ***General Overview***

The current production paradigm of the space industry is the same as in the last 60 years and dramatically influences the design and layout of spacecraft and satellites, as well as the payload, in terms of mass, volume and size. In fact, they must comply with appropriate space requirements to stay inside the launcher that will transfer them into orbit [1][2]. Furthermore, all the components designed and built on the ground need a ruggedized reinforcement to withstand the tough launch phase, which includes several vibrations, acoustic loads, acceleration loads and even thermal loads [1][2]. This same strengthening process involves significant penalties in terms of mass and volumes which therefore limits the payload capacity and increases the launch costs [1]. These penalties are further accentuated by the need for backup redundancy systems to provide security against damage that may occur during the launch phase [1].

Moreover, the launching phase involves the impossibility of realizing some types of components such as, for example, ultra-thin wall structures that can be inflicted as well as damaged subject to the force of gravity [1]. Similar and other constraints limit the profitability and flexibility of use of commercial satellites and spacecraft. The set of these limits also greatly influences the design, capabilities and products of the spatial system that can be realized [1][3].

In the light of these and other considerations, scholars and researchers have proposed in recent years to replace at least partially or totally this type of terrestrial architecture destined to spacecraft, satellites and systems with one destined to production and assembly in a space environment [1]. This concept, known as on-orbit / in-space manufacturing, although it still has a low TRL (technology readiness level), has undergone several advances in recent years [1]. An example of on-orbit manufacturing is the recently demonstrated one of additive manufacturing, carried out onboard the International Space Station, through which various plastic tools were made.

In this regard, in the course of this document, a bibliographical section is presented first, based on bibliographic sources and secondly an experimental section developed at the Polytechnic of Turin and the Turin office of Thales Alenia Space.

As for the bibliographic section, divided into two different chapters, the main topics concern the state of the art of Additive Manufacturing and In-space Manufacturing as well as future trends.

As far as the experimental section is concerned, modern topological optimization techniques are introduced, with the aid of some examples, focusing in particular on the algorithms used by Altair Inspire, software used to obtain the new architecture and layout of a component used for protection from collisions with micrometeorites and space debris. A common design intended for two different scenarios is proposed:

- Scenario 1: ground-based aluminium additive manufacturing production, packaging in the launcher and transfer to orbit where the assembly phase takes place.

- Scenario 2: space-based polymer additive manufacturing production and assembly in situ.

Finally, the conclusions of this thesis work are presented, with reference to possible future developments concerning the same field of analysis of the experimental section and to the possible applications deriving from it.

## **1. In-space manufacturing**

### **1.1 Use of space**

Since the advent of spaceflight technologies, in the late 1950s, space launch services were at the initiative and exclusive use of national government programs that led to the well-known Space Race between the US and USSR [4]. Today, there is a keen interest in space, and there is talk of Billionaire Race Space and NewSpace which sees the entry into the space sector of private billionaires from other industries as well as several companies and startups. NewSpace means the movement or philosophy that includes the new aerospace companies that work independently from governments and traditional contractors in order to be able to develop access to space and related technologies more quickly and with lower costs, no longer driven by political motivations but for socio-economic purposes [5]. The commercial use of space can be defined as follows:

"Commercial use of space is the provision of goods or services of commercial value by using equipment sent into Earth orbit or outer space [4]."

This definition includes several activities, such as satellite navigation, satellite television and others. The drivers of these activities generally assign the ground-based production of satellites and their launch to public or private companies. Recently, several companies and research institutions around the world have proposed to review this production paradigm and replace it with a space-based one [1]. The next step in supporting a human presence in space is to increase current production and assembly capacity in space, integrating advanced additive manufacturing and autonomous robotic assembly technologies. Integrating these abilities, the architectures of space missions are free from the stagnant mass, volume and costs, imposed from the current production and assembly technologies of the space system.

### **1.2 In-space manufacturing. What is it?**

The term in-space manufacturing refers to the set of processes and techniques with which goods are produced outside the earth's atmosphere [6]. This "definition" implies the existence of conditions of microgravity and emptiness (pressure much less than atmospheric, approximately equal to 0). A definition of "manufacturing" is provided by Smokorohov [3]:

*"Manufacturing is considered to be an activity that involves at least one of the following three components: fabrication, assembly and integration:*

- ***Fabrication:*** *the process of producing basic spacecraft or spacecraft subsystem components through 3D printing or traditional industrial methods such as welding, cutting, bending, etc..*
- ***Assembly:*** *combining fabricated or prefabricated components into subsystems or entire spacecraft or direct complex 3D printing;*
- ***Integration:*** *Bringing together subsystems into one system and ensuring that the subsystems function together as such, including software; also includes potential processes associated with activities before or after upgrades, deliberate disintegration, and re-integration of subsystems into a spacecraft."*

The term in-space / in-orbit before the word manufacturing refers to the portion of space around the earth up to the GEO, in the long term even beyond, where the manufacturing activity would take place [3]. ISM in an umbrella term, many activities fall within the definition, those that consider the human presence for technological necessities have to

be considered near-term, while those that foresee the mining activity of the material for example from the lunar soil or from an asteroid have to be considered long-term [3]. In both cases, in-space manufacturing brings with it a series of social-economic considerations that have a substantial impact in terms of feasibility. In agreement with Skomorohov, from which the following image is extracted, there is a gap in the literature regarding the attention given to the technology and business topics related to in-space manufacturing; on the one hand, more considerable attention is given to technology, analyzing the benefits and limitations, on the other hand, attention is given to detailed analyzes of the business such as costs, market size.

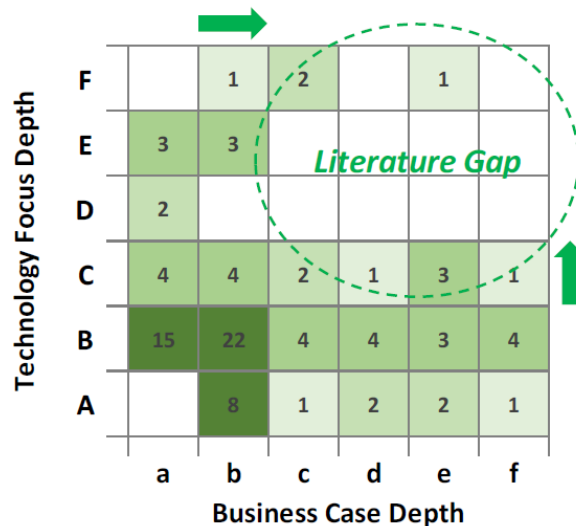


Figure 1: Use cases categorized by depth of technology and business focus [3];

Over the past 20 years, many companies have been born that are interested in investing in the space market and, through experimentation and RD, to help fill this gap. For example: Made in Space, Nanoracks, Tethers Unlimited, Bigelow Aerospace, Space Tango, Techshot, BioServe Space Technologies. Some of these companies' projects are presented later.

### 1.2.1 Challenges for in-space manufacturing

The space environment can be beneficial for the production of a wide variety of components but there are currently different limits and technological problems [1][7]. Economical space access: the largest costs to be faced are those needed to transport the feedstock material into orbit, once this initial cost barrier has been overcome, in-space manufacturing could become very attractive to new investors [1]. The goods produced in space must not merely be better than those produced in space but must be so that in-space manufacturing becomes a critical element in the business plan of a company. Furthermore, the transport to and from the space must be economically advantageous and reliable as well as access to the space production environment must be available as often as required by the customer and must guarantee the quality of the product from launch to recovery [6].

## Change in Launch Costs Over Time

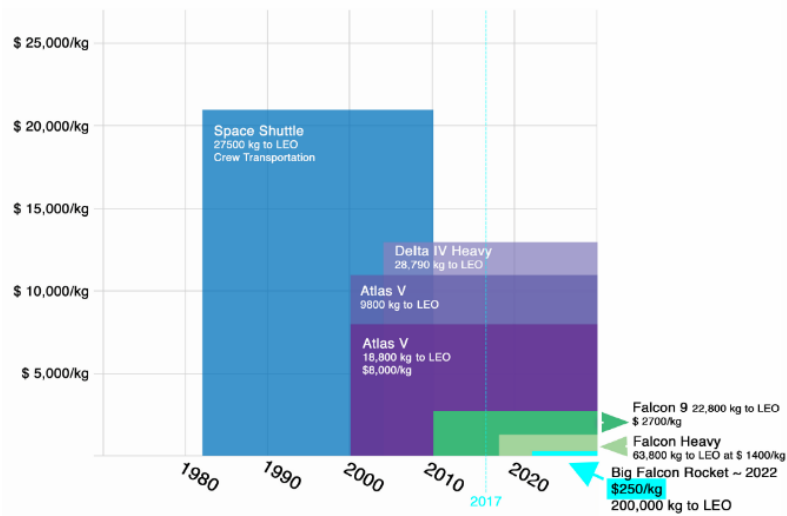


Figure 2: Change in launch cost over time [6];

*Technological Process [1][6]:* there are several limitations to the type of component that can be achieved in space. These are influenced by various factors such as the materials required for that component, the size, the time required to produce it, its configuration and the energy required to feed the process. Most critical spacecraft components are much larger than those demonstrated today in space. The AM process would take days to produce large items, and the printers would absorb much energy. The machines should also guarantee high precision required by the complex structural geometries of some instruments. Many technological processes are influenced by the extreme spatial environment: microgravity, atomic oxygen, radiation exposure. AM processes involving the use of powders cannot be applied because the dust would disperse.

### 1.2.2 Benefits of in-space manufacturing and assembly

The advantages that would derive from the adoption of in-space manufacturing are several and involve different activities, from commercial missions to earth sciences, passing through national security. Among the disciplines and activities that would benefit from ISM, the following are reported [1][6]:

- A. Space science as astronomy and astrophysics: thanks to the ISM it would be possible to produce telescopes too large to be built and assembled on earth and then transferred to orbit. Currently, the main limitations concern the maximum diameter that can be used in the missions and the current capacity to demonstrate the correct functioning of the instrumentation in microgravity conditions. ISM can provide the possibility to release objects and components, such as sensors, on-demand and only when requested, making them independent of the launch schedule.
- B. Science and disciplines on the ground: by producing satellites and spacecraft directly in orbit, it would be possible to significantly decrease the number of satellite launches of various kinds, for example, those for data collection and remote sensing (meteorology, climate, oceans, agriculture);
- C. Exploration: in particular for human-crewed missions, it would be possible to produce on-demand instruments and spare parts by only having the feedstock

material [8][9]; in this way, in addition to increasing safety, a reduction in costs deriving from the optimization of weights and volumes onboard the launch vector would be obtained [8]. It would be possible to produce and assemble entire spacecraft. An excellent example is the ISS, which is too large to be assembled and transported into a single launch. ISS solar panels would collapse under the force of gravity when assembled at once on earth. It is sufficient to think that it was built between 1998 and 2011, employing more than 160 EVAs for more than 1000 hours. Thanks to the ISM, EVAs could be definitively eliminated, reducing the risk of loss of life to zero. Furthermore, it would be possible to significantly increase the duration of space missions, currently limited by the growing likelihood of failure over time for components that could be repaired on-demand thanks to ISM. According to the National Academy of Sciences report, more than 28% of ISS failures concern polymer components and could be repaired on-demand [1].

- D. Commercial missions: in particular for telecommunication satellites placed in GEO, these could be assembled and improved in platforms set up and positioned in LEO and then transferred to GEO. Thanks to the ISM it would be possible to increase the size of the antenna and therefore increase the profit deriving from them, in fact the higher the diameter of the antenna the higher is the capacity of the same to receive and transmit signal [1]. There are two methods to increase the total area of the antenna: the first involves reaching the maximum geometric efficiency in occupying the internal volume of the launcher with antennas already produced and subsequently assembling them in orbit by means of robots, the second thanks to ISM plans to produce antennas larger in size than those currently existing directly in orbit.
- E. National security: for example for surveillance or recognition missions, intelligence and communication. Thanks to the ability to produce larger openings than those obtained today, the spatial resolution capacity would increase, which in the military case must be greater than in the civil case [1]. The potential benefits discussed for space sciences reflect those obtainable for national security. A further benefit lies in the ability to accommodate any changes in the signature to be detected; today it is necessary to launch another satellite that implements the required upgrades or new technologies.

The advantages of space manufacturing, concerning the activities listed above and others, can be classified as follows:

1. The ability to release satellites, spacecraft, hardware components and systems that cannot be subjected to launch constraints;
2. Increased flexibility of the activities of spacecraft allowed by any upgrades and/or repairs that can be carried out in orbit;
3. Reduced costs thanks to an intelligent use of the masses (the strengthening of the structures is no longer necessary). Further reduction of costs thanks to the lower number of ground tests once a certain technological maturity has been reached;
4. Ability to create structures and components that cannot be subjected to the earth's gravitational field;
5. The unique characteristics of the space environment allow the realization of industrial processes that cannot be performed on Earth;

6. The feedstock material can be more easily found and transported to orbit by other bodies/planets at a lower cost than that required in the terrestrial case (The economical movement of material in space is directly related to the  $\Delta V$ , or change in velocity, required to move from the mining sites to the manufacturing plants)
7. Potentially dangerous processes can be performed in space with minimal risks for the terrestrial environment and other planets

In general, each space craft needs to be strengthened to withstand loads of various kinds that are generated in the launch phase (accelerations, vibrations, acoustic loads) and this process imposes significant limitations in terms of mass and volumes and therefore costs; every space mission could benefit from in-space manufacturing [1]. Even more so considering the pre-launch tests that besides being expensive, occupy a good part of the launch schedule.

### **1.3 State of the art in-space manufacturing & assembly**

Historically the first in-space manufacturing application dates back to 1969 when the Vulcan welding unit was shipped into space aboard Soyuz 6. Several welding methods were tested in outer space [1][6]. In 1990, NASA researchers developed a computer-aided and FDM device. Today ISM includes a wide variety of potential techniques, including AM and other welding techniques and chemical processes. It is possible to subdivide the ISM according to the intended use of the products: ISM for space, ISM for land (e.g exotic optical fiber or silicon carbide).

#### **1.3.1 ISM for space**

Currently, there are still a few existing programs supporting the development of ISM techniques. In 2014, Made in Space in partnership with NASA launched a technological demonstrator at the ISS, the first 3D polymer printer for space [10]. It was possible to compare samples produced in space with those on earth, and the equivalence of the properties of the two products was demonstrated. Later, Made in Space launched the Additive Manufacturing Facility (AMF) at the ISS on March 2016.



Figure 3: Additive Manufacturing Facility (AMF) [10];

The AMF is a permanent facility on the ISS that can use different varieties of polymers, including ABS and polycarbonate, also ULTEM and PEEK. Once plugged into the Expedite

the Processing of Experiments for Space Station(EXPRESS) Rack Locker, the crew is only needed to remove finished parts and exchange consumables periodically. AMF is responsible for raising the TRL of space-based polymeric additive manufacturing to 9.

In 2015, Made In Space was selected to develop Archinaut, the Versatile In-Space Robotic Precision Manufacturing and Assembly System. Archinaut is a free-flying space manufacturing and assembly capability that enables advanced spacecraft and structures to be produced in the space environment [10]. Actually, State of the Art of ISM is defined by the EVA performed by astronauts to build ISS [1]. These EVA are cost and mass prohibitive, as well as risky. Archinaut, which should be launched with the Archinaut One in late 2020, advances state of the art with the tool necessary to cut the avoidable and unnecessary risk to human life via the development of the robotic mechanism which enables Archinaut manufacturing and assembly paradigm.

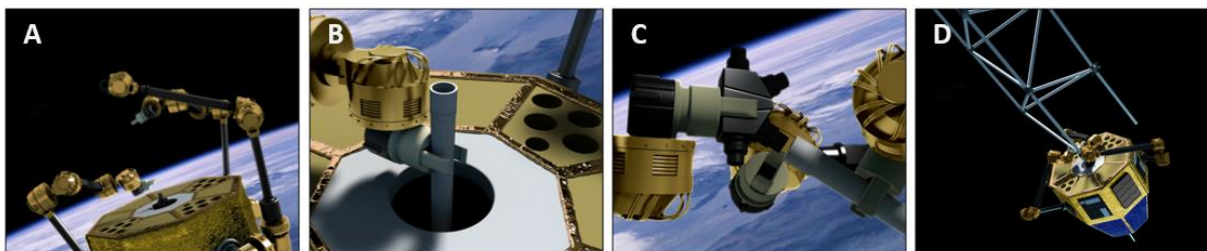


Figure 4: (A) Archinaut manufactures nodes and (B) struts, (C) Archinaut's robotic manipulators, (D) Archinaut autonomous assembles structural element [10];

Archinaut enables new mass efficiency optimizations over current manufacturing and assembly processes. Structures additively manufactured on-orbit do not need ruggedization for launch loads, assemblies allowing for deployment, nor face the constraints of launch fairing geometry. Optimization in this manner is nominal: Archinaut's additive manufacturing process constructs the target structure layer by layer and requires no support material in microgravity.

There are many other projects about ISM. Ames Research Center, and Marshall Space Flight Center, in collaboration with JPL are developing capabilities to produce electronic or photonic components in space [1]. Researchers at the Johnson Space Center and MSFC have worked on a process to repair damaged components in space from debris and micrometeorites. Tethers Unlimited, through a NASA contract, worked on the SpiderFab project for the production of large structures, in particular solar panels and antennas, using compact materials. Other concepts include the MIT fabrication laboratory which is characterised by several ISM tools.

ESA has also investigated the ISM, for example with the Additive Manufacturing Aiming Towards Zero Waste and Efficient Production of High-Tech Metal Component (AMAZE) [8]. The Portable on-Orbit Printer 3D (P3DP) is the first European Additive Manufacturing experiment in space. The printer implements the FDM technique to produce components in PLA, a thermoplastic polymer. The role of the astronauts is limited to the activation of the Built-In Test and to the following activation of the 3D printing process. The goal is to validate 3D printing technology in microgravity and prove that FDM fabrication with a

representative type of polymeric material is not significantly affected by the presence/absence of gravity acceleration field. The experiment nominally consists of performing FDM printing of a single object in the ISS microgravity environment. The full payload is thereafter brought to ground, where the built object is examined and compared to the object printed on the ground in order to investigate the differences concerning the most significant aspects of the manufacturing quality.

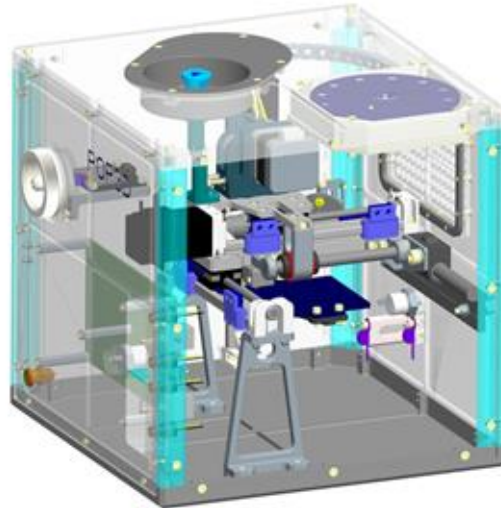


Figure 5: P3DP Overall Architecture [11];

### **1.3.2 The case of in-space repair**

When a satellite or spacecraft is damaged in space, it is not easy to find a way to repair it. Furthermore, in the event of failure of attitude control systems, the satellite becomes potentially dangerous. This is because the satellite could become space debris, posing a danger to satellites and stations that are still operational. It is therefore evident the importance assumed by the ability to be able to repair a spacecraft, or at least be able to remove its debris. As already mentioned, several companies and startups are working to find, one day, a solution to these problems. Some of these have proposed to build spacecraft that orbits in space and function as rendez-vous for failed spacecraft, others have proposed dragging damaged satellites to earth to destroy them with re-entry into the atmosphere. Still, others suggest this solution: generate, in space, via AM and on-demand the spare parts necessary to guarantee the correct functioning of the satellite/spacecraft and assembly on-demand [1][8]. Actually, state of the art for in-space repair consist in Orbital Replacement Unit (ORU) which is a key element of the International Space Station which can be easily and quickly replaced when units pass its design life or fail [12]. None of these parts are intended to be installed inside pressurized modules. Some of these parts are pumps, storage tanks, controller, antennas, battery units. These influence the control of the cooling system, the movement and control of the solar array as well as the flow of energy through the station from the solar array to the heat rejection system as part of the external active thermal control system (EATCS). In addition to oxygen storage tanks as part of the station's environmental support and life support system (ECLSS). The ORUs can be, virtually any element that can be easily removed and replaced

when required. The replaceable modular nature of the station, in theory, makes it possible to extend its duration far beyond its initial design life. As previously said, the capability to produce on-demand instruments and spare parts by only having the feedstock material, replacing the current repair paradigm could represent a great game-changers for future space mission.

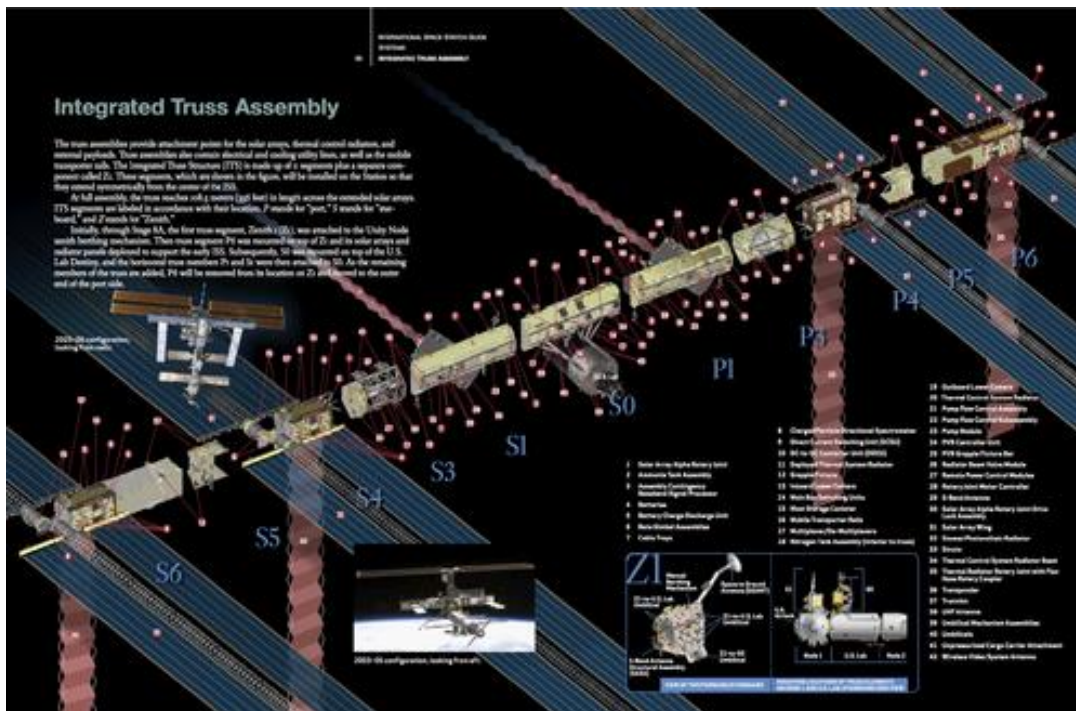


Figure 6: ISS Integrated Truss Structure detailing all ORU in situ [12];

### 1.4 A long-term vision

In 1928, the Austrian engineer Hermann Potočnik Noordung published the book "The problem of navigation in space" in which he showed the Wonhrad (inhabited wheel), which can be considered the first concept of space station [13]. The Wonhrad, consisting of three modules, would have been put in continuous rotation to produce an artificial gravity force, would have been equipped with a power plant powered by solar energy through a parabolic panel and would also have had an astronomical observatory. The three modules, connected to each other by a complex cable system, would have been placed in geosynchronous orbit at an altitude of 36000 km from the earth and with a total diameter of 30 meters, would have made a complete revolution every 8 seconds.

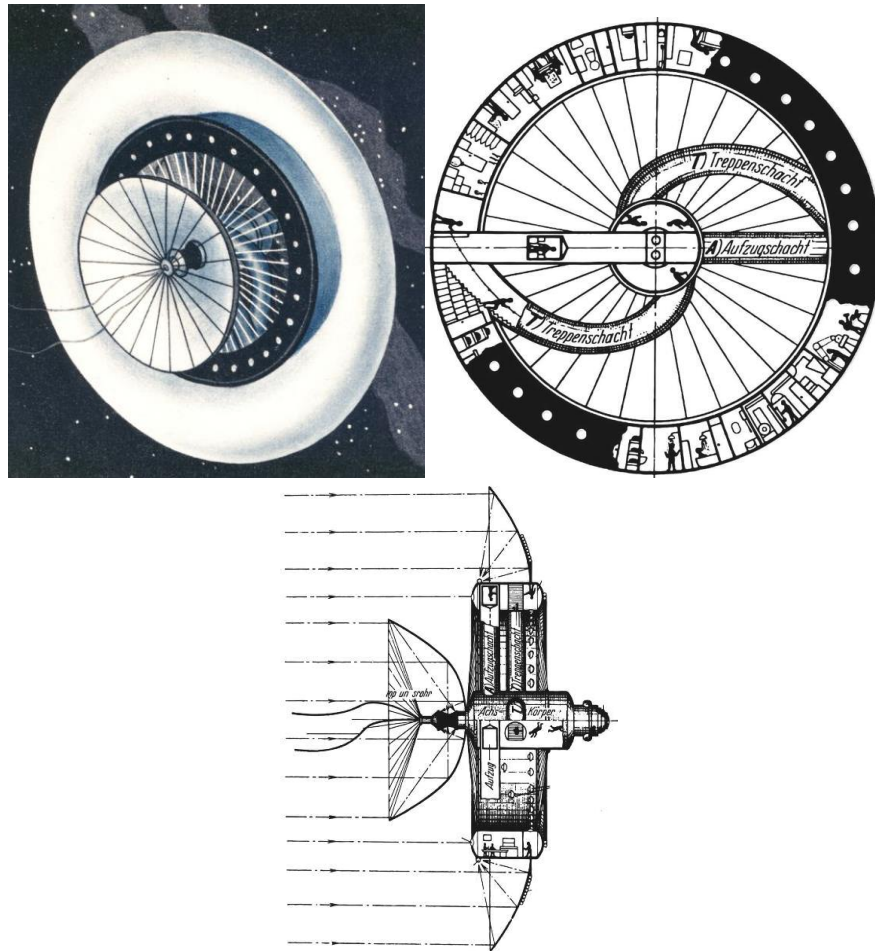


Figure 7: Woonhrad Station, Norduung (1928) [13];

In the coming years many people tried their hand at producing more or less utopian works of innovative spatial architecture, from the Flying City (1928) by Georgii Krutikov to La toroidal station (1957) by Werner von Braun, until in 1963 the same von Braun and writer Willy Ley, consultant for the Air Force and NASA, designed a wheel 75 meters in diameter.

At the end of the 20th century the International Space Station (ISS) assembly was launched, a project born from the collaboration of space agencies from five countries - USA, Europe, Japan, Russia and Canada - and conceived as an orbiting laboratory dedicated to scientific research in low earth orbit (LEO) at 400 Km altitude and continuously inhabited by astronauts since 2000. In any case, several agencies and associations have continued, even in recent years, in the production of futuristic space station concepts. Among the many, we want to present below the Orbitecture project, produced by the Center for Near Space (CNS) and futuristic both for the suggested solutions and for the systemic vision proposed from the point of view of architectural design [13]. Starting from the assumptions of Autonomy, Permanence, Experimentation, Exploration with Orbitecture, a new concept of orbital infrastructure was created, consisting of: resort, terminal, laboratory, hangar. The central unit is the hangar and the creation, management and maintenance of the infrastructure with innovative technologies and processes as well as for the production of electricity and thermal conditioning starting from solar energy is conceived. The concept of Orbitecture is based

on the goal of allocating the station not only to highly qualified and trained personnel - such as the astronauts to date on the ISS - but also for ordinary people. In fact it could host around 100 people divided as follows: 1/3 station operators, 1/3 tourists, 1/3 astronauts and researchers. To reduce the costs of transfer to orbit and weight, Orbitecture would be produced and assembled in situ through inflatable structure technologies and lean manufacturing additive manufacturing processes [13]. For the sustenance of the personnel the structure will be equipped with a green area of 6000 m<sup>2</sup>. Seen from outside the station has a planetomorphic aspect: a central sphere (Miranda) with a diameter of 44 meters crossed by a cylinder with a diameter of 20 meters where the hangar and the laboratory are placed in microgravity, 2 overlapping toroids (Aristarchus) placed at 38 meters from the axis and with lunar gravity and finally at 83 meters another toroid (Galilaei) where gravity would be that of Mars.

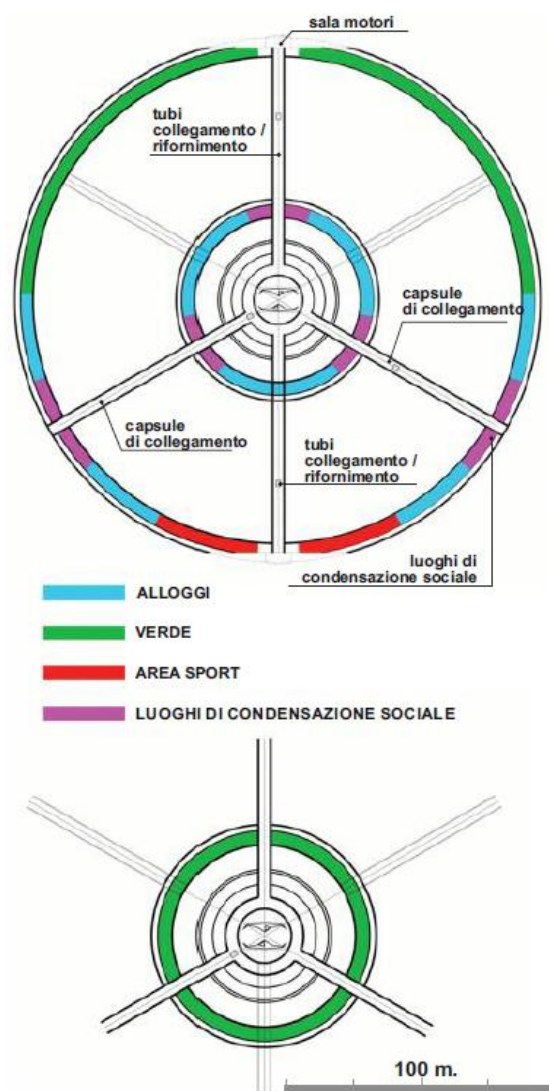


Figure 8: Functional layout of Orbitecture [13];

## 2. Additive Manufacturing

The 3D printing technique, now known as additive manufacturing, is an industrial production process that consists of the realization of three-dimensional objects through the addition of material (typically layer-by-layer) controlled by a computer according to a precise digital model [14].

The 3D printing was born in the first half of the 80s when Chuck Hull, founder of the still existing 3DSystems, realized the first commercial example of rapid prototyping through a process known as Stereolithography for which he obtained the patent in 1986; he was also responsible for the invention of the STL format [15]. In the coming years many people studied the ideas of Chuck Hull and similar techniques were developed but each characterized by an important modification: the Selective Laser Sintering (SLS) in which dust is used instead of resin and Fused Deposition Modeling (FDM ) that is printing with molten material and actually the only technic applicable in orbit.

Today additive manufacturing, defined as disruptive technology, is considered one of the most promising technologies for multiple applications, using metallic, ceramic, plastic or a combination of them [14]. The rapid development of AM is related to the advantages that this technology offers, including high dimensional accuracy, freedom of design, reduction of waste, ability to reproduce structures of complex geometry and variable dimensions, rapid prototyping. The success of the AM is also demonstrated by the number of scientific publications released in the last decade:

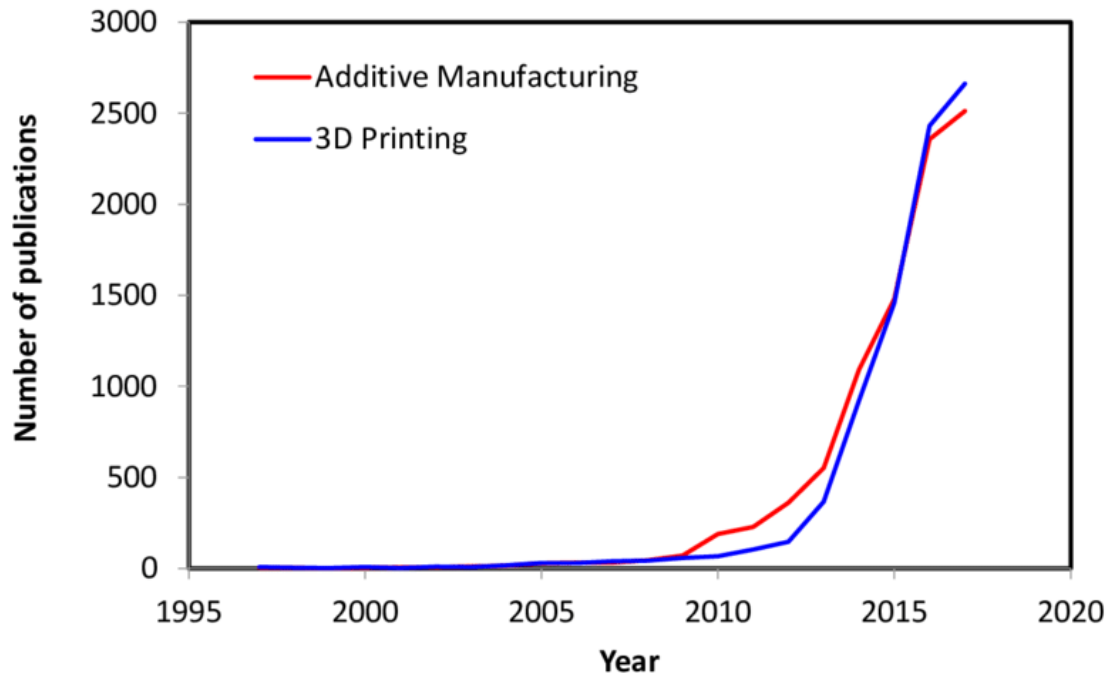


Figure 9: AM publications per year [16];

However, there remain some problems connected with the lower mechanical properties and the anisotropic behaviour of the moulded elements, furthermore for mass production it will be necessary further improvements in the production speed and a decrease in the

costs. [14] This goal could also be achieved through continuous improvements in machine design. In industry, AM was adopted mainly for prototyping in the early stages of the product development process. Lately, some companies have started using metal-based AM for more regular production, but on a small-scale. The space sector, which requires production in small series of components with high performance and sophisticated shape, could particularly benefit from the adoption of AM, in particular as said that practised in space.

### 2.1 Classification AM Process

Metal AM production processes can be classified according to the nature of the raw material, the mechanism used to join the layers of material and the method used to feed the machines [17]. In metals AM, the raw material can be in the form of dust or more rarely of a wire. The supply of energy completely melts it by a laser or an electron beam. Recently, the main techniques of AM, according to ASTM International, can be classified as follows [17]:

Table 1: Classification of AM processes [17];

Categories	Technologies	Material	Power Source	Strengths/Dow nsides
Metal Extrusion	Fused Deposition Modeling (FDM)	Thermoplastics Ceramic slurries, Metal pastes	Thermal Energy	-Inexpensive extrusion machine; -multi-material printing -Limited part resolution -Poor surface finish
	Contour Crafting			
Powder Bed Fusion	Selective Laser Sintering (SLS)	Polyamides/Pol ymer	High-powered laser beam	-High accuracy and details -Fully dense parts -High specific strenght & stiffness -Powder handling & recycling -Support and anchor structure
	Direct Metal Laser Sintering (DMLS)	Atomized metal powder stainless steel, cobalt chromium, titanium Ti6Al-4V, ceramic powder		
	Selective Laser Melting (SLM)		Electron Beam	
	Electron Beam Melting (EBM)			
Vat Photopolymerization	Stereolithography (SLA)	Photopolymer,	Ultraviolet laser	-High building speed

		ceramics, (alumina, zirconia, PZT)		-Good part resolution -Overcuring, scanned line shape -high cost for supplies & materials
Material Jetting	Polyjet/Inkjet Printing	Photopolymer, Wax	Thermal Energy/Photocuring	Multi-material printing -High surface finish -Low-strength material
Binder Jetting	Indirect Inkjet Printing (Binder 3DP)	Polymer powder (plaster, resin), ceramic powder, Metal powder	Thermal Energy	-Full-color object printing -Require infiltration during post process -Wide material selection -High porosities on finished parts
Sheet Lamination	Laminated Object Manufacturing (LOM)	Plastic film, Metallic sheet, ceramic tape	Laser Beam	-High surface finish -Low material, machine, process cost -Decubing issues
Direct Energy Deposition	Laser Engineered Net Shaping (LENS) Electron Beam Welding (EBW)	Molten metal powder	Laser beam	-Repair of damaged parts -Functionally graded material printing -Require post-processing machine

The technologies present in this classification are limited to plastic, metal and ceramic polymers. Other printable materials such as fibers, sand, glass, wood and bio-materials have not been contemplated. Furthermore, it is emphasized that this classification is valid for the technologies used on the ground, it is recalled for example that the technologies that use powders are not practicable in space. For the sake of completeness, the main

ground-based techniques for products intended for space use are presented in the following paragraph.

## 2.2 AM: state of the art

### Electron Beam Freeform Fabrication (EBF3):

Developed at the NASA Langley Research Center, this technique is designed to produce aerospace structures in aluminium or titanium alloy [18]. The metal wire of raw material is inserted into a molten pool generated by an electron beam in a vacuum environment. This technique manages to achieve approximately 100% efficiency. This technique offers practical solutions to deposit rate problems, process efficiency and material compatibility.

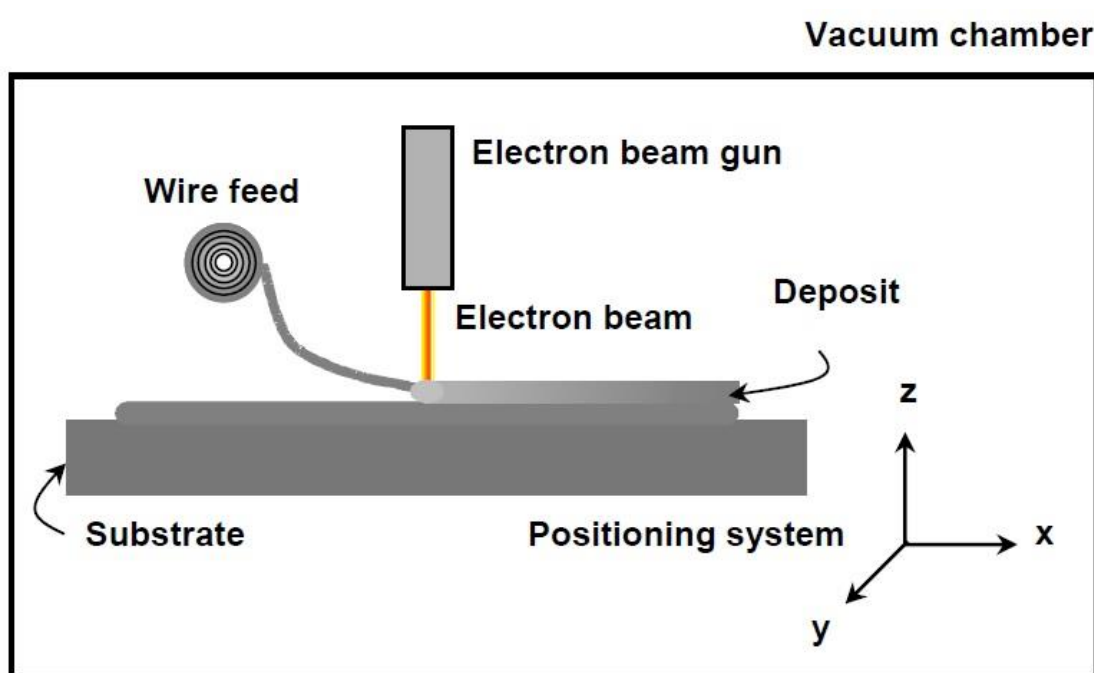


Figure 10: Electron Beam Free Fabrication Process [18];

**Wire plus Arc Additive Manufacturing (WAAM):** This technique is born from the combination of an electric arc as a heat source and wire as feedstock material [19]. The standard equipment includes welding power source, torches and wire feeding system. As for MIG, the wire is the consumable electrode. Adopting Fronius cold metal transfer (CMT), which is a modified variant of MIG, should provide parts with excellent quality, low heat transfer and almost no spatter. While meeting these expectations at the time of depositing materials such as aluminium and steel, unfortunately, with titanium, this process is influenced by the wandering of the arc, which results in greater surface roughness [19]. Consequently, tungsten inert gas, or plasma arc welding, is currently used for titanium deposition. These processes, however, rely on the external power supply of the wire; for consistency of deposition, the wire must always be fed from the same direction, which requires the rotation of the torch, thus complicating the robot programming. An electric arc as a heat source and from the wire as raw material.

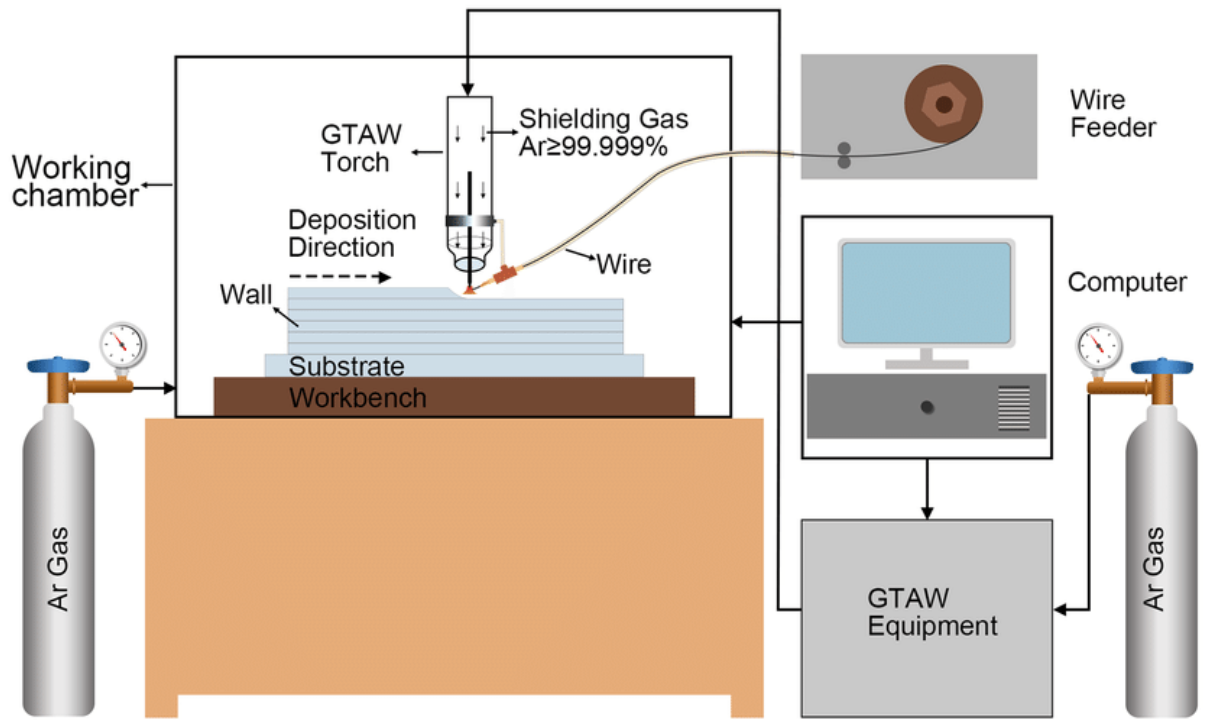


Figure 11: WAAM Equipment [19];

### 3. Optimization: introduction

“A structure is any set of material whose purpose is to support the loads”. Therefore, structural optimization can be defined as the discipline that studies how to make an assemblage of materials sustain loads in the best way possible [20]. The main objective is to make the structure lighter than the original but another goal may be to make the structure as rigid as possible. Such maximizations or minimizations cannot be performed without constraints. The quantities constrained in optimization problems are often displacement, stresses and geometric dimensions.

#### 3.1 The problem of optimization

By optimization problem, we mean the search for minimum or maximum points of a given objective function [21][22]. Added to this is the presence of constraints that must be respected in the search for this stationary point. Generally we can express what has been said in formulas with the following notation [20][21][22]:

$$\begin{cases} \min F(x) & s. t. \\ g_j(x) \leq 0 & j = 1, \dots, m \\ h_k(x) = & k = 1, \dots, l \\ x_i^L \leq x_i \leq x_i^U & i = 1, \dots, n \end{cases}$$

Where:

1. Independent variables  $x \in R^N$
2. Objective function  $F(x)$
3. Constraints of inequality  $g_j(x)$
4. Equality constraints  $h_k(x)$
5. Constraints on upper independent variables  $x_i^U$  and lower  $x_i^L$

In particular, these take on the following meaning [21][23]:

1. The independent variables, or optimization variables, are the parameters that we intend to change within a specifically defined interval in order to obtain the change of the objective function. Their choice is strongly influenced by the type of application the problem has and by the method of solving it. The variables can be discrete or continuous: in the first case they are forced to move from one precise value to another, so they are not free to take values at will. In the second case, on the other hand, the parameters can take any value within the definition interval. This last type is the preferred one since it is much simpler to solve.
2. The objective function represents the criterion for evaluating the validity of the design solution. In fact it is based on the value it assumes to find the optimal condition. This is usually a linear equation and not in the independent variables of point one, it can be either explicit or implicit. Problems may exist with more objective functions to be minimized substantial and therefore we speak of multi-objective optimization; clearly this type of problem is much more complex to solve.

3. Equality constraints very frequently represent the satisfaction of some equilibrium condition, they are often difficult to analyze mathematically because they require to be always active. They are usually linear equations and not in independent variables, both explicit and implicit.
4. The inequality constraints are much more common than those related to point three and divide the space of the solutions into two macro-areas: that of the feasible solutions and that of the ineligible solutions. If the result of the optimization lies in the first space then the solution can be accepted and the constraint is called inactive, viceversa the solution cannot be valid and the constraint is violated. Usually the imposition of constraints of this type is of considerable importance in the definition of the minimization problem and it is reasonable to think that the solution will result to be straddling the two described areas in which it is said that the constraint is active. They are usually linear equations and not in independent variables, both explicit and implicit.
5. The constraints on the optimization variables are also called side constraints: they are treated differently from those of the previous points and define the domain of existence of the solution.

In the engineering field, the calculation codes that solve a problem like the one just described make use of iterative procedures that can be summarized in the following points [22]:

- A. Analysis of the physical problem through the finite element method
- B. Sensitivity analysis, consists in the calculation of the partial derivative of the responses of the system with respect to the project variables
- C. Updating the project variables based on the information obtained from the sensitivity analysis
- D. Convergence test of the result

### **3.2 Structural Optimization**

Entering into the merits of the optimization methodologies developed to date, there are actually three types, the Topological, the Form and the Dimensional [21][22].

- **Topology Optimization:** consists in the definition of an optimized structure, starting from the maximum encumbrance that the latter could potentially have, called the existence domain. This operation is carried out through an iterative process in which the excess material is eliminated until it undergoes particular constraint conditions. Some of these can be, in the structural field, volume, stiffness, natural frequency, maximum admissible tension and others.
- **Shape Optimization:** the goal is to determine the best form of the outline of the project domain. The process is iterative like the previous one in which the variables are the geometric parameters of the surface, these are made to vary in order to verify which is their best combination in order to satisfy the objectives and be subject to the constraints. During this process it is obvious that the topology cannot be modified, in fact it is not possible to create holes or other structural elements but only partially vary the geometry. It can, therefore, be deduced that

this type of optimization is sequential to the topological one and the inverse procedure is not possible.

- **Dimensional Optimization:** The third and last typology, namely the dimensional one, consists in keeping the component geometry completely fixed and making only some significant parameters vary, for example the thickness of a plate. This ensures that this type of optimization is the simplest and can also be performed in a completely analytical way.

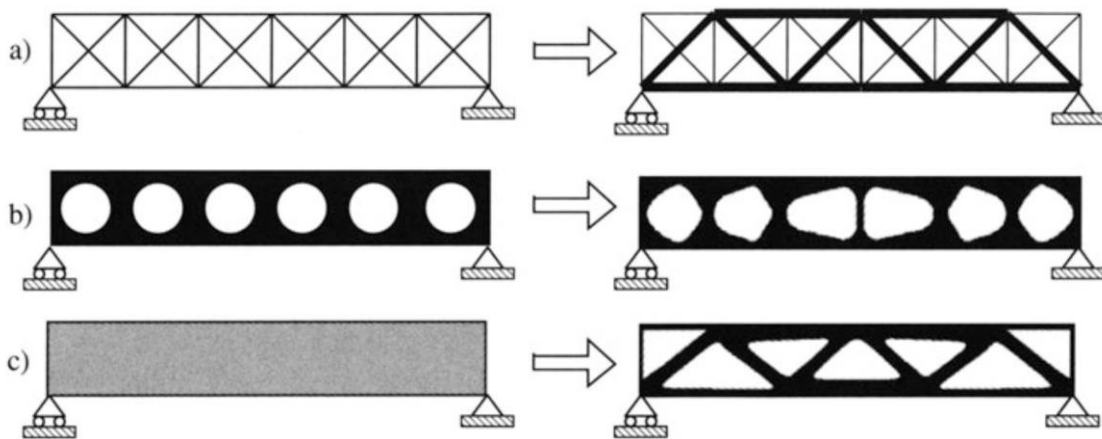


Figure 12: The three types of Structural Optimization [22];

In turn, the three types of optimization can be grouped into two groups:

- *Concept level design:* here we find the topological optimization, it is used in the very early stages of the design process for the best proposal from which to start for product development [22].
- *Fine-tuning design:* here the dimensional and shape optimization are included, which allow variations of the geometry, in order to satisfy the criteria, without modifying the overall topology of the structure [22].

The problem up to now, in the use of this exceptional instrument, is that, although it can achieve a perfectly optimized structure, there are considerable limitations in being able to produce it physically. The commonly used industrial processes do not allow much freedom of design, indeed very often they significantly constrain the latter profoundly affecting the shape that a component must have in order to be realized.

However, combining this exceptional tool together with a technology capable of generating very complex structures in a short time, we obtain a rapid and efficient tool that can be exploited even in fields other than engineering.

### 3.2.1 Topology Optimization

Typically this type of optimization provides for the maximization of rigidity, hence the minimization of the compliance of the structure [21][22]. The solution to this problem would be to distribute the material continuously throughout the project domain, but it is necessary to introduce a constraint on the total amount of material. A similar formulation is of great interest in the engineering field because it allows reducing the weight of the

structure (hence the cost), preserving its qualities in terms of stiffness. In oratory, the designer wants to determine which full and empty ones must occupy points of the domain.

The figure below shows a body in a domain  $\Omega$  (design space) defined in  $R^2$  o  $R^3$ .  $\Gamma_t$  is the edge on which the surface forces act  $t$  while  $\Gamma_u$  is the border on which the U displacements are assigned. Finally,  $f$  are the forces of volume. In the domain  $\Omega$ , there may be regions defined as non-design spaces.

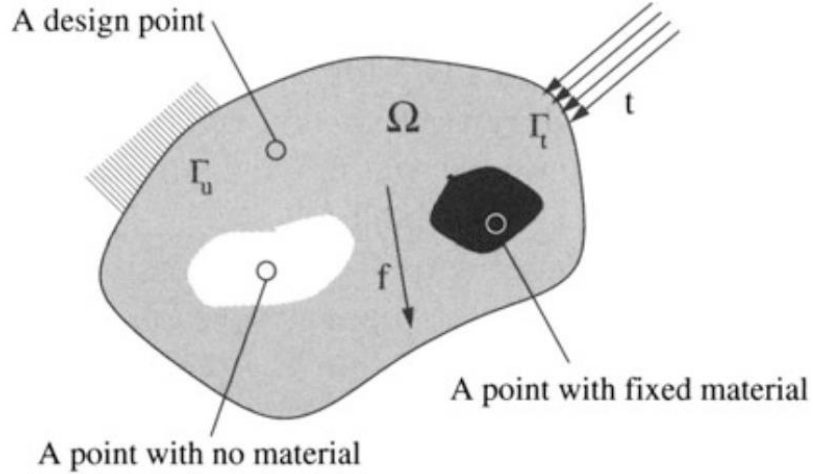


Figure 13: Domain for Optimization [22];

So we want to evaluate, throughout the domain  $\Omega$ , the best distribution of a fictitious material density  $\rho$  normalized to the nominal density  $\rho_0$  of the material taken into consideration, which can, therefore, take values between 0 and 1 (which correspond to 0% - empty - and 100% - full of  $\rho_0$ ) [21][22].

Through the principle of virtual works, we can express the problem of minimizing compliance with the following mathematical formulation :

$$\underbrace{\min}_{\rho} C(\rho) = U^T f = U^T K U$$

$$con \begin{cases} KU = f \\ V(\rho) = V_0 \\ 0 \leq \rho_e \leq 1 \end{cases}$$

K is the stiffness matrix, U and f are the displacement vector and that of external loads. rho is the vector of the material densities, ie the design variables.  $V(\rho) = V_0$  represents the limit on the quantity of material.  $V_0$  is the volume of  $\Omega$ .  $V(\rho)$  is calculated as [20][21]:

$$V(\rho) = \sum_{e=1}^N \rho_e v_e$$

With N number of elements that discretize the domain,  $v_e$  is the volume of the generic element. In literature, the most used approach to solve the problem is Isotropic Solid or

Empty Elements (ISEE) [20][22]. It provides that after the optimization process, the assigned material density can assume a discrete binary value (0-1) in which the zero corresponds to the void and the unit to the full. The same applies to the elementary elastic tensor  $E_{ijkl}$ , necessary to calculate the stiffness matrix  $K$ , which takes zero value if the density is zero and the value  $E_{ijkl}^0$  if the density value assigned is 1. The problem is that for large models the calculation times would become very long, so the problem is relaxed by allowing the material density to assume values between 0 and 1. Thus, considering that the FEM method requires that the density is constant, element for element, the number of variables is reduced to the number of elements that discretize the model. It should be noted that the solutions to the problem that include values of intermediate density, therefore attributable to fictitious materials, are devoid of physical meaning. Penalisation techniques are then introduced that force the final design to be represented only by elements with a density close to 0 or 1. The most commonly used penalty scheme is the SIMP (Solid Isotropic Material with Penalization) [20][21]. This involves describing the elastic tensor through a power law as a function of the assigned density:

$$E_{ijkl} = \rho_e^p E_{ijkl}^0$$

The penalty coefficient  $p$  must be chosen greater than 1 so that the intermediate densities are disadvantaged, this means physically that the stiffness obtained is small compared to the volume of material [20][21]. Then the global stiffness matrix is rewritten as:

$$K = \sum_{e=1}^N \rho_e^p K_e^0$$

By replacing within the compliance minimization problem, we obtain the expression of the compliance of the written system according to the project variables  $p$ :

$$C(\rho) = \sum_{e=1}^N \rho_e^p U_e^T K_e^0 U_e$$

Where  $U$  is the vector of the nodal displacements of the generic element.

The topological optimization problem is solved numerically by iterative procedures. At each step, the material densities associated with each finite element are updated using different approaches based on the result of the sensitivity analysis [20][21]. This involves the calculation of the partial derivative of the system responses with respect to the second project variables:

$$\frac{\partial C}{\partial \rho_e} = -U^T \frac{\partial K}{\partial \rho_e} U = -p \rho_e^{p-1} U_e^T K_e^0 U_e$$

From which it can be observed that an increase in density leads to a reduction in compliance or an increase in stiffness.

As already mentioned, in order to form topologies, it is necessary to introduce the penalty scheme. However, the solution still contains elements with an intermediate density value.

Then we use the iso-density curves. In essence, a cut-off value is defined and all those elements whose density is lower than the threshold value are discarded from the solution [20][21]. Typically choose a value such that the topology is fully connected. The remaining elements are promoted to unit density and thus the final topology is obtained which can be used as a starting point for the design of the structure.

## **4. Case Study**

The main target of this thesis is to explore the use of structural optimization *Altair Inspire* codes in the design process, in particular, for this project it is re-design, taking as a case study the aluminium structure of a subsystem for collision protection from micrometeorites and space debris. The focus of the work was to optimise the existing thin-wall structure, initially produced by conventional subtractive production technologies, developing a “organics” structure design feasible only by additive manufacturing production technologies.

Two different hypotheses have been evaluated and considered as most likely scenarios in the frame of International Space Station projects or, better, in the frame of next-generation deep space mission exploration actually under evaluation by TAS-I:

- production/assembly on the ground and transfer to orbit.
- (ii) production/assembly in-orbit and in-situ installation.

The first allows faster and more efficient product design, reducing material consumption, costs and production times. The second scenario combines these advantages to the benefits discussed in the second chapter.

First, the CAD model of the secondary structure being studied is shown. Next, the load and constraint conditions and the theory with which they were derived are shown. The focus of this chapter concerns the description of the procedure adopted to obtain the final component and the presentation of the results to demonstrate the advantages gained in terms of material and weight savings. This process is of an iterative type and in some case, become quite time-consuming. Therefore, it requires accurate knowledge of the model, of its physical-mechanical characteristics, of the loading and constraint conditions and of the structural context in which it will operate, especially mechanical interfaces and boundary condition are considered critical points for the optimization process. The software used is solidThinking Inspire and the laptop used has the following features:

- Processor Intel® Core i7-8750H;
- Ram: 16 Gb;
- Video Card: NVIDIA GeForce GTX 1050 Ti;

### **4.1 Altair solidThinking Inspire**

Altair is an American software house, founded in Michigan in 1985, operating in the CAE sector [25]. solidThinking Inspire is a powerful tool dedicated to design engineers, product designers to create and analyse efficient structural concepts quickly and easily. Traditionally, structural simulations allow engineers to verify that the designed structure resists loads. Inspire improves this process, allowing to increase the mechanical performance of the structure by generating a new layout of the material using only the loading conditions and constraint as an input. The software integrates a CAD tool allowing a correct design phase the first time, reducing costs, product development time, material consumption and product weight. The software integrates the following tools:

- CAD modeller: it allows to create and modify 2D and 3D geometries;

- Pre-processor: enables simulation inputs to be defined and a finite element numerical model to be created extremely quickly;
- Solver: it allows the resolution of linear and non-linear elastic static analyses, normal and buckling modes as well as topological and dimensional optimisations;
- Post-processor: enables the display of results;

Although this software aims to be used as a concept design tool, in this thesis, it is used to allow a rapid redesign of existing structures to exploit the maximum potential of the ISM.

#### **4.2 Geometry and materials**

The study case treated in this thesis is a part of an innovative Micro-meteor & Debris Protection assembly actually under development in the frame of R&D Thales Alenia Space.

In particular the study case analysed in the following chapter is represented by a petal devoted to protect a circular window and it is shown below:

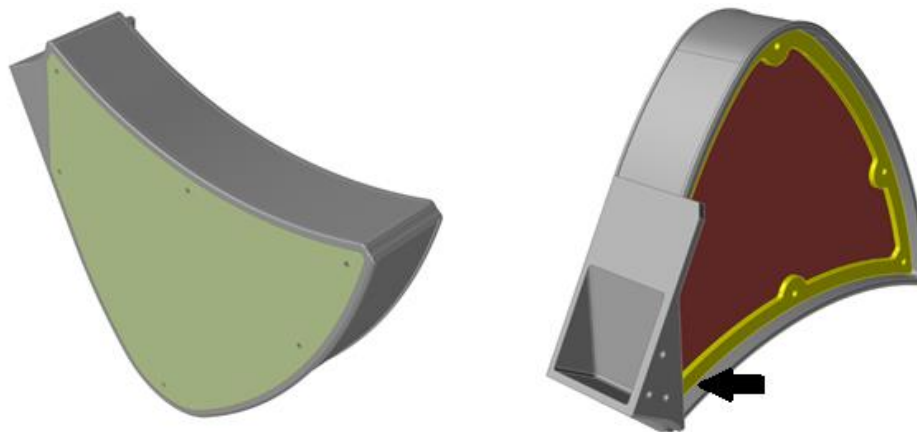


*Figure 14: View 1 (left) and view 2 (right) of the model;*

The proposed design is mainly composed of the following elements:

- BODY (in grey in figure 14);
- FRAME (yellow, figure 6 view 2);
- Primary Bumper (green, view 1);
- Secondary Bumper (brown, view 2);

As for their function, that of the BODY is to contain the two layers together, that of the FRAME is to hold the Secondary Bumper together with BODY. The model has several holes, of which the three indicated by the arrow in Figure 14 are those through which the subsystem is bound to the rest of the structure (not available for the analysis). The remaining holes are used to fix the layers to the main. However, none of these holes can be modified/deleted so parts will be created, defined as NDS, to safeguard the holes themselves.

The material of all the components is a 6000 series aluminium alloy (Anticorodal), except Secondary Bumper which is Kevlar. The mechanical characteristics, already present in the Inspire library, are the following:

Table 2: Mechanical properties of Aluminium;

<b>Material</b>	<b><math>E</math> [MPa]</b>	<b><math>\nu</math></b>	<b>Densità</b> <b><math>\left[\frac{kg}{mm^3}\right]</math></b>	<b>Carico di snervamento</b> <b>[MPa]</b>	<b>Coefficiente di espansione termica</b>
Alluminio (6061-T6)	$75 \cdot 10^3$	0.33	$2.7 \cdot 10^{-6}$	241.3	$23.5 \cdot 10^{-6}/K$

Table 3: Mechanical properties of Kevlar;

<b>Material</b>	<b><math>E</math> [MPa]</b>	<b><math>\nu</math></b>	<b>Densità</b> <b><math>\left[\frac{kg}{mm^3}\right]</math></b>	<b>Carico di snervamento</b> <b>MPa</b>	<b>Coefficiente di espansione termica</b>
Kevlar	$62 \cdot 10^3$	0.29	$1.4 \cdot 10^{-6}$	59	$2.3 \cdot 10^{-6}/K$

Table 4: Original model weights;

	<b>Material</b>	<b>Peso [g]</b>
<b>BODY</b>	Aluminium	969.74
<b>Secondary Bumper</b>	Kevlar	42.169
<b>Primary Bumper</b>	Aluminium	101.66
<b>FRAME</b>	Aluminium	98.208
<b>Overall</b>		1250.9

#### 4.3 Load and constraints conditions: Mass Acceleration Curve

For the structure object of this thesis, considering the launch phase, loads of different nature must be considered (acceleration, acoustic, vibration). An easy and quick way to do this is to use MACs [24]. JPL has successfully used the theory on which the Mass Acceleration Curve is based for several years in the preliminary structural sizing of several spacecraft [24]. The acceleration to which a physical mass is subjected, the spacecraft, is limited by a curve, the MAC. In particular, the smaller the mass of the component and the higher the acceleration it perceives. The MAC is a semi-empirical tool. Two curves are distinguished, as reported in the JPL document:

1. “a curve corresponding to the physical masses of the Spacecraft, this is called the Physical Mass Acceleration Curve (MAC). This curve is chronologically the oldest .”
2. The second curve, the most recent, is that which refers to the acceleration of the effective mass of each mode of the spacecraft, the Modal Mass Acceleration

Curve. The MMAC is used as a forcing applied to the model of the spacecraft or the model of the subsystem if available.

The second one is more precise because it allows tracing the envelope of the Forcing Function that can be used to estimate the loads acting on each component of the payload. However, according to TAS-I, in this thesis the simplest but still effective physical curve was used; this makes the problem more conservative [24]. The procedure to use the MAC is clear and straightforward but can be used only if essential hypotheses are respected:

- The subsystem must consist of a single concentrated mass;
- The mass must be less than 500 kg;
- The structure of the subsystem must be in "appendage like" configuration with a static attack on the rest of the spacecraft or the remaining structure.

So, this curve can be used for the preliminary design of subsystems for:

- Determine the preliminary acceleration of the concentrated mass
- Then determine the loads acting on the support of the subsystem structure

For any other condition, a finite element model is required, or the MDMAC approach must be used. The following images show the Mass Acceleration Curves for physical masses of spacecraft subsystems for STS / IUS and Titan 4 / IUS.

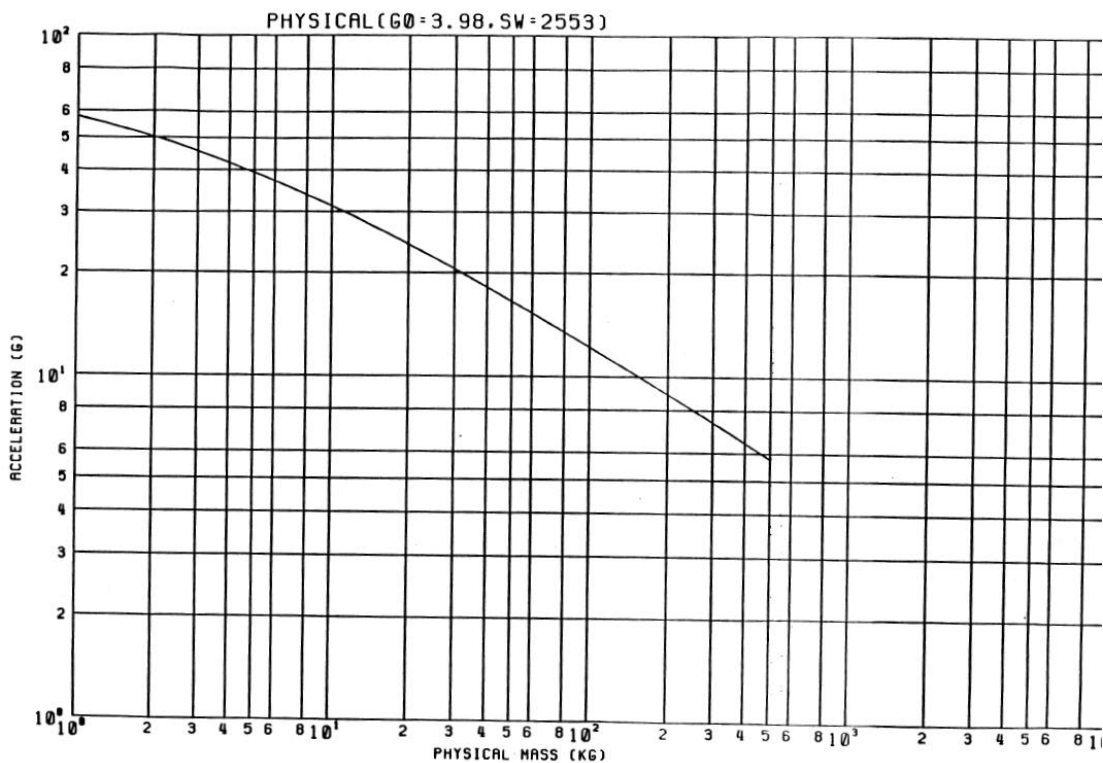


Figure 15: Physical Mass Acceleration Curve for STS/IUS [23];

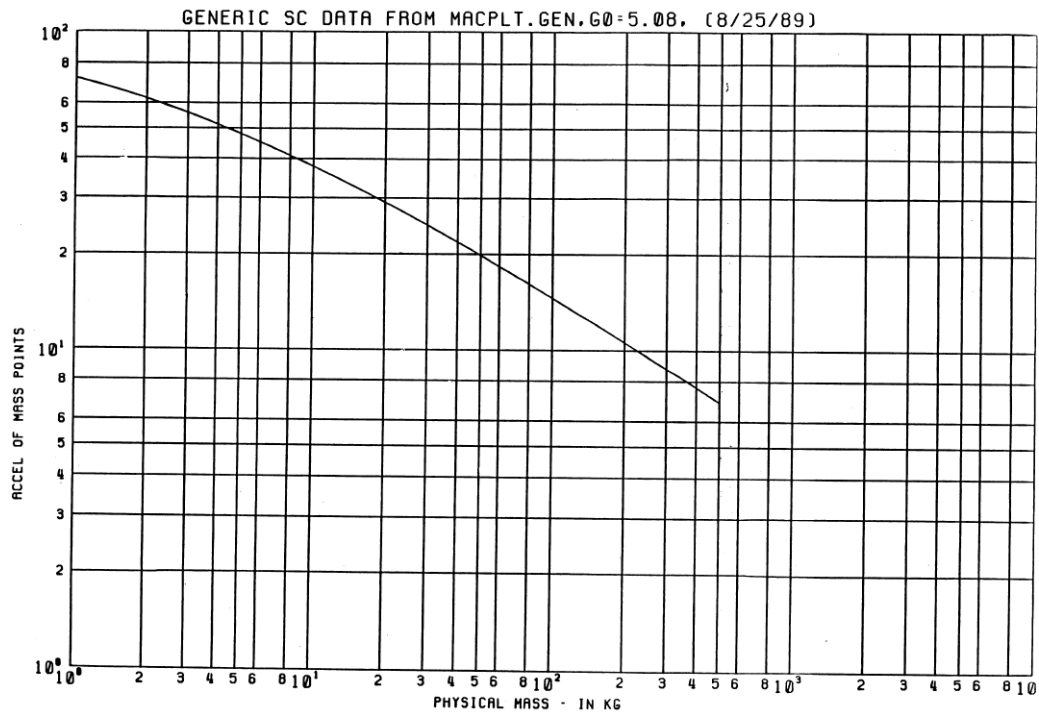


Figure 16: Physical Mass Acceleration Curve for Titan 4/IUS [23];

In this thesis, the first curve is used. The use of the MAC is quite simple. Once the total weight of the concentrated mass is known, it is sufficient to enter the graph from the abscissa axis and move up until it meets the MAC, then it moves left to the ordinate axis where it is possible to read the value (in g) of the acceleration to which the subsystem is subjected. Then the value of the acceleration is multiplied by the concentrated mass and by the terrestrial gravitational acceleration (in the case of the earth precisely). Thus the value of the inertial forces to which the subsystem is subject is derived.

$$F_{x,y,z} = m \cdot gs \cdot g$$

Where  $m$  is the concentrated mass,  $gs$  is the value obtained by MAC and  $g$  is the terrestrial gravitational acceleration. The weight of the component is derived from the software after assigning the materials to the individual parts.

The theory foresees, at this point, to create eight load cases each defined by a different combination in the direction of application of the forces. According to the MAC theory, in the direction along which gravity is supposed to act, the acceleration value obtained from the MAC is increased for a factor of  $g_0 = 3.98$  [24].

Table 5: Load Case Original Model;

	$F_x [N]$	$F_y [N]$	$F_z [N]$
<b>Load case 1</b>	724	675	675
<b>Load case 2</b>	-724	675	675
<b>Load case 3</b>	724	-675	675
<b>Load case 4</b>	724	675	-675
<b>Load case 5</b>	-724	-675	675
<b>Load case 6</b>	-724	675	-675

<b>Load case 7</b>	724	-675	-675
<b>Load case 8</b>	-724	-675	-675

The constraint conditions, as shown in the following figure, are made up of three joints placed in the holes through which the part is connected, through three bolts, to the rest of the structure. Therefore in the three holes all 6 degrees of freedom, three rotational and three translational are eliminated by inserting anchored steel bolts. In fact, according to the load conditions of the problem, it is possible to constrain the structure through Supports, Anchored Fasteners, Anchored Joints. This last type has been rejected because the joint does not respect the real fixing conditions between the parts. The supports are used to set the model so that it is not moved when the loads are applied, and they simulate the conditions of constraints of the joint. The Grounded Fasteners also act as supports in the loading conditions and are used to simulate the nut, and the bolt fixed to another part not available in the model. The latter are those chosen in the model.

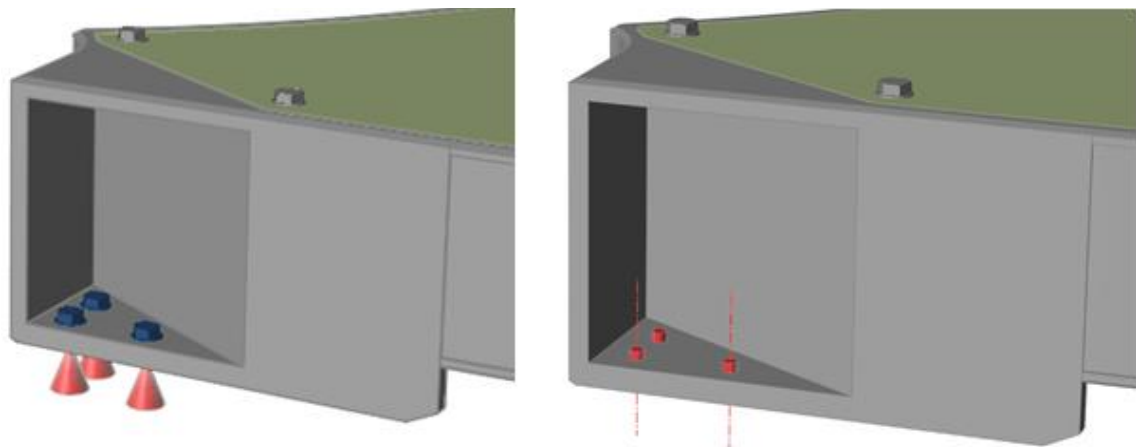
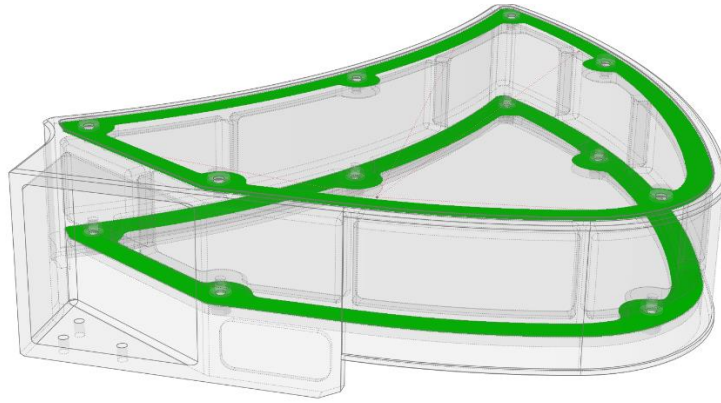


Figure 17: Fasteners (left), support (right);

#### 4.4 Set-up linear static analysis

By the hypotheses on which the theory of Mass Acceleration Curves is based, a point is created and placed in coincidence with the center of gravity of the model. The eight load cases described in the previous paragraph are applied to the point. Then a rigid type connection is generated, through which the forces will be transferred to the other parts of the model.

Since the model is composed of several parts, is essential to correctly define the fixing and contact conditions between the parts to obtain correct results. The following are the contact conditions between the parts of the original model:



*Figure 18: Original model contacts;*

The coupled contacts are displayed in green. In particular, the reference is to the two layers, which are simply in contact (therefore not welded) with the BODY. Furthermore, following the actual fastening conditions between the parts, nut and bolt type fastenings automatically detected by the software have been applied.

#### **4.4.1 Model 0 - the original component**

In this phase, the static structural analysis has been carried out. The FEM linear static analysis is not only useful to verify that the original component resists the applied loads but still to compare the mechanical performance of the optimized model.

Moreover, we have tried to determine for which average dimension of the mesh elements we can obtain the right compromise between the quality of the result and computational time. This through a process of h-refinement, the mean size of the element has been progressively decreased, to which corresponds an increase in the degrees of freedom of the problem. From the FEM theory it is known that as the number of elements in which the domain is discretized increases, the result tends asymptotically to the value of the analytical solution (ideally being able to have an infinite number of elements). On Inspire you can change the order of the element by selecting More accurate (second-order) instead of Faster (first-order) while setting up the analysis, but the computational time is too high, and it needs too much disk space to be performed. The convergence of the result is evaluated on the module of the maximum displacement of point A.

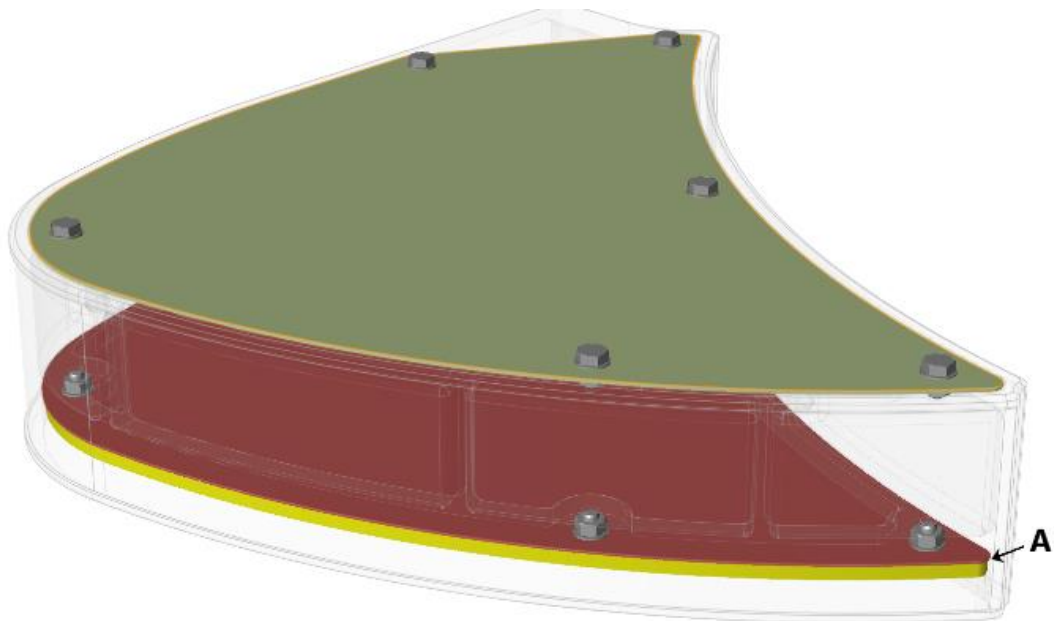


Figure 19: Point A of the model;

The inverse proportionality relationship between the number of finite elements, in which the model is automatically discretized, and the mean size of the elements is shown below.

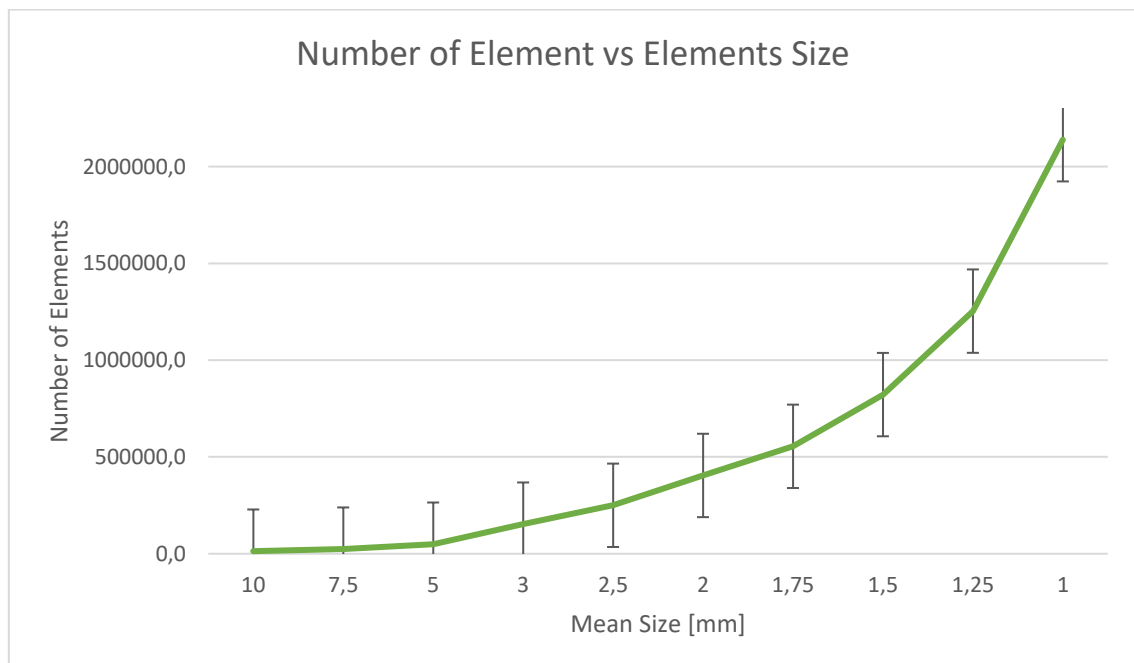


Figure 20: Number of elements VS Mean size;

Below, is the exponential trend of the calculation time as the mean size of the elements decreases:

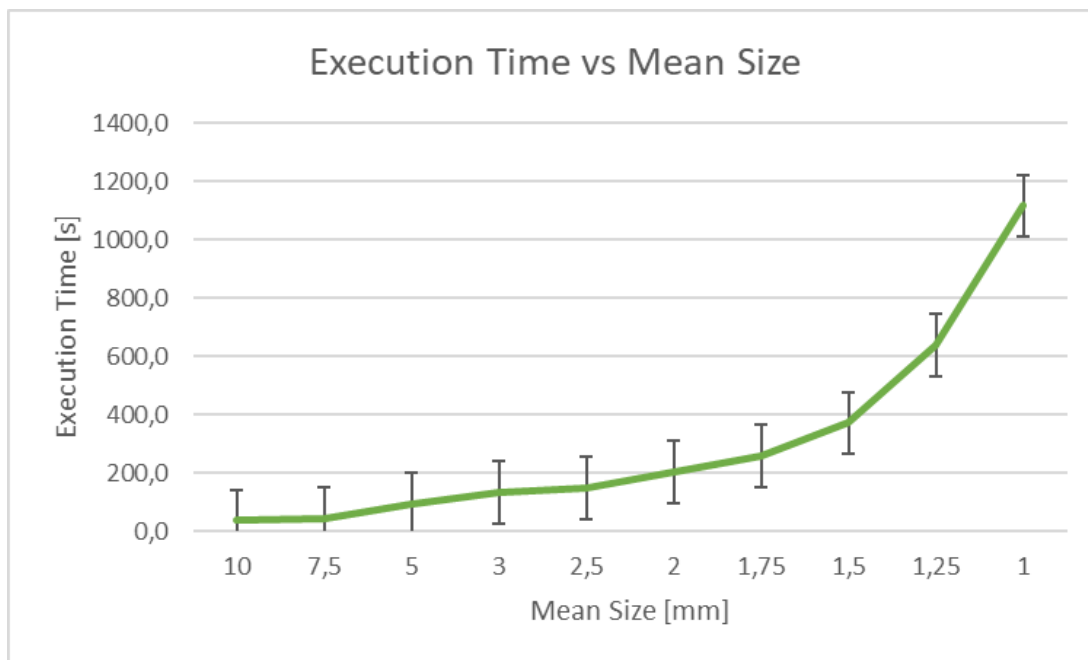


Figure 21: Execution Time VS Mean Size;

It is clear that the smaller the elements that discretize the domain, the more time is required to complete the analysis, this is also due to the larger dimensions of the algebraic system that the computer will have to solve.

Once the static analysis is complete, *Inspire* allow to view the results of the safety factor. The safety factor shows which areas of a model are at risk of loss due to stress. The safety factor is calculated as follows:

$$SF = \frac{\text{material yield stress}}{\text{actual von Mises stress}}$$

A safety factor less than 1 indicates that the part at that point could produce errors. The accuracy of the safety factor analysis depends on an accurate input of loads, materials and models. In general, there is no definitive safety factor suitable for all applications.

The minimum safety factor, the maximum modulus of the displacements of point A, the max yield in percentage and the maximum von Mises tension are reported below in the tabular form. Moreover, with *Inspire* there is the possibility to see the results with Result Envelope mode, that shows the maximum value for each result type across all load cases.

Table 6: Original model: result envelope for different mesh size;

Mean Size [mm]	S.F.	$u_{max}$ [mm]	$\epsilon$ [%]	$\sigma_{VM_{max}}$ [Mpa]
10	3.3	1.071	30.64	7.393e+001
7.5	2.3	1.213	43.24	1.043e+002
5	1.3	1.440	74.54	1.799e+002
4	1.5	1.672	68.52	1.653e+002

3	0.7	1.922	142.78	3.445e+002
2.5	1.4	1.542	72.35	1.746e+002
2	1.3	1.640	77.19	1.863e+002
1.75	1.1	1.597	90.58	2.186e+002
1.5	1.0	1.606	100.54	2.426e+002

The minimum safety factor obtained is less than 1, for some mean sizes of the element, only in some very small areas, negligible due to errors in the minimum dimension of the mesh element. In the rest of the component, the safety factor is always greater than 1.2. Near the constrained holes there are the lowest values of the factor of safety, moving from there the factor of safety increase.

The following is the trend of the maximum module of the displacement of point A depending on the mean size of the mesh elements.

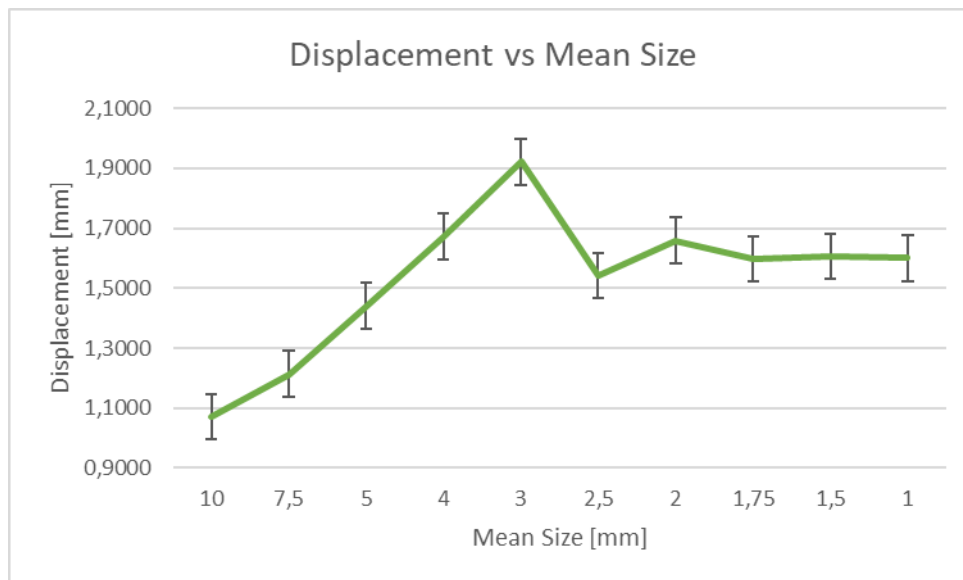


Figure 22: Displacement (point A) VS Mean Size;

Considering asymptotic value the results relative to  $MS=1[mm]$ , the model with the mean size of the elements equal to 2 mm is chosen to take as a reference. This size represents a good compromise between quality of results, calculation times and number of elements in which the model is discretized. For this size, the results for all load case are shown below.

Table 7: Results Original-Model,  $MS=2[mm]$ ;

	S.F.	$u_{max}[mm]$	$\epsilon[\%]$	$\sigma_{VM_{max}}[Mpa]$
Load Case 1	4.3	0.416	23.18	5.594e+001
Load Case 2	1.3	1.265	76.41	1.844e+002
Load Case 3	1.4	1.640	72.83	1.757e+002
Load Case 4	2.1	0.7185	46.82	1.130e+002
Load Case 5	2.1	0.7185	46.82	1.130e+002
Load Case 6	1.4	1.640	72.83	1.757e+002

Load Case 7	1.3	1.265	76.41	1.844e+002
Load Case 8	2.8	0.8205	35.90	8.663e+001
Results Envelope	1.3	1.640	76.41	1.844e+002

The contour plot of the factor of safety is presented in figure 23;

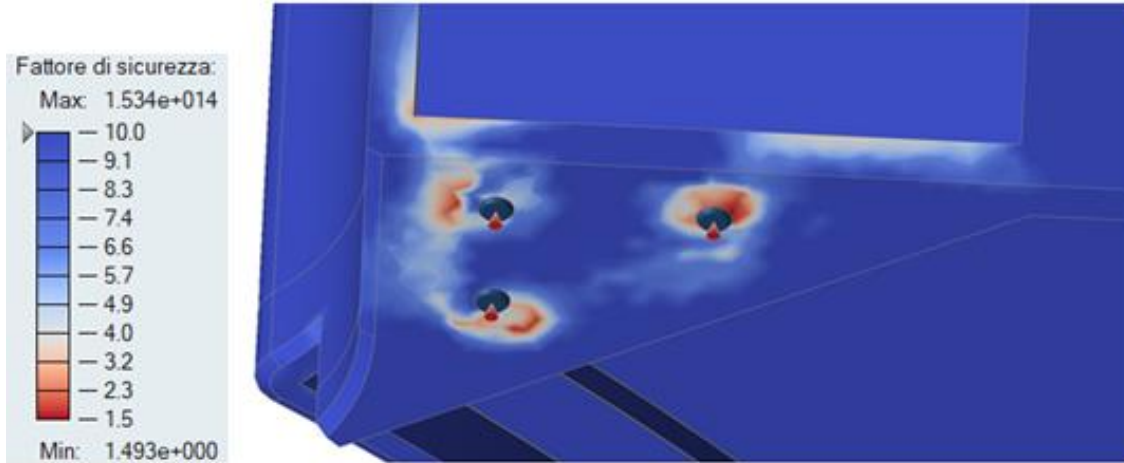


Figure 23: Factor of Safety Original-Model;

The results of displacement are presented below, figure 24.

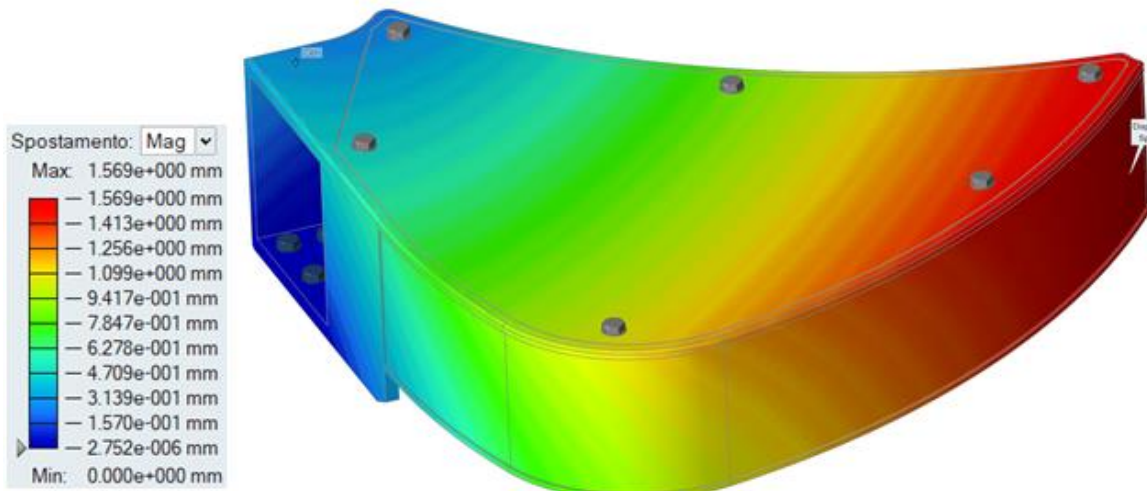


Figure 24: Displacement Original-Model;

The contour plot of von Mises stress is shown below, figure 25.

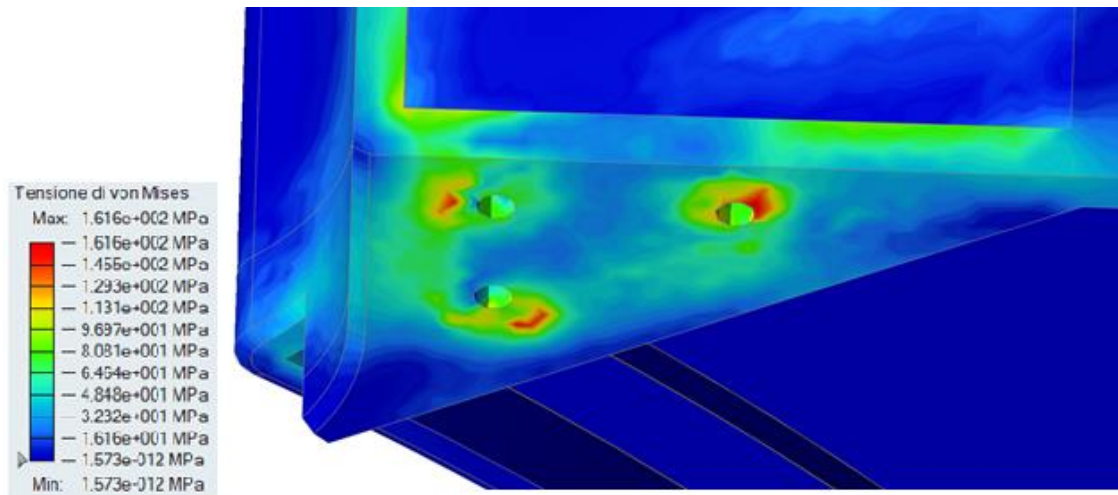


Figure 25: von Mises stress Original-Model;

#### 4.5 Project specifications

During the redesign of the part, a series of technological, physical and geometric constraints must be respected. These define the project specifications and can be summarized in the following points:

1. The material of the Layer2 has to be a 6000 series aluminium alloy (Anticorodal), the material of the Layer1 has to be Kevlar.
2. The maximum displacement of point A is set equal to 5 mm;
3. The minimum SF must be equal or greater than 1.2;
4. The maximum size of the optimized part must be equal to or less than the original one;
5. The connection and the interface between the parts cannot be altered;

## 5. Optimization phase

As regards the types of optimization, those of most considerable interest for this thesis are topology and lattice. For these, it is also possible to choose the target of optimization between maximize stiffness, maximize frequency, minimize mass. For each of these, it is possible to define the constraints of minimum and maximum thickness, which the optimized design space must respect. As for the minimum thickness, it is set at the minimum value suggested by *Inspire*.

First, it is necessary to prepare the CAD model for the phase in which it will be optimized. The Simplify functions present in the Geometry ribbon have been used to eliminate those features such as rounds, fillets and traces to simplify the DS modification phase.

Then the model was subdivided into design space (DS) and non-design space (NDS). The design space is that portion of space, occupied by the model, that we want to optimize. To establish the DS, it is necessary to know all those portions of the volume of the model that cannot be altered; therefore constrained parts, particular holes, interface points and elements whose geometry is closely related to the correct functioning of the equipment are not defined as DS. The subdivision of the model in DS and NDS is carried out through the Boolean functions: Intersect, Combine, Subtract.

### 5.1 Non-Design Space

The NDS is that region of the model that cannot be altered by the optimization algorithm because it competes with other parts or simply for functional reasons. The usefulness of the NDS is also from the numerical point of view: the loads and the constraints must always be applied to NDS parts to prevent the point of application moving during the optimization and obtaining results without physical meaning. In particular, circular crowns have been generated in correspondence with the fixing holes of the primary and secondary bumper (also defined as NDS for functional reasons) and in correspondence with the constrained holes. The above can be observed in the following image:

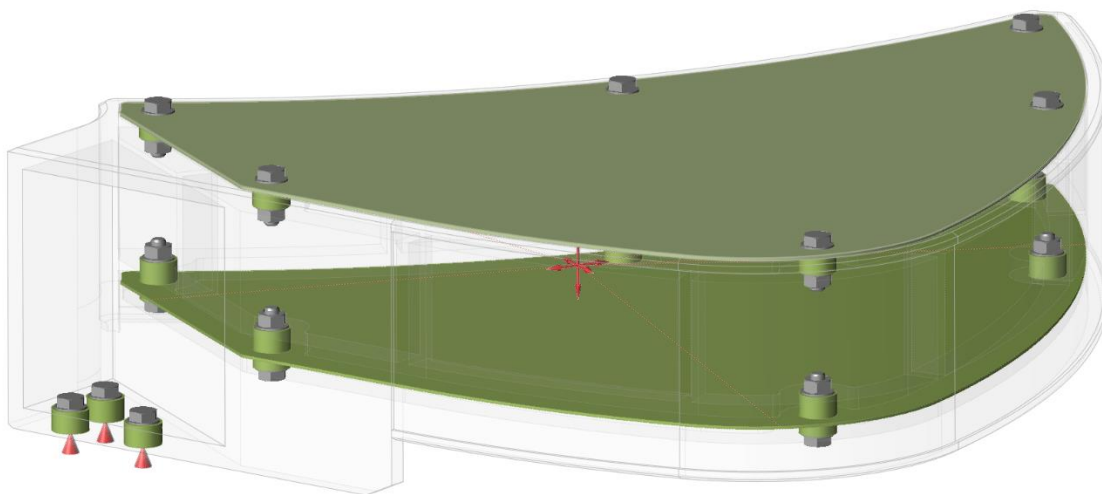


Figure 26: NDS;

## 5.2 Design Space

The DS represent the optimization domain, where the optimal distribution of material will be sought to withstand precise loading and constraint conditions. The best design practice recommend to create a DS as large as possible (in compliance with the project requirements) to leave the maximum freedom of exploration to the optimization algorithm. In the beginning, two alternative DSs have been defined for topological optimization, DS-Original and DS-Full. The DS-Original coincides with the original model, except for those regions defined as NDS, in order to assess whether and where it would be possible to remove material.

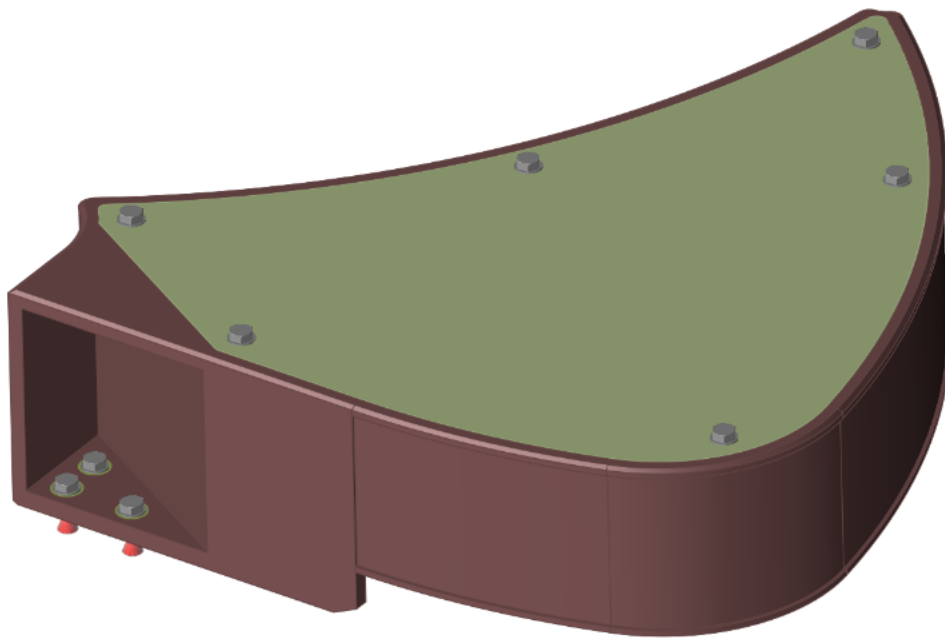


Figure 27: DS-Original, view 1;

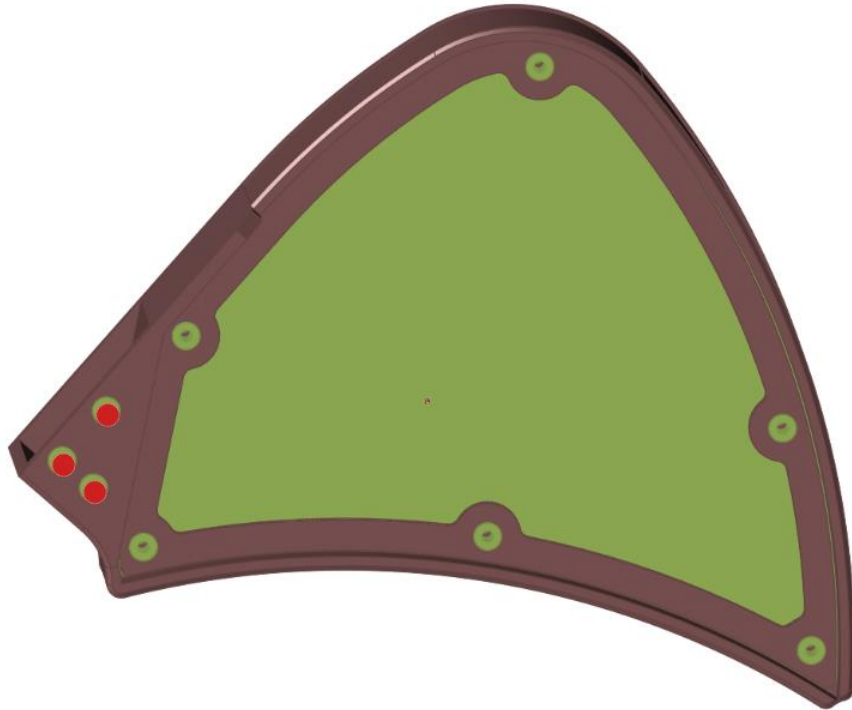


Figure 28: DS-Original, view2;

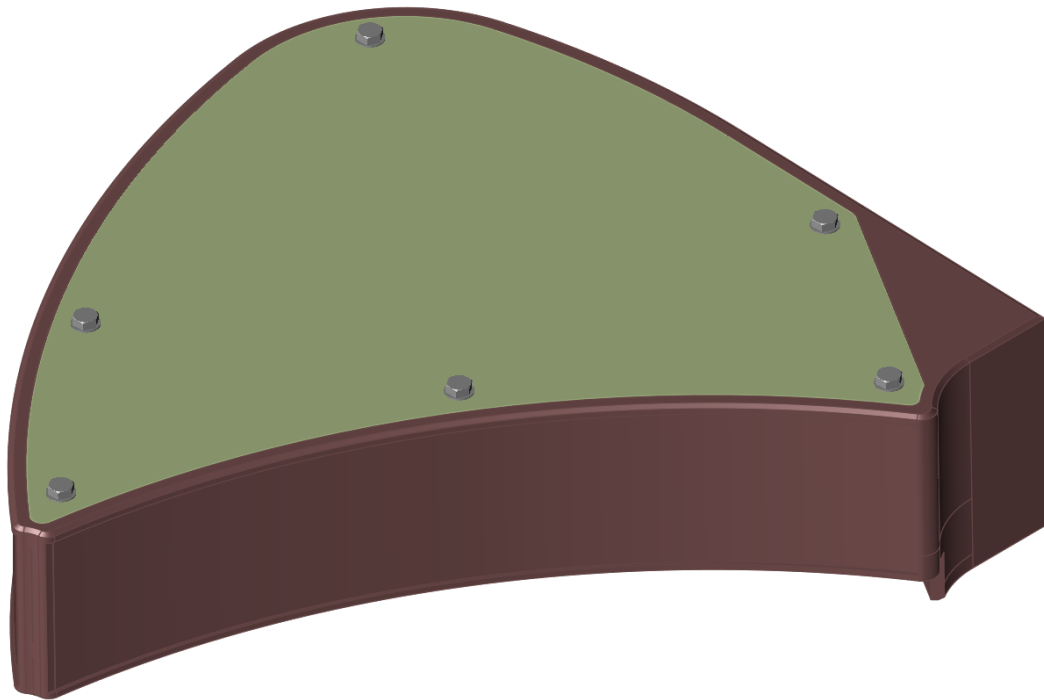


Figure 29: DS-Original, view3;

The DS-Full is for a drastic redesign of the model and consists of the volume occupying the maximum dimensions of the model with 6 through holes to prevent that material being positioned in correspondence with the NDS circular crowns (for assembly reasons). The parts defined as NDS are the same in both cases; therefore the ratio between the volumes of the two DS was calculated, obtaining a value equal to 0.17, to know how much material

will have to be removed in the optimization process to obtain a weight reduction compared to the original. As can be seen in the figures below, 3 through holes are created to allow the assembly phase.

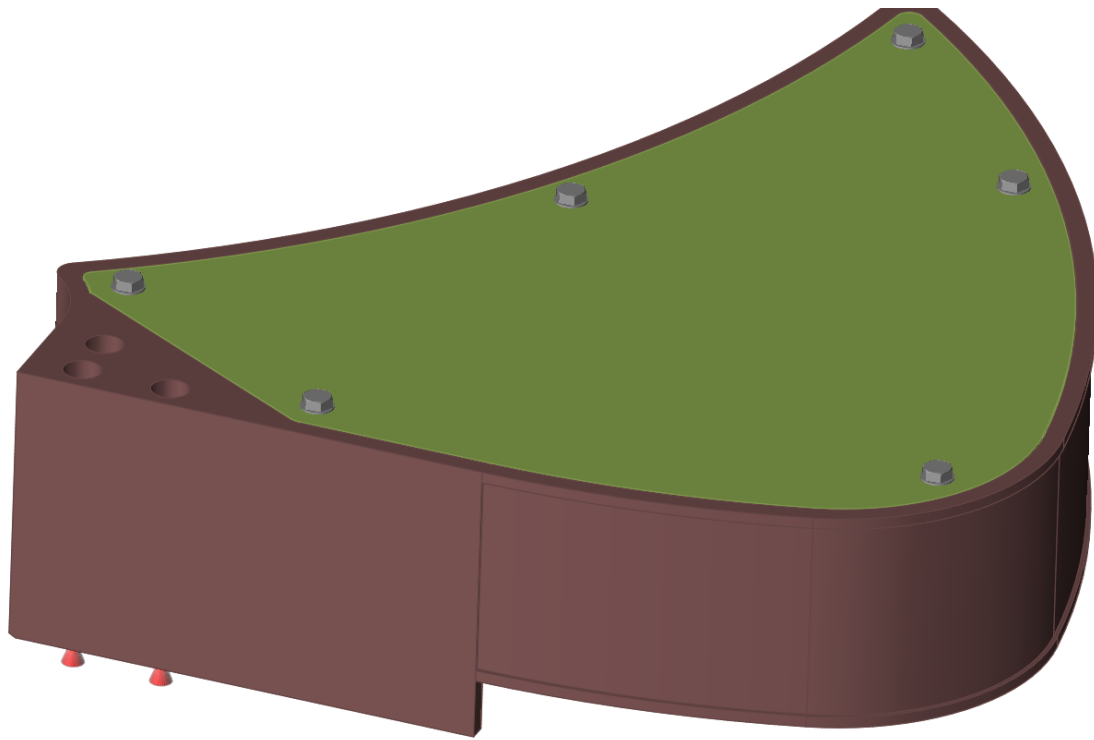


Figure 30: DS-Full, view1;

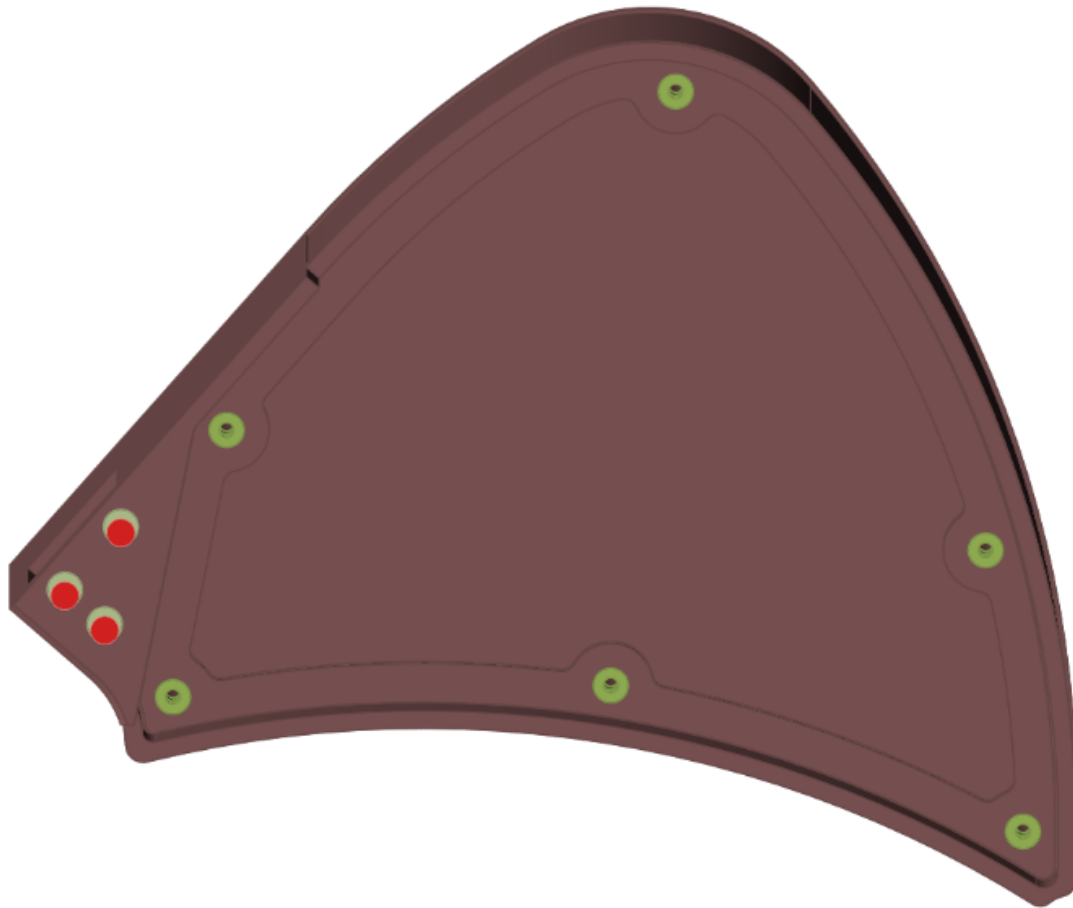


Figure 31: DS-Full, view2;

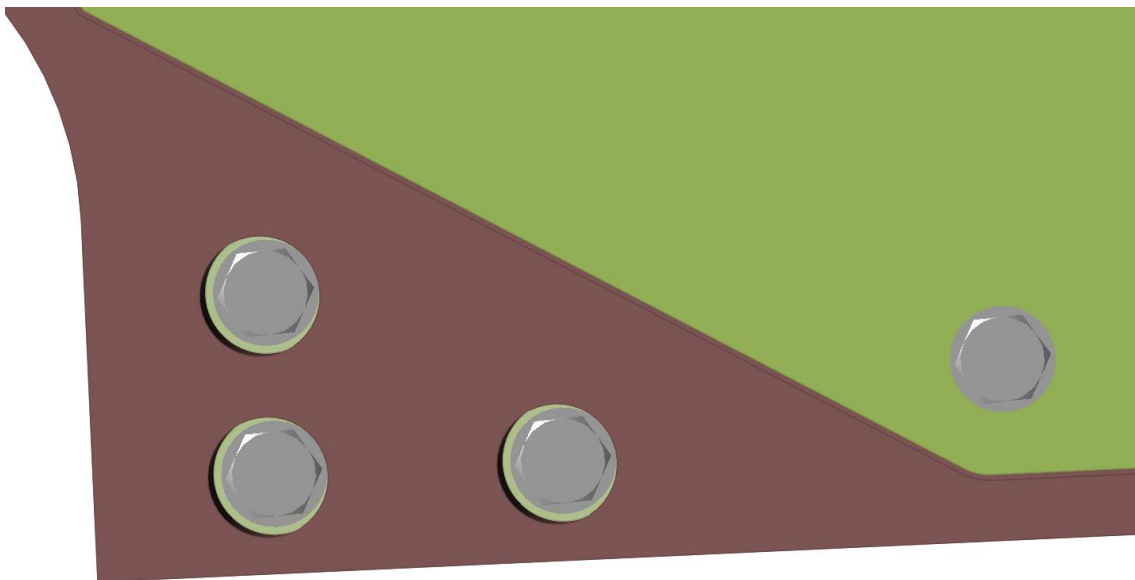


Figure 32: View of the three through-holes of DS-Full;

As for the optimization process, it is necessary to choose the objective function. In Inspire, you can choose between:

- maximizing stiffness;

- minimizing mass.

The first generates a form that produces the least amount of movement of the model and it is necessary to choose the percentage objective of the total volume of DS. The second produces the lightest topology able to withstand loads (in this case it is necessary to choose a constraint on global stress via SF). In minimizing mass, it is also advisable to insert a constraint on the maximum displacement to avoid excessive deviations of the structure.

### 5.3 Results DS-Original and DS-Full

#### 5.3.1 DS-Original

Optimization was carried out for the DS-Original to minimize compliance (maximize stiffness) with 30% as the objective of the DS. The minimum value allowed by the software was entered as the minimum thickness, this is equal to 2.6 [mm]. Inspire allows you to interpret the optimization result using the iso-density curve method, so a threshold value (cut-off) is expected on which an iso-density curve is drawn that describes the contour of the resulting topology: all the elements that have been assigned a density value below the threshold are discarded, while all the others are promoted to a unit density value. This process is semi-automatic in Inspire, through the shape explorer, it is possible to move a sliding cursor by specifying the value of the cutting density and automatically the software carries out the reject and promotion operation. Typically, set the threshold value to have all connected topologies.

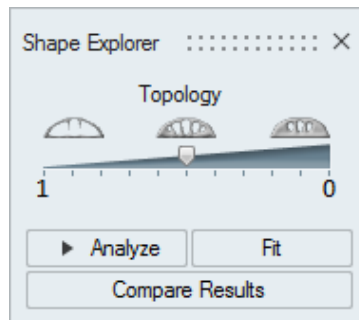


Figure 33: Shape Explorer

The results obtained in the case of DS-Original, stiffness maximization, are shown below.

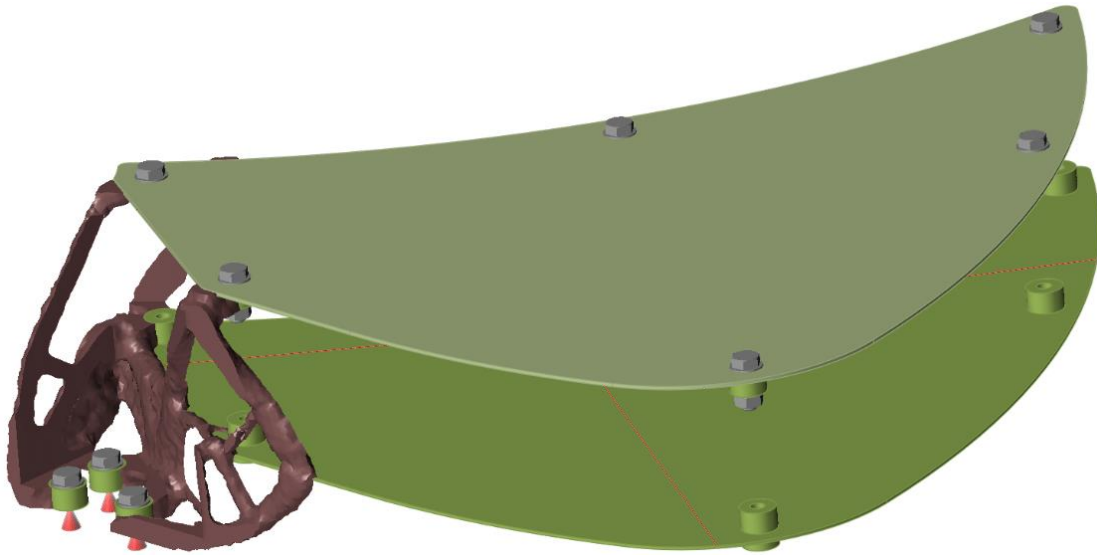


Figure 34: Optimized DS-Original max stiffness, view1;

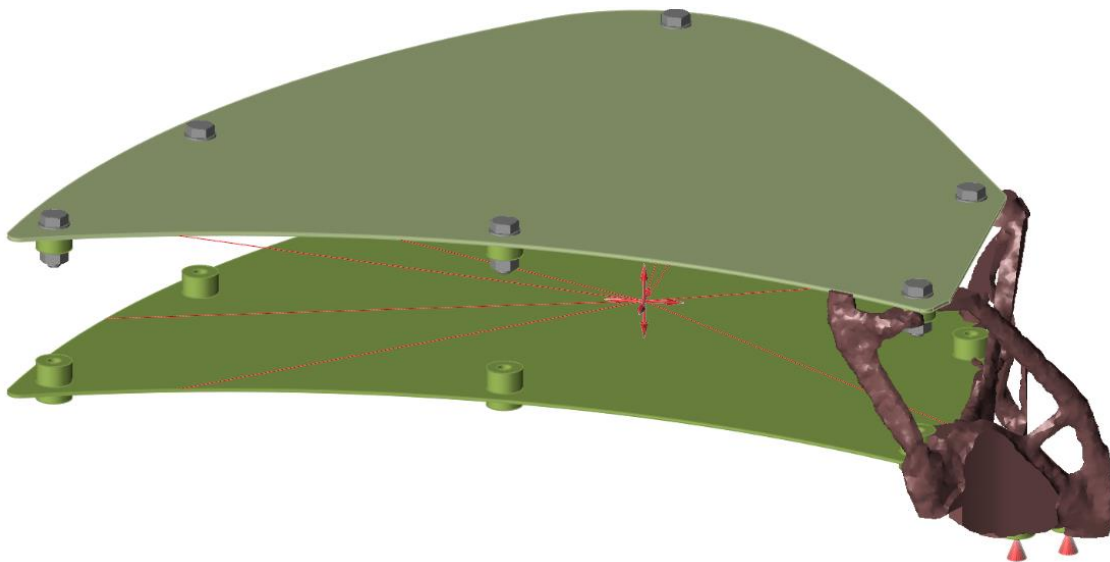


Figure 35: Optimized DS-Original max stiffness, view 2;

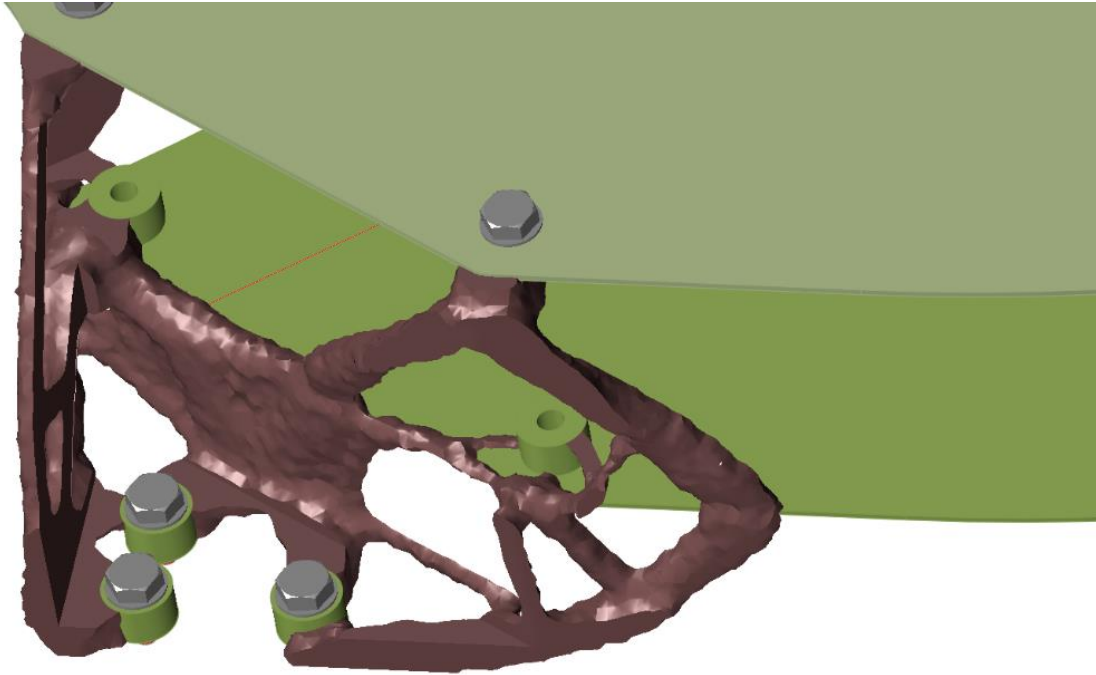


Figure 36: Optimized DS-Original max stiffness, view 3;

There is clearly a drastic reduction in the weight of the model. Which is about 30%, in weight, of the original model. Observing the optimized solution, we realize that this is only a numerical result of the optimization problem. Globally, the optimization algorithm solves the problem with a cantilever solution where the two layers have infinite stiffness. Locally, near the constraints, correctly a very organic topology was generated. Finally this solution must be discarded since it does not take on any usefulness for the function of the system. The cause of this solution lies in the incorrect modelling of the stiffness of the layers. Modelling the stiffness of the layers accurately should result in a better solution.

### 5.3.2 DS-Full

As made for DS-Original, also for DS-Full a topology optimization to minimize compliance is carried out. This time, considering the ratio between the volume of DS-Full and DS-Original, which is 0.17, 5% of the total volume is selected as objective. The minimum value allowed by the software was entered as the minimum thickness, this is equal to 4.6 [mm]. Unfortunately, it is not possible to finish the analysis due to the warning message “The loads are insufficient to generate a shape”.

A second optimization was carried out for the DS-Full to minimize mass with a minimum factor of safety equal to 1.5. The minimum value allowed by the software was entered as the minimum thickness, this is equal to 4.6 [mm]. As shown in figure 38, a *Displacement Constraint* of 2 [mm] is set in point A. The results obtained in the case of DS-Original mass minimization are shown below.

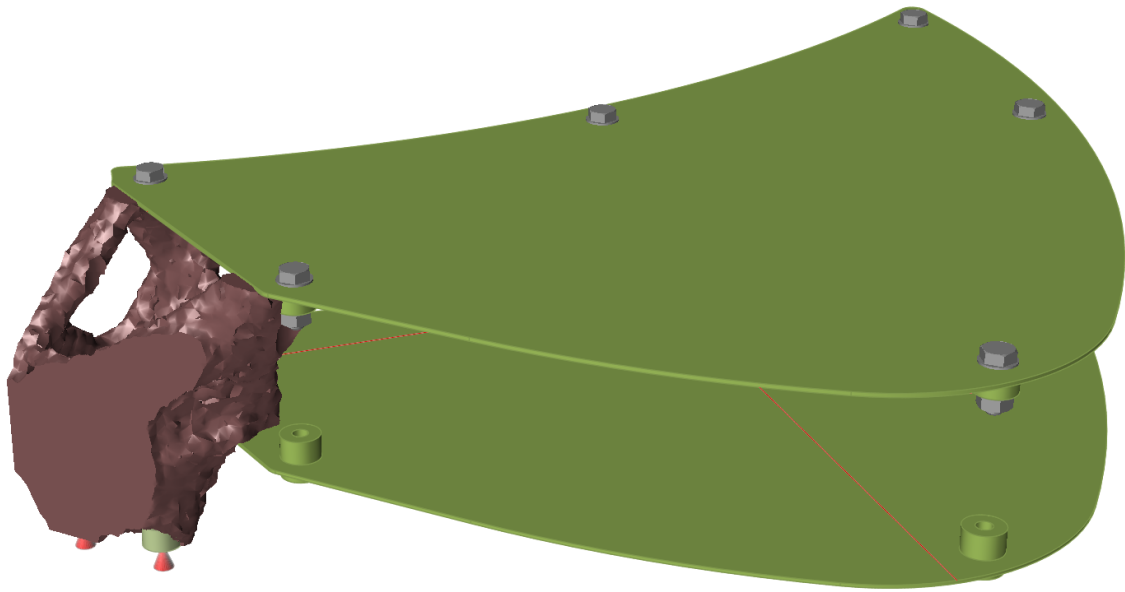


Figure 37: Optimized DS-Full, minimize mass, view1;

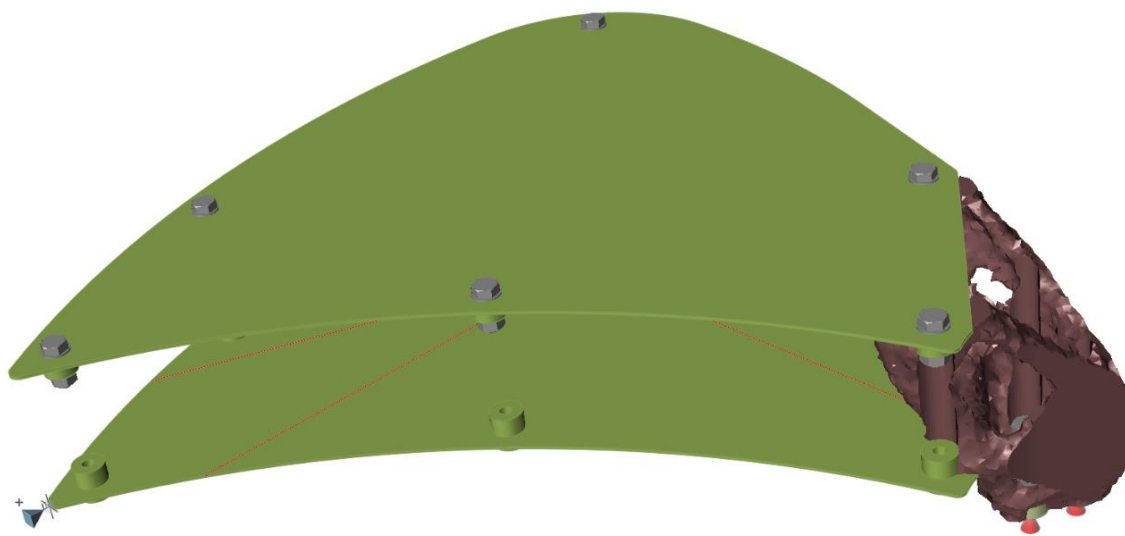
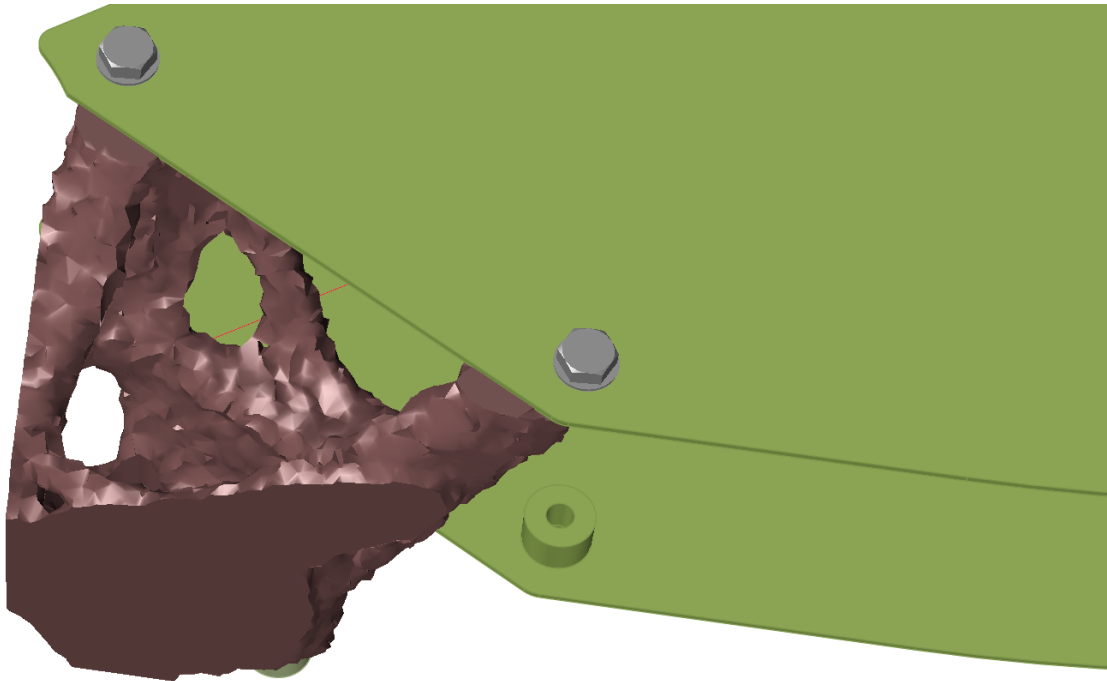


Figure 38: Optimized DS-Full, minimize mass, view2;



*Figure 39: Optimized DS-Full, minimize mass, view3;*

As for the DS-Original, for the same reasons, this solution is discarded. At this point, interpreting the results provided by the first two optimizations, a new subdivision between DS and NDS is chosen to be used.

#### **5.4 DS-Hybrid – Model 1**

In consideration of the results obtained with the DS-Original and DS-Full, a new DS was created that allowed to correctly exploit the optimization algorithm. It is recalled that the structure is thin-wall type and that it is not suitable for topological optimization. So starting from the DS-Original, the entire perimeter area of the BODY was excluded from the DS. Furthermore, as in the case of DS-Full, the area near the constrained holes was filled and three through-holes were drilled to allow fixing to the rest of the structure. The DS-Hybrid aims to use the optimization algorithm correctly, that is, only where the first analyzes have provided correct results. The above is shown in the following figure:

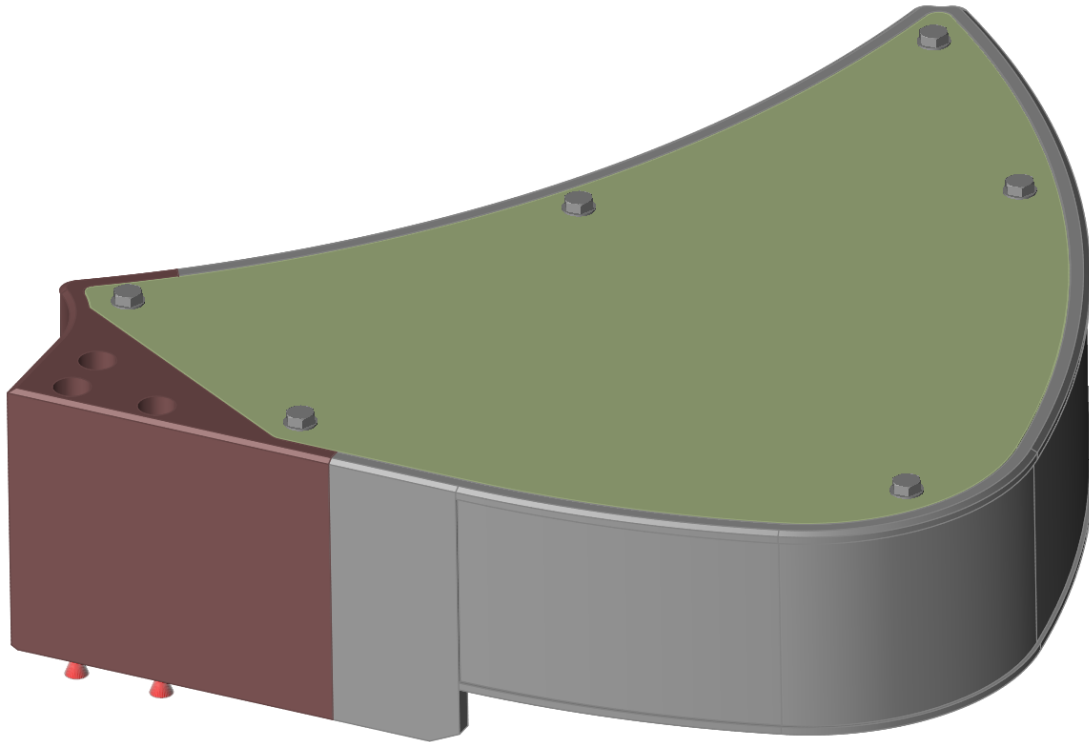


Figure 40: DS-Hybrid, view1;

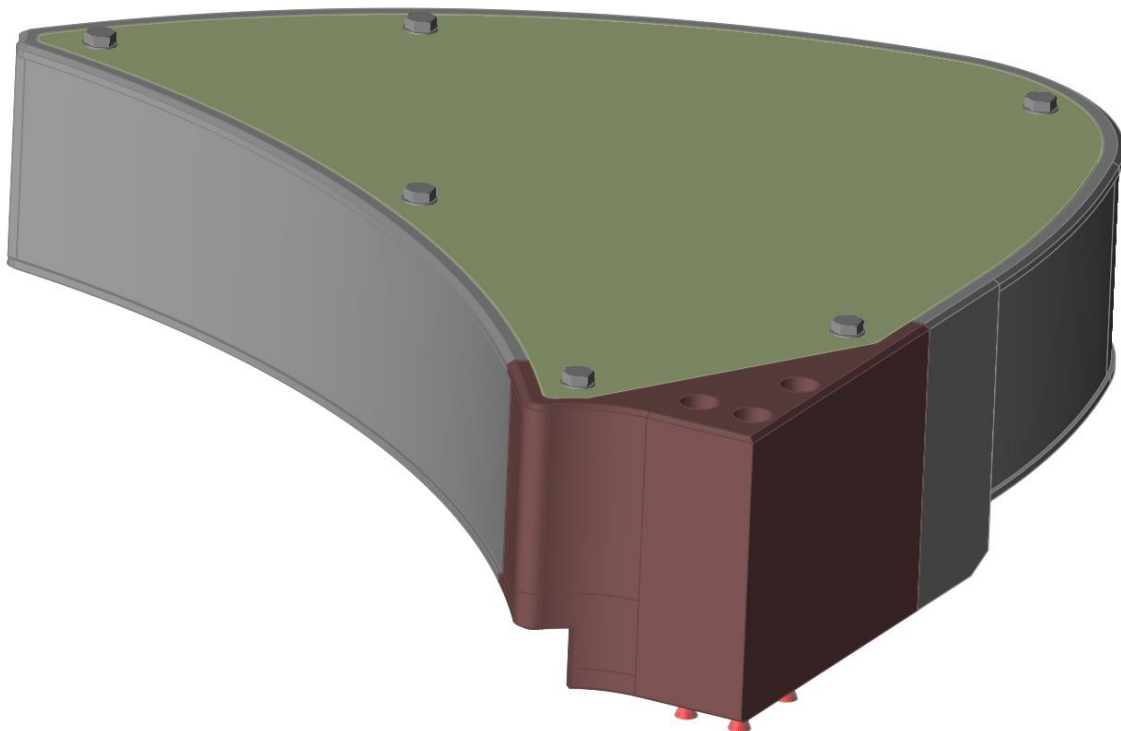


Figure 41: DS-Hybrid, view2;

#### 5.4.1 Result DS-Hybrid

Also, in this case, the ratio between the volumes was calculated in order to know the target percentage. The ratio is 0.45, so 20% has been chosen as the target, which is abundantly below. The minimum thickness, as in other cases, has been set to the

minimum value suggested by the software, in this case 3mm. The results are shown in the following figure:

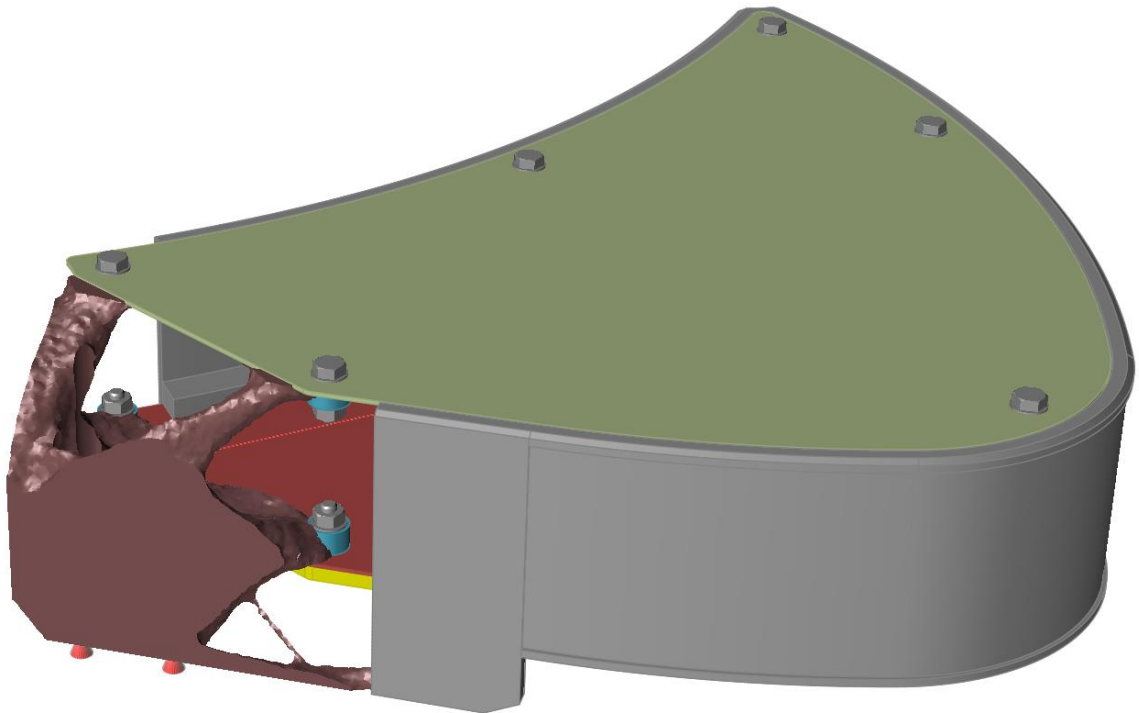


Figure 42: Optimized DS-Hybrid, max stiffness, view1;

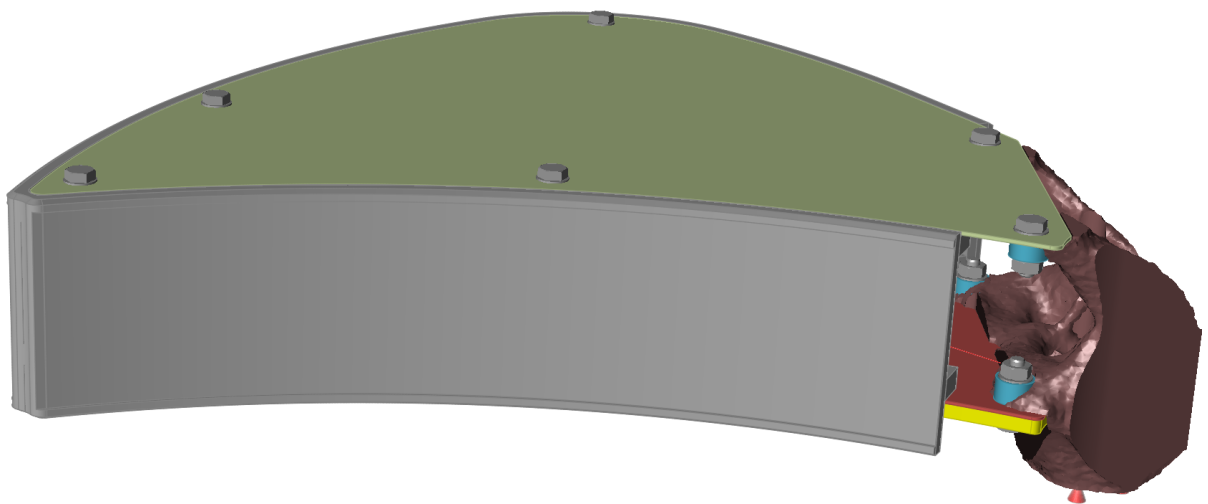


Figure 43: Optimized DS-Hybrid, max stiffness, view2;

This solution has been considered valid from a technical point of view, and for this reason, through Inspire's PolyNURBS functions, a solid part is created following the input generated by the software, considering the constraint of manufacturing (mechanical interface surface) and integration requirement (tool passages and envelopes) moreover. Above is shown in the following figures.

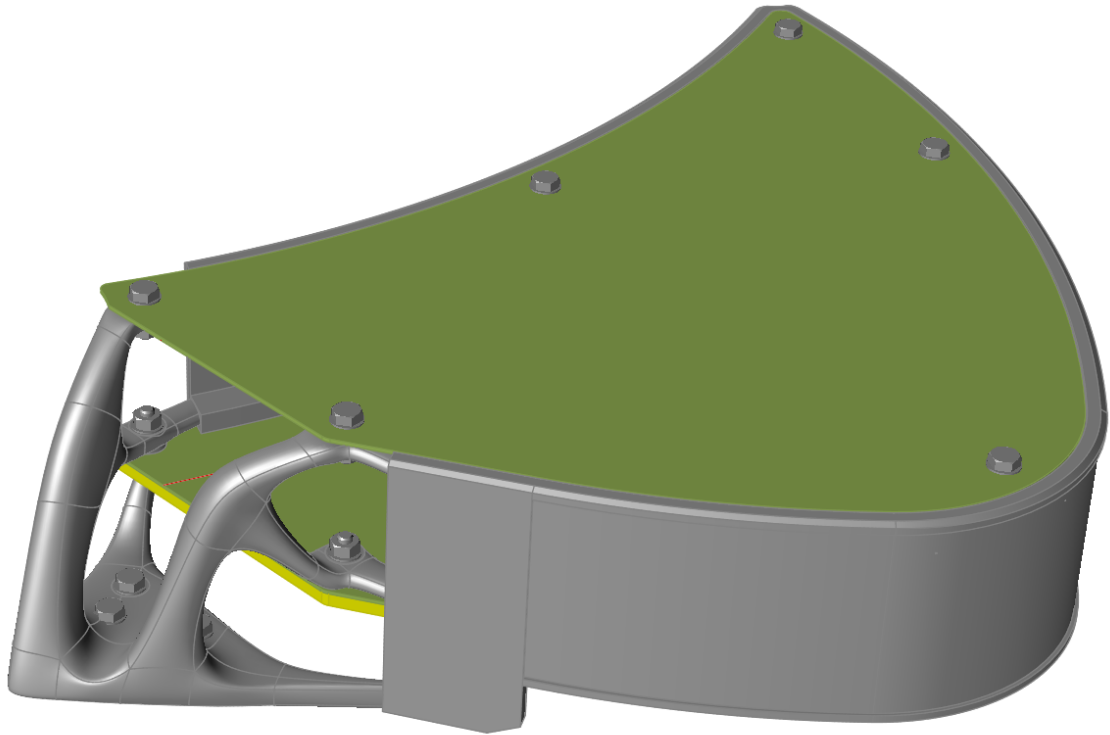


Figure 44: Hybrid-Model, view1;

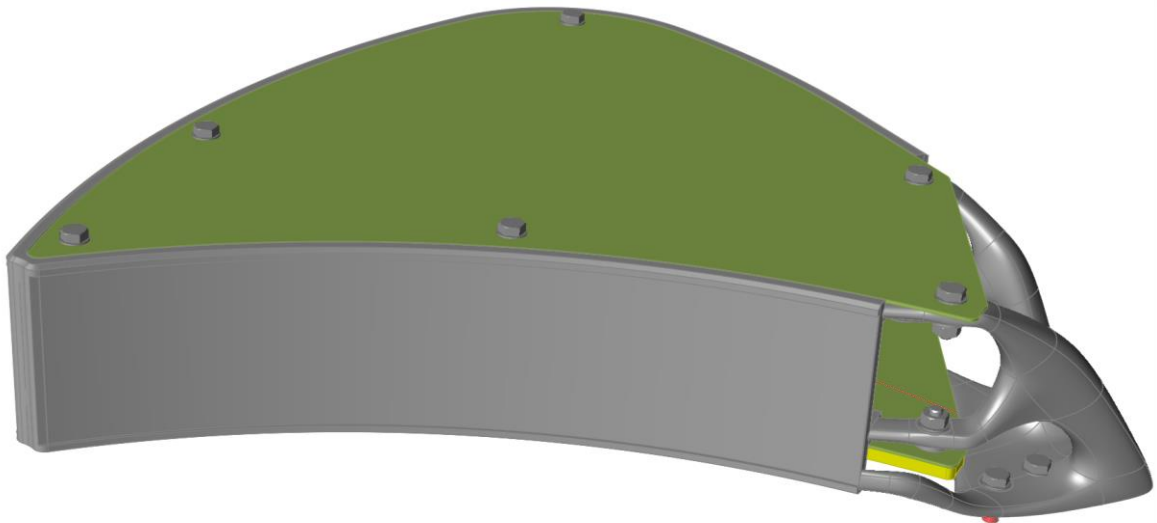


Figure 45: Hybrid-Model, view2;

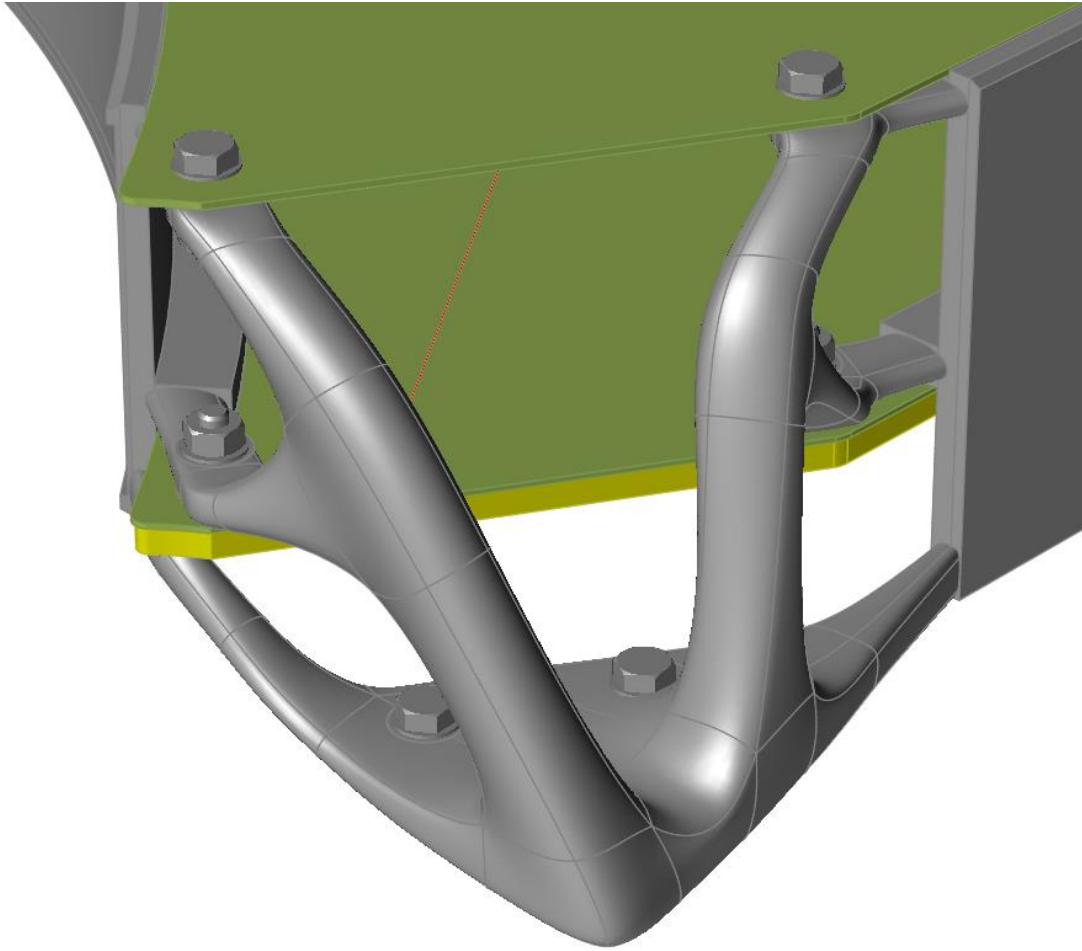


Figure 46: Hybrid-Model, view3;

Taking into account the overall mass of the model which is 1138 [g], actually, there is a saving in mass of 11.5%. The optimized support in figure 46 is under production at EOS Finland as a demonstrator for evaluating powder bed production processes.

#### 5.4.2 Analysis of Hybrid-Model

At this point, linear static analysis is carried out in Inspire to verify the performance of optimized model respect project requirements. The mean size of the mesh element is equal to 2[mm] as for the reference original model. It is essential to point out that once the weight of the model has decreased it is necessary to adopt the MAC again to calculate the modulus of acting forces and accordingly change the eight Load Case. Moreover, the application point must be moved again in the center of gravity of the current model.

Table 8: Acting forces of Hybrid-Model;

	$F_x$ [N]	$F_y$ [N]	$F_z$ [N]
Modulus of forces	675	630	630

The results for the Hybrid-Model are shown below.

Table 9: Hybrid Model, results linear static analysis;

	S.F.	$u_{max}$ [mm]	$\epsilon$ [%]	$\sigma_{VM_{max}}$ [Mpa]
Load Case 1	1.1	1.882	90.69	2.188e+002
Load Case 2	0.8	3.279	124.36	3.001e+002
Load Case 3	0.8	3.066	131.13	3.164e+002
Load Case 4	1.1	2.899	94.81	2.288e+002
Load Case 5	1.1	2.899	94.81	2.288e+002
Load Case 6	0.8	3.066	131.13	3.164e+002
Load Case 7	0.8	3.279	124.36	3.001e+002
Load Case 8	1.1	1.882	90.69	2.188e+002
Results Envelope	0.8	3.279	131.13	3.164e+002

We underline the fact that for this model, it is the Load Case 2 and 7 that generates the maximum displacement, not the 3 and 6 anymore.

#### 5.4.3 Result Hybrid-Model Lightened – Model 2

To achieve another mass reduction, the model was modified in Inspire through CAD tool. In particular, a reticular structure was generated in the NDS as shown below.

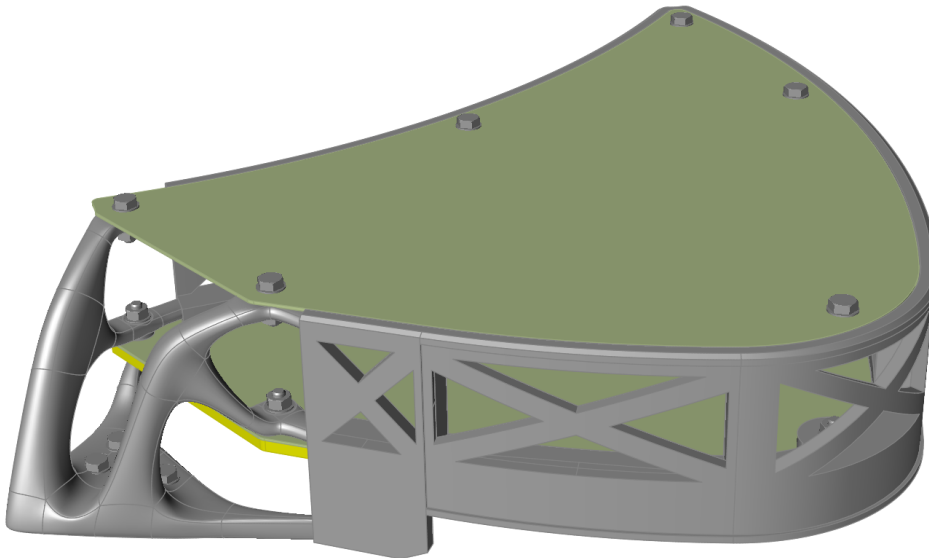


Figure 47: Hybrid-Model lightened, view1;

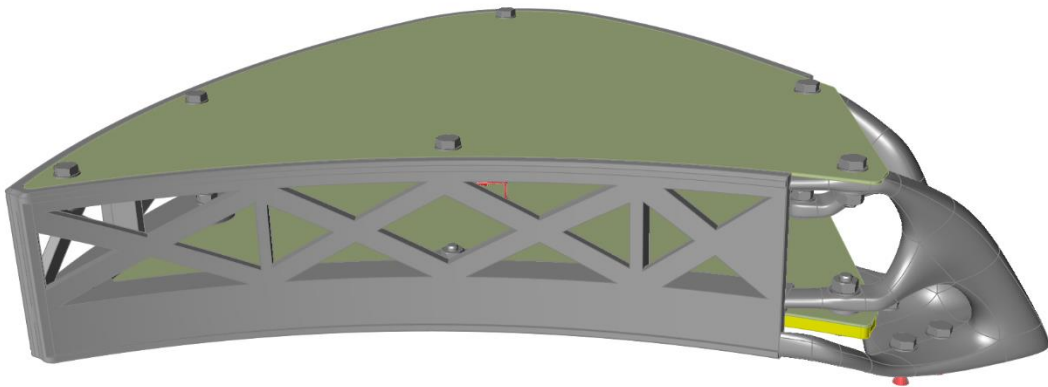


Figure 48: Hybrid-Model lightened, view2;



Figure 49: Hybrid-Model lightened, view3;

In order to carry out the linear static analysis, considering a mass equal to 1 [kg], as made for the Hybrid-Model, the force modules were recalculated, and the point of application positioned in the center of gravity.

Table 10: Acting forces on Hybrid-Model Lightened;

	$F_x$ [N]	$F_y$ [N]	$F_z$ [N]
Modulus of forces	608	568	568

The results for the Hybrid-Model Lightened are shown below.

Table 11: Hybrid-Model Lightened, results linear static analysis;

	S.F.	$u_{max}$ [mm]	$\epsilon$ [%]	$\sigma_{VM_{max}}$ [Mpa]
Load Case 1	1.5	1.613	66.33	1.600e+002
Load Case 2	1.1	2.800	88.51	2.136e+002
Load Case 3	1.0	2.577	99.84	2.409e+002
Load Case 4	1.4	2.437	70.88	1.710e+002

Load Case 5	1.4	2.437	70.88	1.710e+002
Load Case 6	1.0	2.577	99.84	2.409e+002
Load Case 7	1.1	2.800	88.51	2.136e+002
Load Case 8	1.5	1.613	66.33	1.600e+002
Results Envelope	1.0	2.800	99.84	2.409e+002

Also in this case, the Load Case 2 and 7 generate the maximum displacement of the point A which is smaller than in the case of Hybrid-Model. The envelope mode result for the factor of safety and displacement are shown below.

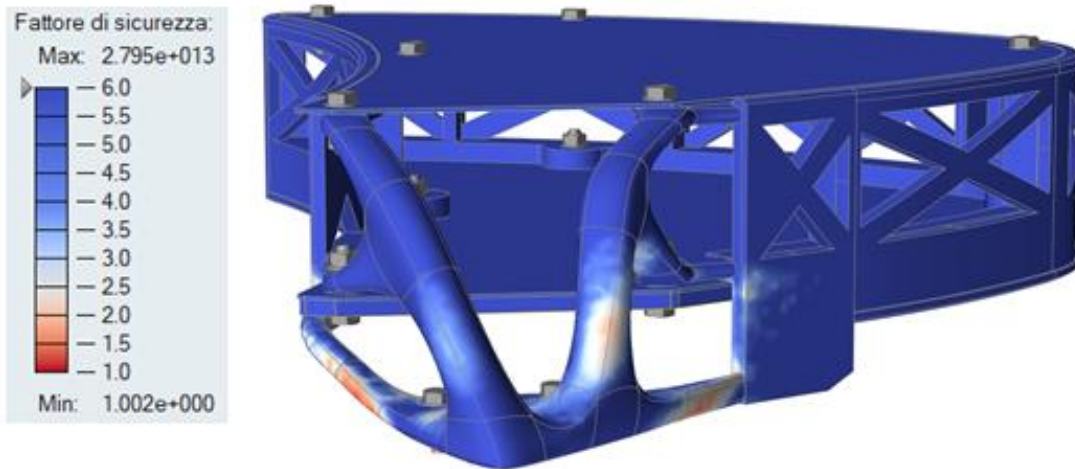


Figure 50: Factor of Safety of Hybrid-Model Lightened;

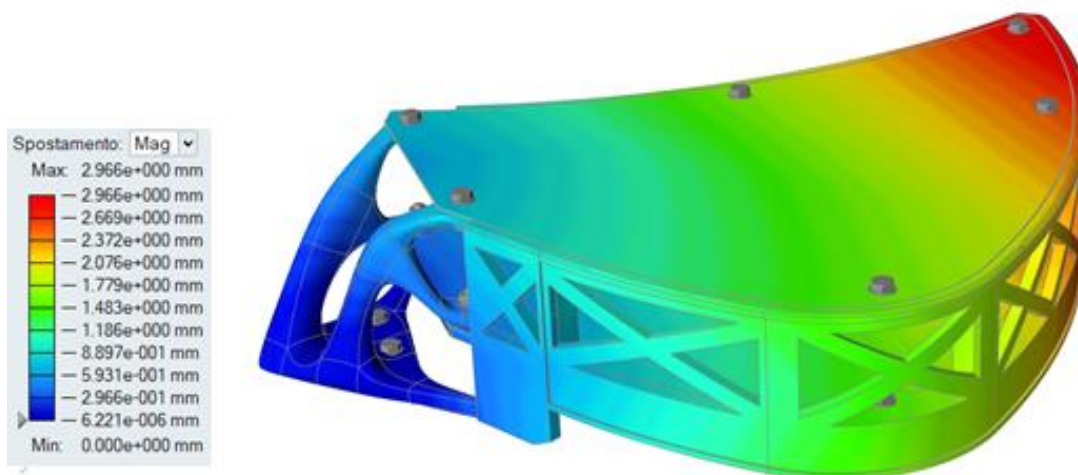
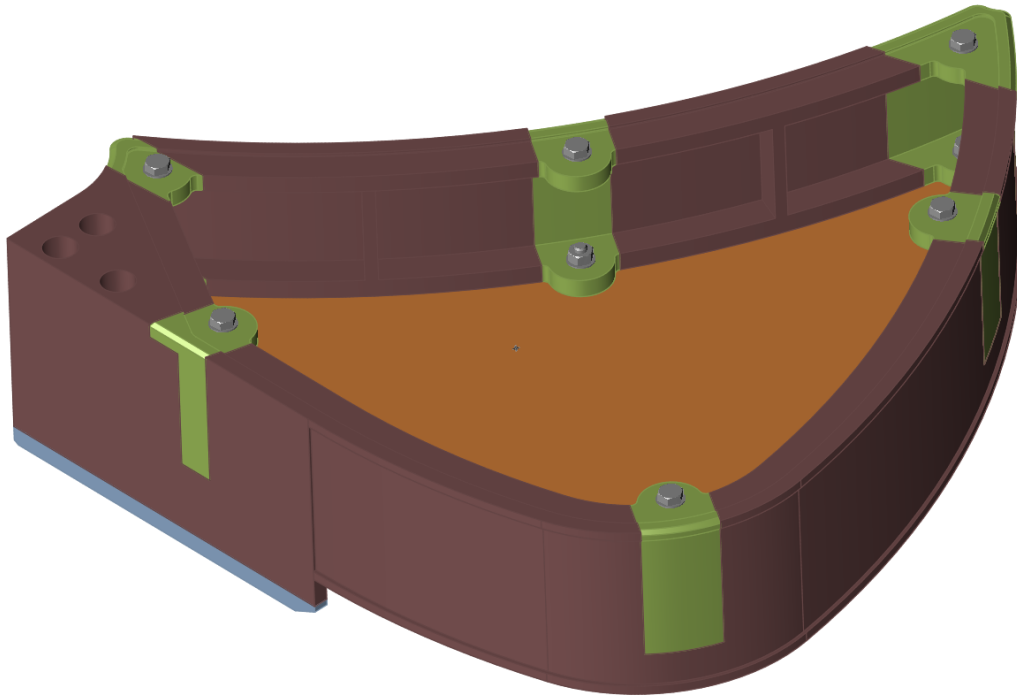


Figure 51: Displacement of Hybrid-Model Lightened;

### 5.5 DS-Lattice – Model 3

Lattice-type optimization fills the DS with an optimized reticular structure. In essence, it is the traditional optimization where the solid elements are replaced with a truss structure. It is, however, possible to choose whether to minimize the mass or to maximize the stiffness, also to insert the available constraints for the topological optimization. In

the lattice optimization, it is possible to check the target length, the minimum and maximum diameter that the beams of the optimized form must respect. The results of the lattice optimization are provided in the form of a result analysis instead of optimization results. Despite this, it would be possible to perform the covering of the optimized lattice through *PoliNURBS* functions, but the process would become too time-consuming. The lattice optimization was performed on the original component defining, in compliance with the requirements, the DS and the NDS as follows:



*Figure 52: DS-Lattice, view1;*

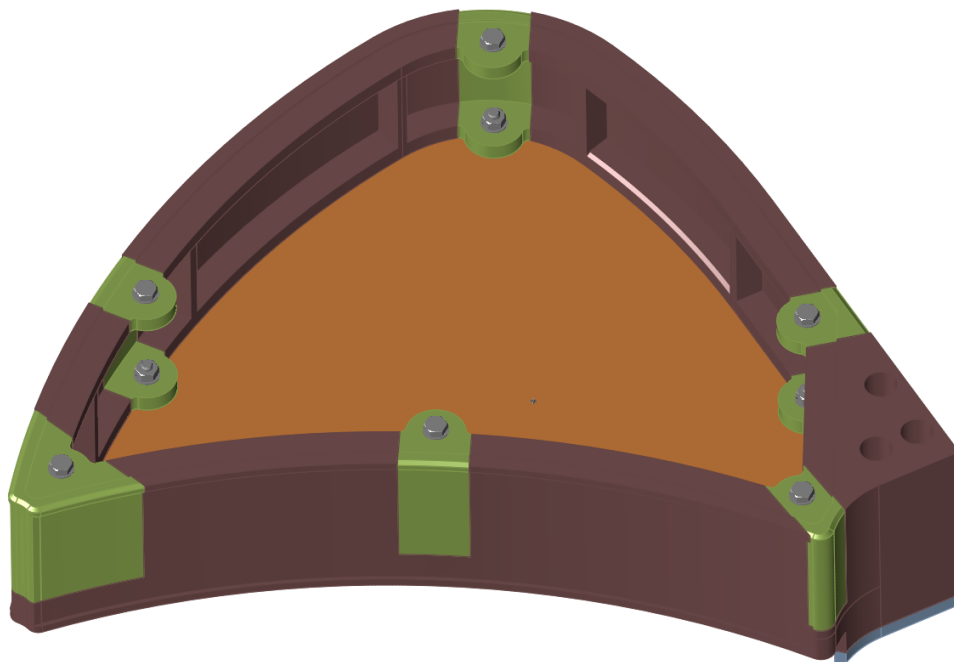


*Figure 53: DS-Lattice, view2;*

It was decided to create “cradles” in correspondence with the holes, as well as to safeguard the holes themselves, to ensure absolute ease in tightening the bolts. For the safeguarding of the constrained holes, the circular crowns were not used but were included in a single component. This choice was made, after having carried out the first attempts, to obtain a more homogeneous distribution of the stresses. In the beginning, a target length equal to 25 [mm] was used. Finally, a good layout which respects project requirements is achieved decreasing this value. The lattice optimization constraints, used to run the last analysis, are shown below.

Table 12: Lattice optimization constraints;

	<b>Target Length</b>	<b>Minimum Diameter</b>	<b>Maximum Diameter</b>
<b>Length [mm]</b>	16	1.8	2.5

### 5.5.1 Results of Lattice-Model

The applied force modules are the same as the original model. The results of lattice optimization are shown below.

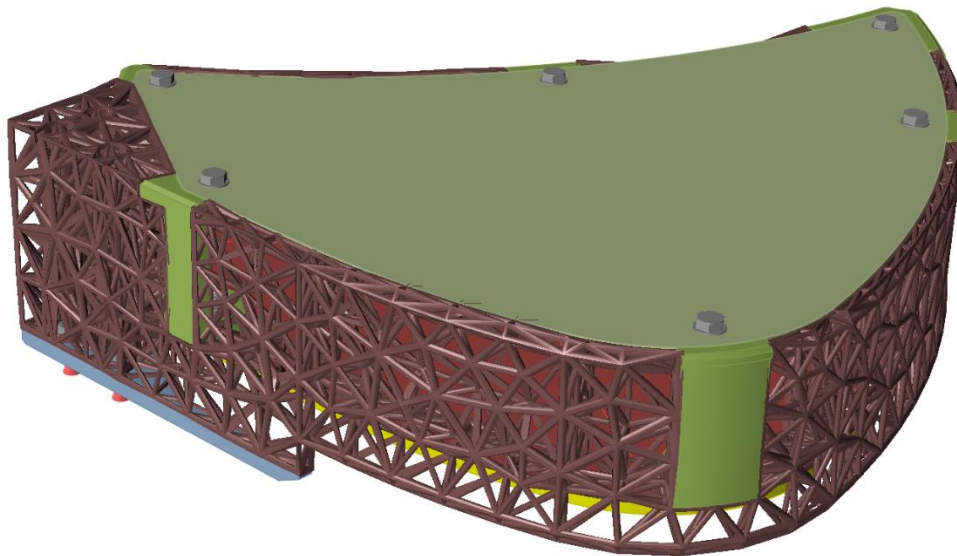


Figure 54: Lattice-Model, view1;

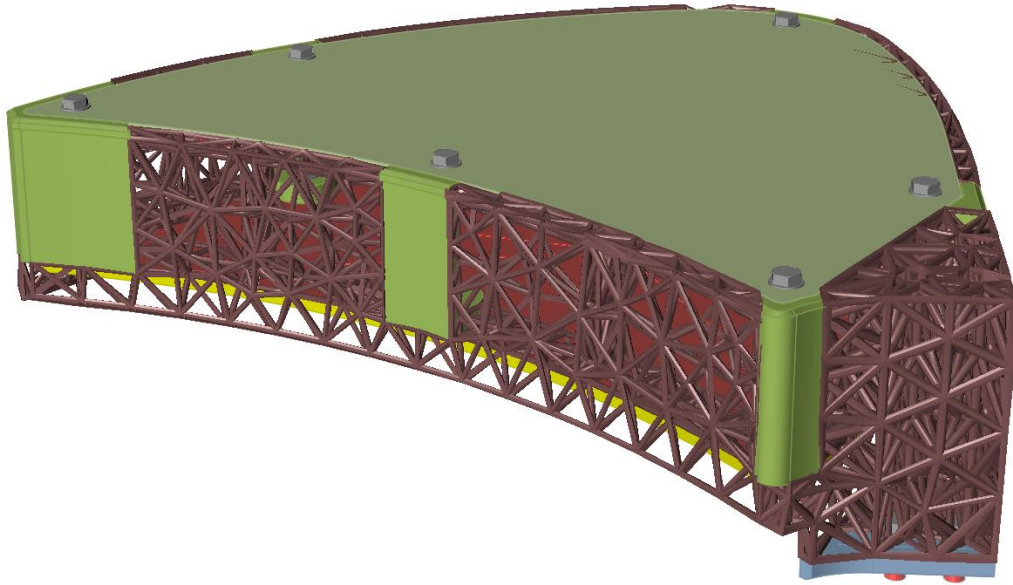
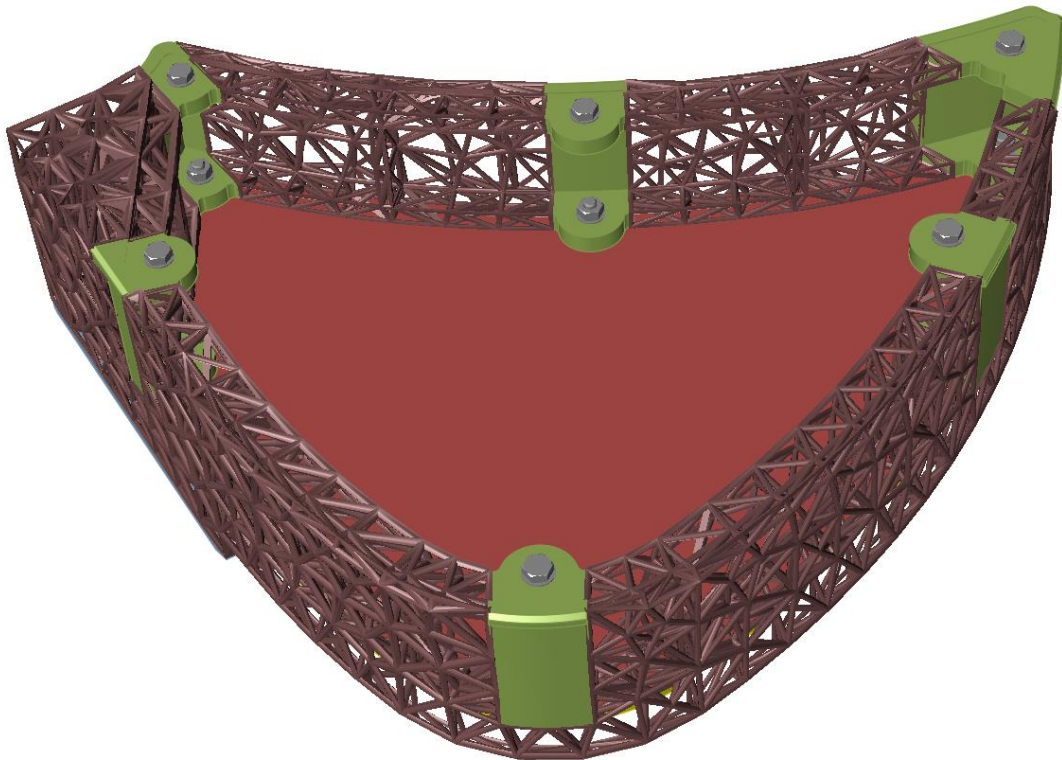


Figure 55: Lattice-Model, view2;



The results of the linear static analysis, obtained for lattice optimization, are shown below.

Table 13: Lattice-Model, linear static analysis results;

	S.F.	$u_{max}$ [mm]	$\epsilon$ [%]	$\sigma_{VM_{max}}$ [Mpa]
Load Case 1	0.7	1.283	152.15	3.671e+002

Load Case 2	0.3	1.977	310.35	7.489e+002
Load Case 3	0.3	2.230	315.40	7.611e+002
Load Case 4	0.6	1.412	173.71	4.192e+002
Load Case 5	0.6	1.412	173.71	4.192e+002
Load Case 6	0.3	2.230	315.40	7.611e+002
Load Case 7	0.3	1.977	310.35	7.489e+002
Load Case 8	0.7	1.283	152.15	3.671e+002
Results Envelope	0.3	2.230	315.40	7.611e+002

The contour plot of the factor of safety and displacement are shown below.

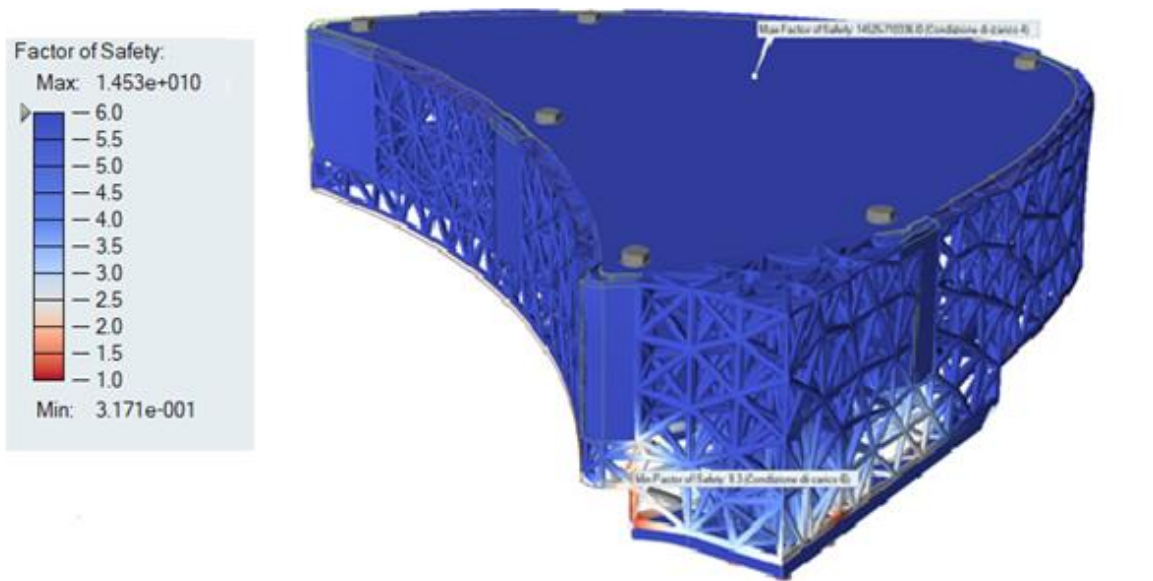


Figure 56: Factor of Safety of Lattice-Model;

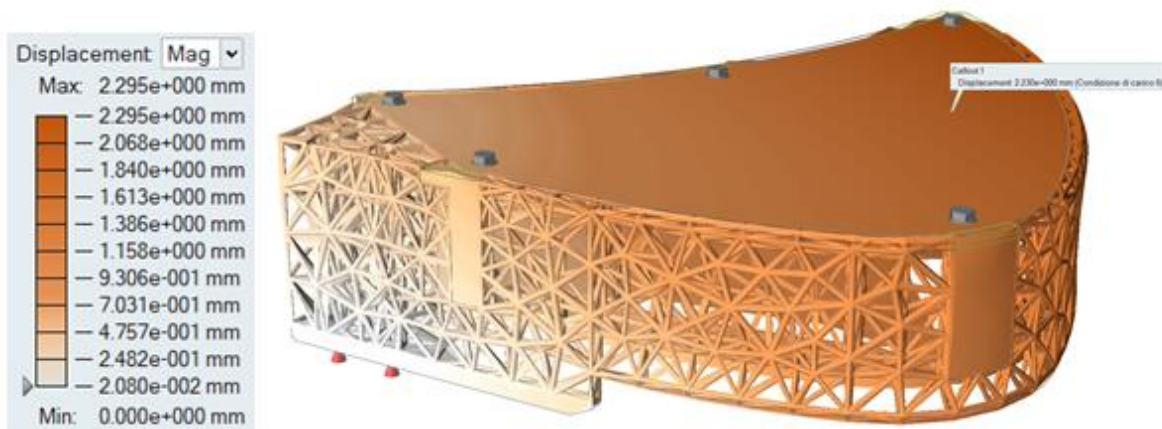


Figure 57: Displacement of Lattice-Model;

The values of the factor of safety reported in table 12 are probably due to meshing error. In fact, as can be seen in figure 56, the minimum safety factor is about 1.3.

## 5.6 Final-Model

Considering the previous solutions to the optimization problem, and drawing inspiration from them, considering the need to have a homogeneous distribution of material between the two bumpers, a new design was created. This paragraph aims to present another design intended for two different scenarios:

1. a ground-based Additive Manufacturing production (structure in aluminium), via a powder bed method
2. a space-based Additive Manufacturing production (structure in ULTEM 9085, specialized polymer for space applications).

The final design of the model is obtained, taking into account the previous results, in particular those of *Hybrid-Model Lightened*. Two different scenarios and thus load conditions have to be used.

### Scenario 1

In the case of ground-based production, the MAC (figure 15) has to be adopted. Unfortunately, MAC curves cannot be used directly for masses lower than one kilogram; the *Final Model*, with the BODY part in aluminium, weighs 475 [g]. So, the data used in the previous analyses, obtained via MAC, are interpolated in Matlab using a second-degree interpolation polynomial. Three couples of data are used.

Table 14: Data for interpolation;

	1.	2.	3.
<i>m</i>	1	1.138	1.25
<i>gs</i>	58	56.5	55

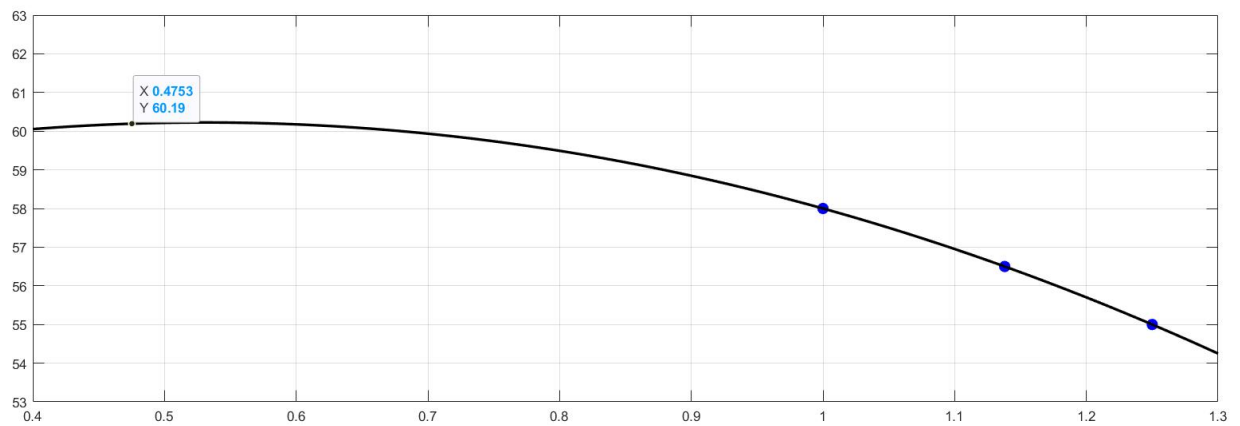


Figure 58: MAC Data Interpolation;

Considering the final mass of 475 g, a value of *gs* equal to 60.2 was obtained. According to the theory of MAC, the modulus of the forces are calculated:

Table 15: Acting forces on Final-Model;

	$F_x$ [N]	$F_y$ [N]	$F_z$ [N]
Modulus of forces	301	282	282

## Scenario 2

For space-based production, two different load sets are used.

Case 1: is the standard method for equipment which is not in EVA path. So, five load cases are created and an acceleration value equal to 0.2 g is considered, this value is due to the shock-induced by docking operation. As for the previous model, a rigid link is generated from the two layers to center of gravity where the acceleration vectors are applied. For Load Case 1, the acceleration is applied orthogonally to the layers, in other case is turned 45° in the plane xz and xy in both senses positive and negative.

Case 2: taking into account the function of the device, which has to be considered as equipment and not as a system, a literature search was carried out to define mission loads, ie those due to the impact with spatial deditris. There are different categories of space debris, based on the size as shown in figure 56. The debris from 10 [cm] to 1 [cm] can be tracked and therefore evasive manoeuvres can be performed to avoid collision. For size lower than 1 [cm] this cannot be done. Statistically, there is a greater probability of being hit by the smallest fragments because there are many more [26].

Debris size	Mass (g) aluminum sphere	Kinetic Energy (J)	Equivalent TNT (kg)	Energy similar to
1 mm	0.0014	71	0.0003	Baseball
3 mm	0.038	1910	0.008	Bullets
1 cm	1.41	70,700	0.3	Falling anvil
5 cm	176.7	8,840,000	37	Hit by bus
10 cm	1413.7	70,700,000	300	Large bomb

Figure 59: Space debris classification [26];

Taking into account the fragment of 1 [mm] and its mass of 0.0014 [g], the momentum of the debris is calculated by multiplying the mass for the speed. Looking into literature, a speed of 12 [km/s] is quite a common value for LEO debris.

$$QDM_{Debris} = (0.0014 \cdot 10^{-3}) \cdot (12 \cdot 10^3) = 0.0168 \left[ \frac{kg \cdot m}{s} \right]$$

Then, by dividing the QDM for the time interval of the impact, which here is considered 0.001 [s], a value of force equal to 17 [N] is obtained.

Then, five load cases are created. The constraints conditions are the same used for the previous analysis. For Load Case 1, a single force of 17 [N] is applied near the center of the *Primary Bumper* and orthogonally to it. For other cases, the force vector is turned 45° in the plane XZ and XY in both sense positive and negative (figure 60). Below are shown the mechanical properties of ULTEM 9085.

Table 16: Mechanical Properties of ULTEM 9085;

<b>Material</b>	<b><math>E</math> [Mpa]</b>	<b><math>Nu</math></b>	<b>Densità [kg /mm<sup>3</sup>]</b>	<b>Carico di snervamento Mpa</b>	<b>Coefficiente di espansione termica</b>
ULTEM 9085	$2.15 \cdot 10^3$	0.350	$1.034 \cdot 10^{-6}$	47	$65 \cdot 10^{-6}/K$

The *Final Model* is shown in the following figures. The final design result is a strong organic, streamlined structure which can be made on the ground, in aluminium, using a powder bed process to guarantee excellent mechanical properties. Once the machine, adequate to print such a volume, is in orbit then it would be possible to use the same design to produce the only plastic structure via FDM in space.

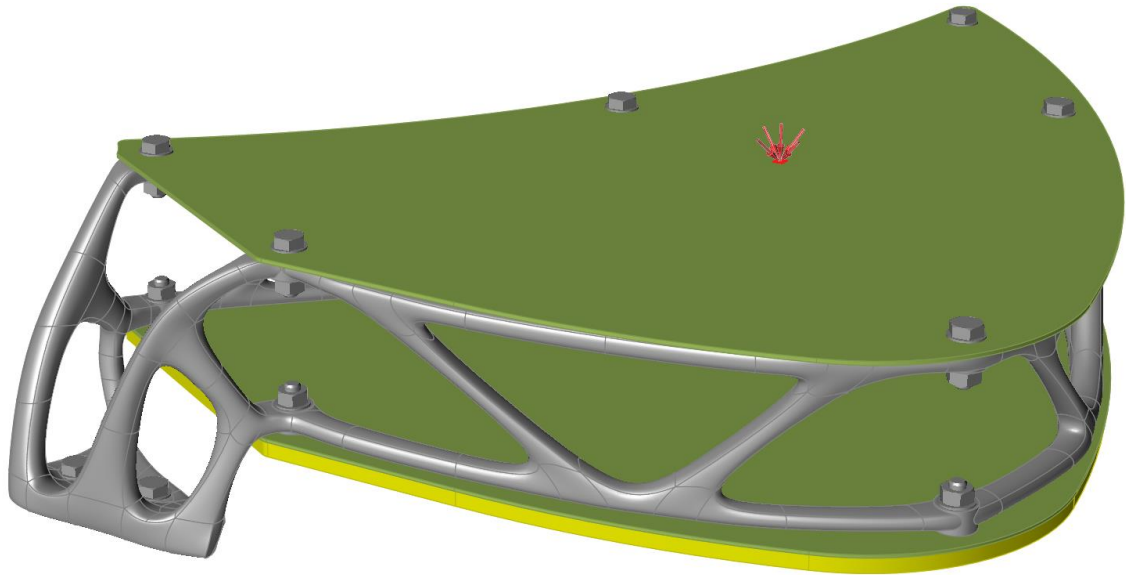


Figure 60: Final-Model, view1;

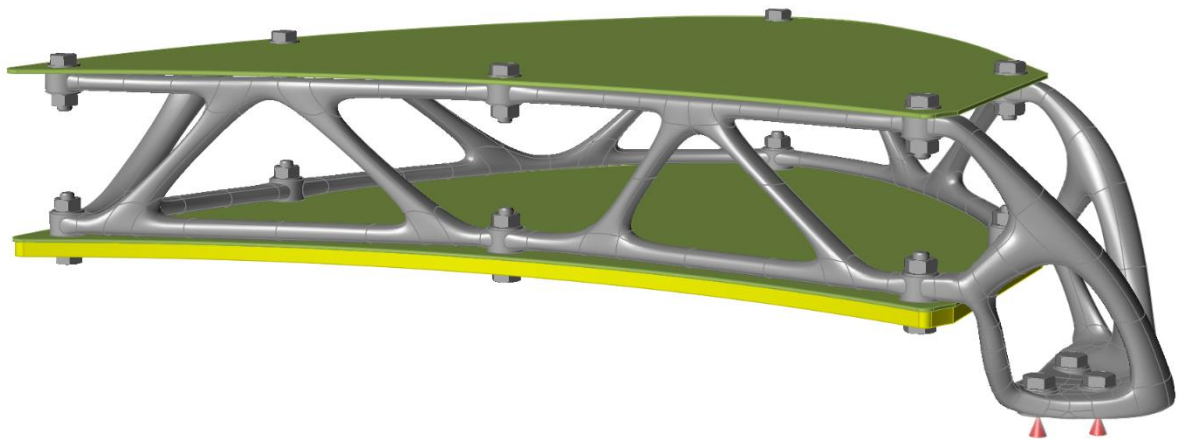


Figure 61: Final-Model, view2;

### 5.6.1 Result of ground-based scenario – Model 4

The results of linear static analysis, useful to validate the *Final Model*, in the case of ground-based production, are shown below.

Table 17: Results for Final Model, ground-based production;

	S.F.	$u_{max}$ [mm]	$\epsilon$ [%]	$\sigma_{VM_{max}}$ [Mpa]
Load Case 1	1.6	1.511	62.64	1.511e+002
Load Case 2	1.7	1.164	59.24	1.430e+002
Load Case 3	1.2	2.333	82.52	1.991e+002
Load Case 4	1.6	1.145	64.25	1.550e+002
Load Case 5	1.6	1.145	64.25	1.550e+002
Load Case 6	1.2	2.333	82.52	1.991e+002
Load Case 7	1.7	1.164	59.24	1.430e+002
Load Case 8	1.6	1.511	62.64	1.511e+002
Results Envelope	1.2	2.333	82.52	1.991e+002

The following is the contour plot of the safety factor and the displacement of the Final Model in case of ground-based production.

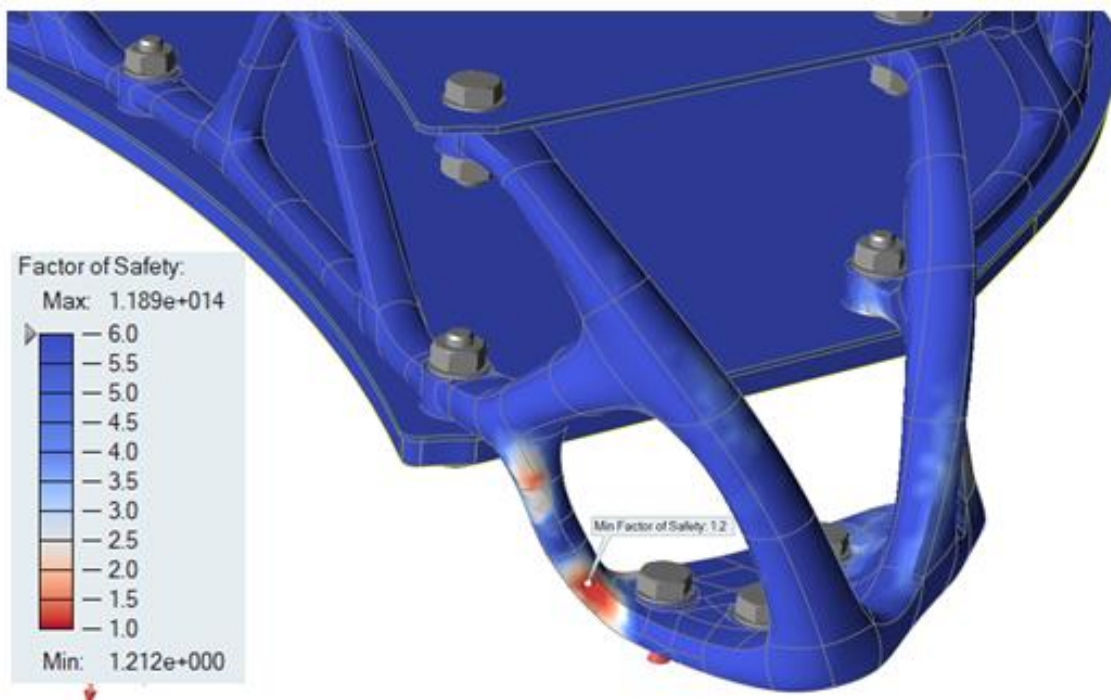


Figure 62: Factor of safety of Final-model, ground-based;

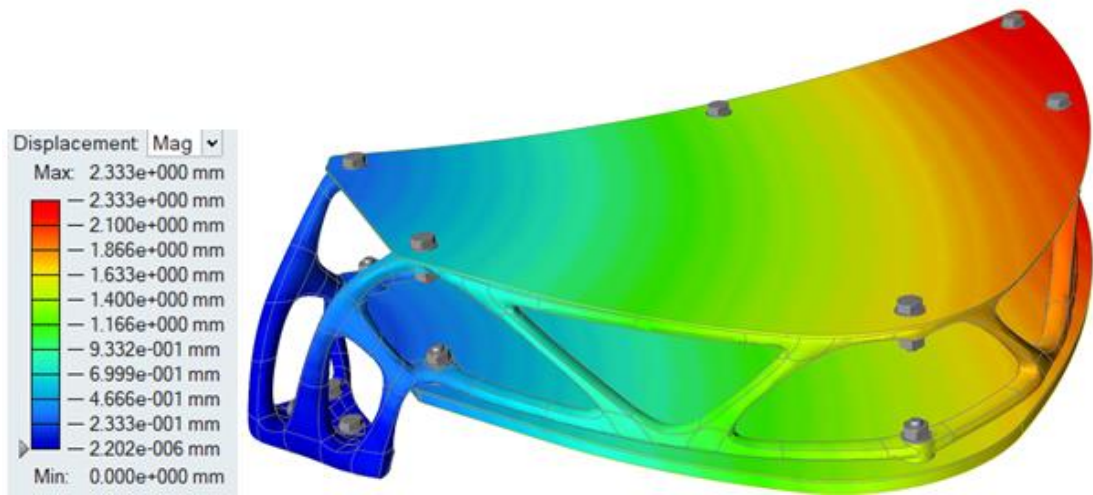


Figure 63: Displacement of Final-model, ground-based;

### 5.6.2 Result for space-based scenario – Model 5/6

The results in case 1 provided, as expected, small values of displacement with respect to case 2. For this reason, case 2 in this case study is assumed to be dimensioning one. The results of linear static analysis, in the case of space-based production and load condition standard of 0.2 g, are shown below.

Table 18: Results for Final Model, space-based production, standard 0.2 [g];

	S.F.	$u_{max}$ [mm]	$\epsilon$ [%]	$\sigma_{VM_{max}}$ [Mpa]
Load Case 1	77.2	0.1615	1.30	6.092e-001
Load Case 2	54.2	0.2010	1.84	8.664e-001
Load Case 3	27.2	0.4242	3.68	1.728e+000
Load Case 4	10.5	1.065	9.48	4.456e+000
Load Case 5	13.1	0.8416	7.65	3.594e+000
Results Envelope	10.5	1.065	9.48	4.456e+000

The following is the contour plot of the safety factor and the displacement of the Final Model in case of space-based production and application of standard 0.2 [g].

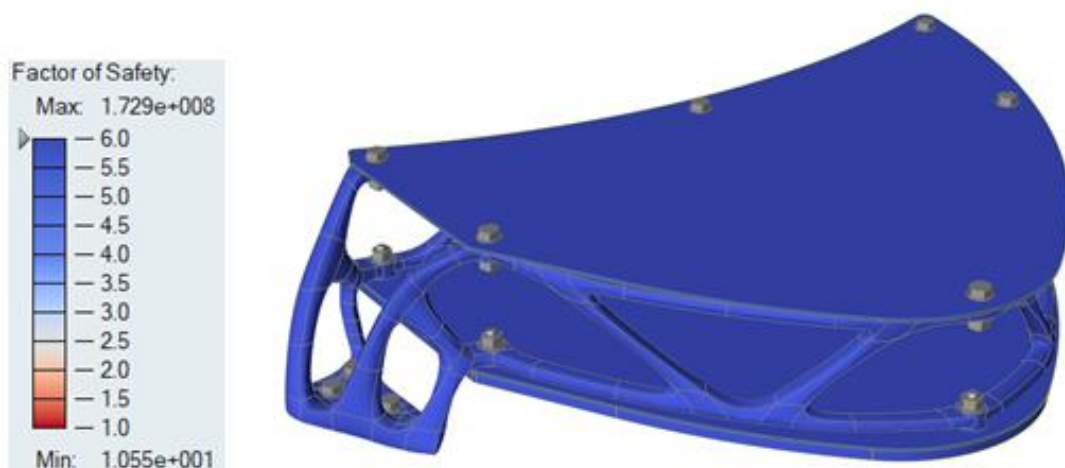


Figure 64: Factor of Safety of Final model, space-based production, standard 0.2[g];

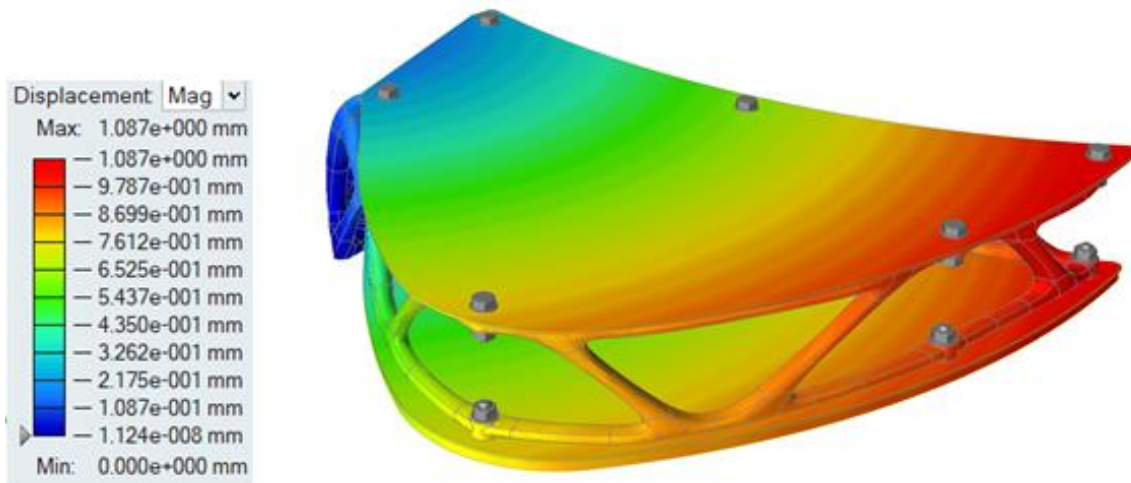


Figure 65: Displacement of Final model, space-based, standard 0.2 [g];

The results of linear static analysis, in the case of space-based production and load condition equivalent to the impact with space debris, are shown below.

Table 19: Results for Final Model, space-based production, impact with debris;

	S.F.	$u_{max}$ [mm]	$\epsilon$ [%]	$\sigma_{VM_{max}}$ [Mpa]
Load Case 1	6.6	3.670	15.21	7.150e+000
Load Case 2	5.6	3.673	17.85	8.391e+000
Load Case 3	5.6	2.449	17.77	8.352e+000
Load Case 4	6.1	3.795	16.51	7.761e+000
Load Case 5	10.8	1.549	9.28	4.423e+000
Results Envelope	5.6	3.795	17.85	8.391e+000

The following is the contour plot of the safety factor and the displacement of the Final Model in case of space-based production and application of forces equivalent to the impact with space fragment.

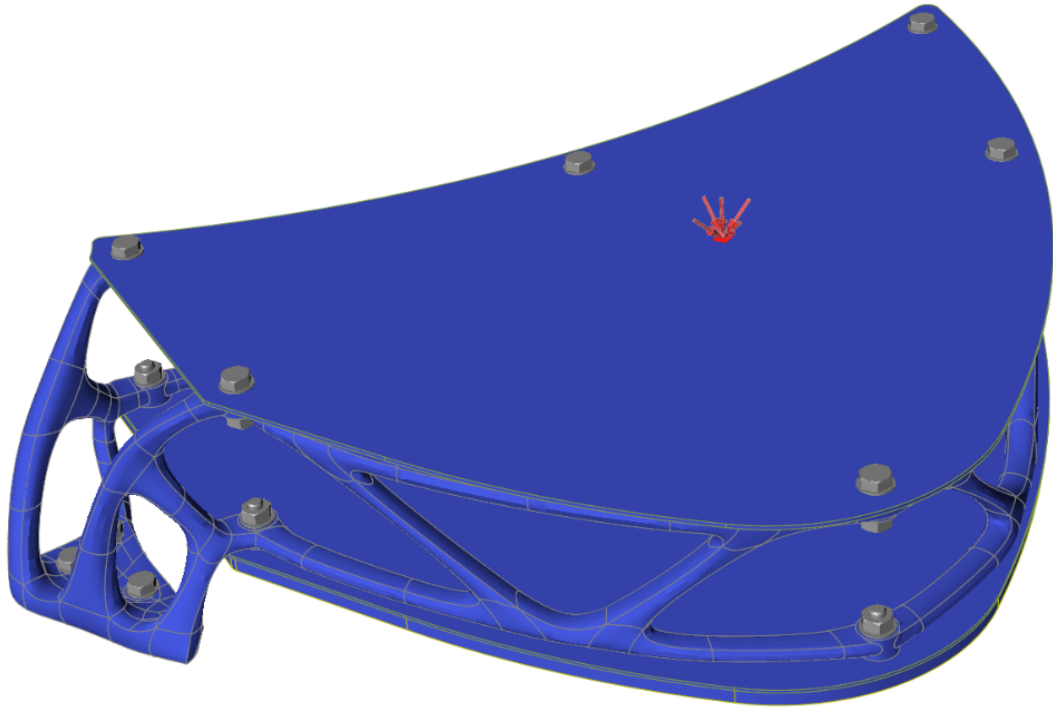


Figure 66: Factor of safety of the final model, space-based, debris impact;

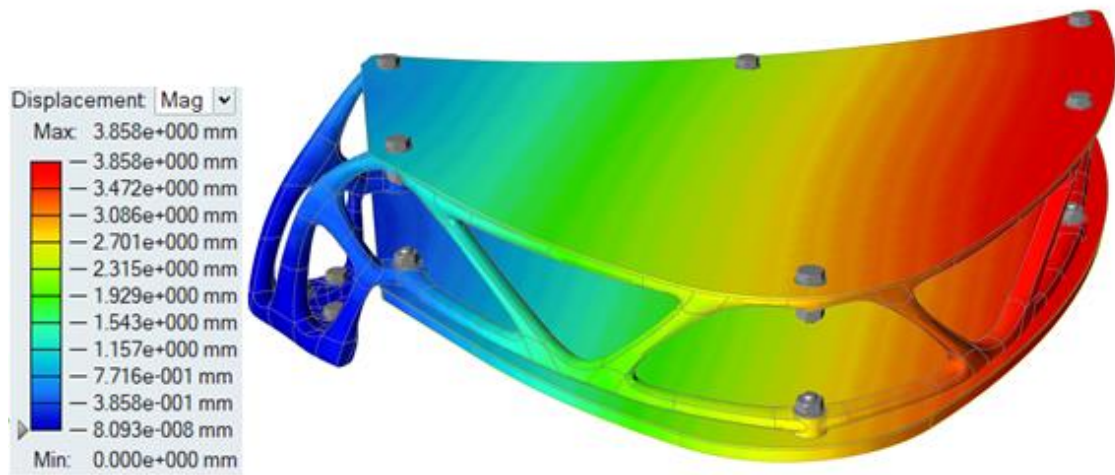
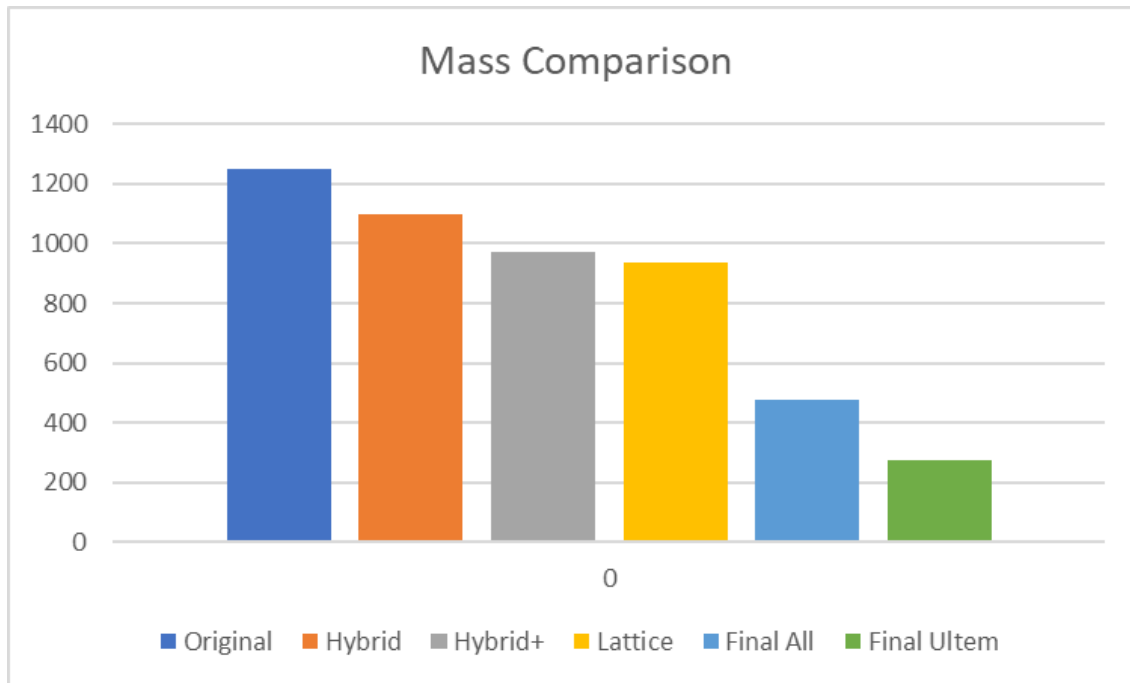


Figure 67: Displacement of the final model, space-based, debris impact;

### 5.7 Model Comparison

As can be seen from the following graph, each optimization step has led to a mass reduction up to a value, in the case of the final design, of 38% compared to the original model. A further mass saving is obtained in the case of production in orbit in ULTEM.



Below a comparison of some of the most indicative parameters for each model. The value in the column  $m$  [%] represents the weight of the model indicated in line with respect to that of the original model. Globally, all the models have safety factors and displacement values such as to respect the project requirements.

Table 20: Review of the model;

	<b>Figure</b>	<b>Material of BODY</b>	<b>Overall Mass [g]</b>	<b>Mass of BODY [g]</b>	<b><math>m</math> [%]</b>	<b>Max Force [N]</b>	<b>Max Displacement [mm]</b>
Model 0	14	Alluminium	1250	969		724	1.659
Model 1	44-46	Alluminium	1098	856	87.84	675	3.279
Model 2	47-49	Alluminium	970	728	77.6	608	2.800
Model 3	54-55	Alluminium	937	483	74.96	724	2.230
Model 4	62-63	Alluminium	475	232	38	301	2.333
Model 5	64-65	ULTEM	273	91	21.84		
Model 6	66-67	ULTEM	273	91	21.84	17	3.795

## ***6. Conclusion and future developments***

The work carried out shows that the use of the topological optimization tool allows a component to be redesigned in a short time, guaranteeing enormous savings in material and thus costs. In some cases, the new design can be exploited both for production on the ground and in space when required. In a long-term vision, imagining the case of long-term exploration missions, huge benefits for crew safety would be derived. However, this method is valid only if you have in-depth knowledge of the component, its functions, the context in which it operates, interfaces with other components. It is crucial to correctly interpret the results and find the right compromise between the optimal solution provided by the software, the project requirements and the technological feasibility constraints.

In the present thesis project, it was possible to redesign the structure of an impact protection shield, reducing its weight by more than 60%. Moreover, thanks to the availability of Ellena S.p.a., a Piedmontese company operating for years in precision mechanics, this structure is currently in production in the final aluminium configuration.

About possible future works and developments, a study of the integration of the model with the rest of the structure is proposed as well as a process of testing and data acquisition through impact tests on the part produced in polymer material.

## References

- [1] I. Boyd, R. Buenconsejo, D. Piskorz, B. Lal., K. Crane, E. Blanco. "On-Orbit Manufacturing and Assembly of Spacecraft" Science & Technology Policy Institute, IDA Paper P-8335, 2017
- [2] A. Trujillo, M. Moraguez, S. Wald, A. Owens, O. de Weck. "Feasibility Analysis of Commercial In-Space Manufacturing Application" AIAA Space Forum, 2017
- [3] R. Skomorohov, C. Welch, A. Hein. "In-orbit Spacecraft Manufacturing: Near-Term Business Cases Individual Project Report." [Research Report] International Space University /Initiative for Interstellar Studies. 2016.
- [4] [https://en.wikipedia.org/wiki/Commercial\\_use\\_of\\_space](https://en.wikipedia.org/wiki/Commercial_use_of_space)
- [5] <https://it.wikipedia.org/wiki/NewSpace>
- [6] [https://en.wikipedia.org/wiki/Space\\_manufacturing](https://en.wikipedia.org/wiki/Space_manufacturing)
- [7] L. Harper, Integrative Studies Space Portal. "Manufacturing in Space Workshop" NASA Ames Research Center, 2017
- [8] G. Musso, L. Enrietti, C. Volpe, E.P. Ambrosio, M. Lorusso, G. Mascetti, g. Valentini. "1st European portable on orbit 3D printer demonstrator on the ISS"
- [9] N. Werkheiser. "In-space Manufacturing: Pioneering Space Exploration" NASA Marshall Space Flight Center, 2015
- [10] S. Patanè, E. Joyce, M. Snyder, P. Shestople. "Archinaut: In-Space Manufacturing and Assembly for Next-Generation Space Habitats" AIAA Space Forum, 2017
- [11] [https://www.esa.int/Our\\_Activities/Space\\_Engineering\\_Technology/Europe\\_s\\_3D\\_printer\\_set\\_for\\_Space\\_Station](https://www.esa.int/Our_Activities/Space_Engineering_Technology/Europe_s_3D_printer_set_for_Space_Station)
- [12] [https://en.wikipedia.org/wiki/Orbital\\_replacement\\_unit](https://en.wikipedia.org/wiki/Orbital_replacement_unit)
- [13] "Orbitecture progetto di habitat spaziale: rapporto tecnico" Center for Near Space, Italian Institute for the future, 2017
- [14] A. Busachi, J. Erkoyuncu, P. Colegrove, F. Martina, C. Watts, R. Drake. "A review of Additive Manufacturing Technology and Cost Estimation Techniques for the Defence Sector" CIRP Journal of Manufacturing Science and Technology, Volume 19, 2017
- [15] M. Anni. "3D Printing: analisi della tecnologia e studio delle potenzialità di mercato" Politecnico di Milano, 2016
- [16] [https://www.researchgate.net/figure/Research-interest-in-additive-manufacturing-as-indicated-by-the-number-of-publications\\_fig2\\_330778615](https://www.researchgate.net/figure/Research-interest-in-additive-manufacturing-as-indicated-by-the-number-of-publications_fig2_330778615)
- [17] W. Gao, Y. Zhang, D. Ramanujan, K. Ramani, Y. Chen, C. Williams, C. Wang, Y. Shin, S. Zhang, P. Zavattieri. "The status, challenges, and future of additive manufacturing in engineering" ScienceDirect, 2015

- [18] K. Taminger, R. Hafley, "Electron Beam Freeform Fabrication for Cost-Effective Near-Net Shape Manufacturing" NASA Langley Research Center, 2019
- [19] S. W. Williams, F. Martina, A. C. Addison, J. Ding, G. Pardal, P. Colegrove. "Wire + Arc Additive Manufacturing" Material and Science Technology, Vol. 32, Iss. 7, pp. 641-647
- [20] N. Manfredi. "Lightweight structures: topology optimization and 3D printing" Università degli Studi di Pavia
- [21] R. Caivano. "Ottimizzazione topologica termo-strutturale per componenti realizzabili in Additive-Manufacturing" Politecnico di Torino, 2018
- [22] G. Briganti. "Scelta e interpretazione del risultato di un'ottimizzazione topologica in funzione della tecnologia di produzione" Politecnico di Torino, 2018
- [23] A. Toscano. "Topology Optimization and design for Additive Manufacturing: the case study of a hydraulic module for automotive application", Politecnico di Torino, 2018
- [24] M. Trubert, "Mass Acceleration Curve for spacecraft structural design" JPL, 1989
- [25] [https://solidthinking.com/help/Inspire/2018/win/en\\_us/tutorials.htm](https://solidthinking.com/help/Inspire/2018/win/en_us/tutorials.htm)
- [26] "Understanding space debris: causes, mitigation, and issues" Crosslink, The Aerospace Corporation magazine of advances in aerospace technology, 2015